University College Cork, Ireland
Coláiste na hOllscoile Corcaigh

An Investigation into the Utilisation of Ethanolamine by Uropathogenic *Escherichia coli*

Thesis presented by

Katherine Dadswell, BSc

for the degree of

Doctor of Philosophy, PhD

University College Cork

School of Microbiology

Head of School: Professor Gerald F. Fitzgerald

Supervisors: Dr John MacSharry, Professor Michael B. Prentice

2019

Table of Content

Declaration

I declare that the research presented in this thesis is my own work and that it has not been submitted for any other degree, either at University College Cork, or elsewhere. Wherever contributions of others are involved, every effort has been made to indicate this clearly, by reference to the literature and by acknowledgement of collaborative research.

This work was completed under the guidance of Dr John MacSharry at the APC Microbiome Institute and Professor Michael Prentice at the School of Microbiology and APC Microbiome Institute, University College Cork, Ireland.

Katherine Dadswell
April 2019

Acknowledgements

I would like to take this opportunity to thank all those that helped me over the last three year and made completing this research possible.

Firstly, I would like to thank my supervisors Prof. Michael Prentice and Dr John MacSharry, for all their help, support and guidance throughout this project. An additional thank to Mike for his help with the bioinformatics analysis in this thesis.

Secondly, I would like to thank the School of Microbiology, the APC Microbiome Institute and Science Foundation Ireland who provided me with the funding and the facilities to carry out this research.

I would also like to thank all the technical staff in the School of Microbiology. I would like to thank Dan Walsh for teaching me all I know about HPLC, and Maurice O'Donaghue for his expertise in cell culture. I would also like to thank John O'Callaghan for helping chance up my orders and finally James Wood and Paddy O'Reilly who have answered all my questions along the way. I would also like to thank Dr Mingzhi Liang, our collaborator at the University of Kent, Canterbury who carried out the TEM in this thesis.

Next, I would like to say an absolutely huge thank you to all members, past and present of Office 435. To Dana, Alli, Marc, Vanessa, Justin, Nuno, thank you for your constant help and friendship over the course of this research. Thank you for the constant stream of random conversation that really helped on those days when everything seems to be going wrong and for the odd trip to KC's for lunch. A particular thank you to the member who were there when I started and took me under their wing, without you my research really wouldn't have taken off! I would also like to mention Ashley Sullivan, who has been my qPCR saviour, helping me setting up runs when I have forgotten how to use the machine, and constantly lending me SYBR green.

Finally, I would like to thank everyone outside of UCC who have supported me over these three year. Firstly, I would like to mention my boyfriend Zsolt. Thank you for listening to me rambling about lab work and endure many evenings alone as I struggled to get those 12-hour time points. Thank you for

your support and love, without which I would have crumbled; you are my rock! Next to my family, my parents Neil and Rosemary, and my sister Lizzie, thank you for supporting me living everywhere but home for the last 7 years and for believing I have a plan even if I don’t think I do. Finally thank you to my little niece Poppy who arrived along the way, you have motivated me to get finished so I can fly home and be there to watch you grow into a great scientist of the future (no pressure!).

Abbreviations

°C	Degrees Celsius
µg	Microgram
µl	Microlitre
µM	Micromolar
AdoCbl	Adenosylcobalamin
Amp	Ampicillin
AMP	Antimicrobial Peptides
AUM	Artificial Urine Media
BEC	Bladder epithelial cells
BMC	Bacterial Microcompartment
cDNA	Complementary deoxyribonucleic acid
CFU	Colony forming unit
Cm	Chloramphenicol
Co-A	Coenzyme A
CUH	Cork University Hospital
ddH_2O	Distilled water
DMEM	Dulbecco Modified Eagle media
DNA	Deoxyribonucleic acid
dNTPs	Deoxyribonucleotide triphosphates
EHEC	Enterohaemorrhagic *E. coli*
ELISA	Enzyme-Linked Immunosorbent Assay
EPEC	Enteropathogenic *E. coli*
Eth	Ethanolamine
EtOH	Ethanol
eut	Ethanolamine utilisation operon
FBS	Foetal Bovine serum
g	Gram
GI tract	Gastrointestinal tract
HPLC	High Performance Liquid Chromatography
Hrs	Hours
IBC	Intracellular bacterial communities
IL-10	Interleukin 10

IL-1β	Interleukin 1 beta
IL-6	Interleukin 6
IL-8	Interleukin 8
Km	Kanamycin
kV	Kilo Volts
LB	Luria broth
LEE	Locus for Enterocyte Effacement
LPS	Lipopolysaccharide
M	Molar
mg	Milligram
min	Minute(s)
ml	Millilitre
ml^{-1}	Per millilitre
mM	Millimolar
Mod M9	Modified M9
MOI	Multiplicity of Infection
mRNA	Messenger Ribonucleic Acid
ng	Nanogram
nm	Nanometre
PAI	Pathogenicity Island
PBS	Phosphate buffered saline
PCR	Polymerase chain reaction
PE	Phosphatidylethanolamine
pg	Picogram
PRR	Pattern Recognition Receptor
PUF	Putative Urovirulence Factor
QIR	Quiescent intracellular reservoir
qRT-PCR	Quantitative reverse transcription PCR
RNA	Ribonucleic acid
SPI-2	Salmonella Pathogenicity Island -2
T3SS	Type Three Secretion Systems
TCA	Tricarboxylic acid
TEM	Transmission Electron Microscopy

TLR	Toll like receptors
UPEC	Uropathogenic *E. coli*
UTI	Urinary tract infection
UV	Ultra Violet light
V	Volts
v/v	Volume by volume
w/v	Weight by volume
xg	G- force/ Relative Centrifugal force (RCF)

Abstract

Urinary tract infections (UTIs) are one of the most common bacterial infections worldwide with *E. coli* as the causal organism responsible for 75% of all cases (1). Uropathogenic *E. coli* (UPEC) naturally reside in the gastrointestinal tract (GI tract) and infect the urinary tract via migratory ascension of the urethra. Ethanolamine, an amino alcohol found naturally in phospholipids as phosphatidylethanolamine, can be metabolised by bacteria to be used as an alternate source of nitrogen and carbon (2). Within the GI tract ethanolamine provides pathogenic bacteria with a competitive advantage over the commensal bacteria (3, 4). The ability of bacteria to utilise ethanolamine is dependent on the presence of the ethanolamine utilisation (*eut*) operon encoding enzymes and bacterial microcompartment packaging (5). Recent studies suggest the regulator of the *eut* operon, *eutR,* can modulate the expression of virulence factors in Enterohaemorrhagic *E. coli* (EHEC) (6-8). Transcriptome analysis of UPEC in active UTIs has found that the *eut* operon is expressed within the urinary tract and confers a competitive advantage in the murine urinary tract, but the exact mechanism conferring this advantage is not known (9, 10).

The aim of this thesis was to investigate the utilisation of ethanolamine by UPEC. This thesis provides evidence that ethanolamine is present in the urine at concentrations of approximately 0.57mM and correlated with the expression of the *eut* operon in UPEC infected urine. Additionally, the ability to metabolise ethanolamine by the *eut* operon is conserved across UPEC in this cohort (Cork University Hospital, Cork). Ethanolamine provides UPEC with a growth advantage as a sole nitrogen source in modified M9 minimal medium and an artificial urine medium (AUM). Metabolite analysis shows that the growth advantage observed in both media correlates with ethanolamine metabolism. Expression of *eut* operon genes and electron microscopy evidence of bacterial microcompartment formation was found in UPEC strain U1 metabolising ethanolamine in AUM. Mutational analysis confirmed a requirement for a functional *eut* operon to metabolise ethanolamine and suggests that ethanolamine is utilised by UPEC as an additional carbon source. Ethanolamine provide U1 with a competitive

growth advantage at 10mM concentrations *in vitro*. RT-PCR provides evidence that suggests ethanolamine regulated the expression of type 1 fimbriae in U1. In conclusion, this thesis supports the hypothesis that ethanolamine provides UPEC with a growth advantage in urine with a potential role in the pathogenicity of UTIs.

Chapter 1 Ethanolamine Utilisation by UPEC in the Urinary Bladder.

1.1 Abstract

Urinary tract infections (UTI) are a significant cause of morbidity and cause significant burden on health care systems worldwide. *Escherichia coli* is the leading cause of UTI with 75% prevalence (11). Uropathogenic *E. coli* (UPEC) are known to reside in the gastrointestinal (GI) tract and transition to the urinary tract to cause infections. UPECs have to adapt to the change in environment when transitioning into the urinary tract. To adapt to the urinary tract UPECs express virulence factors to aid colonisation and subvert the host immune response. Additionally, UPECs adapt their metabolism to utilise the limited nutrients available in the urinary tract (12).

Ethanolamine is an amino alcohol that has found to be utilised by bacteria as a source of nitrogen and carbon (3, 13). Ethanolamine metabolism is mediated by the ethanolamine utilisation (*eut*) operon (5). Proteinaceous structures called bacterial microcompartments (BMC) encase the metabolic reaction protecting the bacteria from toxic intermediates (14, 15). In addition to being metabolised, induction of the *eut* operon has been found to regulate the expression of virulence factors of pathogen in the gastrointestinal tract (7, 8, 16). There is evidence that the *eut* operon is upregulated in urinary tract infection and promotes a colonisation advantage in the murine urinary tract(10, 17). It is however not understood whether this is to be utilised as a potential nutrient or whether it is utilised as a regulatory molecule.

1.2 Urinary Tract Infections

Urinary tract infections (UTIs) result from the colonisation of the urinary tract by microbial pathogens. The human urinary tract is one of the most common sites for bacterial infection affecting 150 million people annually worldwide (18). In 2007 UTIs accounted for 10.2 million doctor visits in the United States, representing US$3.5 billion of economic costs from healthcare to time lost from work (11). Women have a higher risk of contracting UTI compared to men. This is attributed to the shorter length of women's urethra and close proximity of the female urethra opening to the gastrointestinal (GI) tract (19). Almost 50% of all women will experience a UTI once in their lifetime, with 1 in 3 women experiencing a UTI by the age of 24 (20). This is compared to 12% of men who are likely to experience a UTI in their lifetime. Around 20-30% of women who are diagnosed with a UTI will experience a second infection within 6 months of their primary infection (21, 22).

UTIs are diagnosed by identification of clinical urinary symptoms and positive bacterial culture ($>1x10^3$ colony forming units per ml) (CFU ml^{-1}) (23). UTIs are categorised as either lower or upper urinary tract infection, being confined to the bladder (cystitis) or ascending into the kidney (pyelonephritis) (9, 11). Additionally, UTIs are also categorised as either uncomplicated or complicated. Uncomplicated UTIs are typically seen in otherwise healthy individuals. Risk factors associated with uncomplicated UTIs include female gender, prior UTI, sexual activity, diabetes, vaginal infections, and genetic susceptibility (11). In contrast complicated UTIs occur in individuals who have compromised urinary tracts or immune systems, which include urinary obstruction, renal damage, pregnancy and the presence of foreign bodies such as indwelling catheters or other drainage devices (24). The most common cause of complicated UTI is the use of indwelling catheters, accounting for 70-80% of complicated UTIs in the USA (25). Additionally, catheter associated UTIs are the most common cause of secondary bloodstream infections (11).

Gram positive and Gram negative bacteria can cause UTIs. These include *Escherichia coli*, *Klebsiella pneumoniae*, *Proteus mirabilis*, *Staphylococcus*

saprophyticus and *Enterococcus faecalis* (11). Uropathogenic *E. coli* (UPEC) are the most common of these bacteria being responsible for 75% of all cases and 95% of all community acquired infections (1, 22, 26).

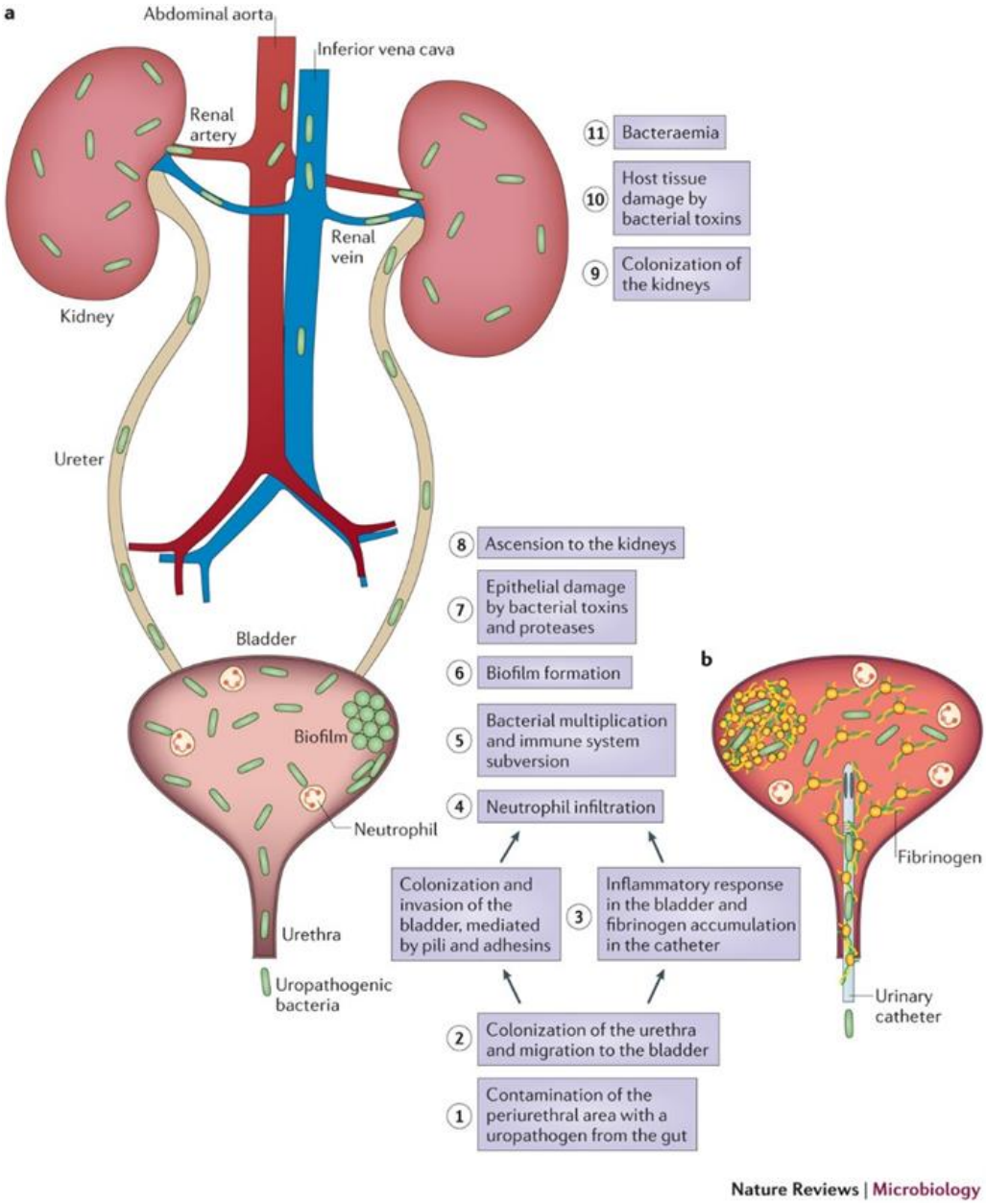

Figure 1.1. **Pathogenesis of A. uncomplicated and B. catheter associated complicated urinary tract infections.** In both situations uropathogen that reside in the GI tract contaminate the periurethral area and colonise the urethra before migrating into the bladder. Within the bladder **A.** uncomplicated UTI, colonise the bladder via pili mediated attachment, **B** complicated UTI, colonise the bladder by binding to fibronectin covered catheters. Neutrophils invade the bladder lumen to clear the infection, however bacteria are adapted to evade the immune system to replicate and form biofilm. Continual colonisation of the bladder results in epithelial damage and ascension to the kidneys. Adapted from Flores-Mires et al*.* 2015 (11)

1.3 Uropathogenic *Escherichia coli* (UPEC)

As mentioned previously *E. coli* infections account for the majority of UTIs (1). *E. coli* is a Gram negative, rod shaped facultative anaerobe that is found to naturally colonise the lower gastrointestinal (GI) tract of mammals and reptiles (27, 28). The majority of *E. coli* in the gut reside as commensal bacteria forming part of the gut microbiota. While *E. coli* typically exists as commensal bacteria in 90% of the population, subtypes of bacteria have acquired virulence factors enabling *E. coli* to cause infection (28). *E. coli* exhibiting pathogenicity in the GI tract mainly cause diarrhoeal disease, and can be separated into: Enterohaemorrhagic *E. coli* (EHEC), Enteropathogenic *E. coli* (EPEC), Enterotoxigenic *E. coli* (ETEC), Enteroinvasive *E. coli* (EIEC), Enteroaggregative *E. coli* (EAEC) (29). Another category of *E. coli* exists within the GI tract. These bacteria are believed to reside as commensals in the gut but have the ability to colonise other site within the body to cause infection. These are known as extra-intestinal pathogenic *E. coli* (ExPEC) and are associated with urinary tract infections (UTIs), septicaemia, and neonatal meningitis (29).

The variable nature of the *E. coli* genome is responsible for its ability to colonise a broad range of niches in mammals. The *E. coli* genome ranges in size from 4.6 to 5.6 Mbp (28, 30). With advances in sequencing over 60,000 genes have been identified to make up the *E. coli* pangenome, the total number of gene identified in *E. coli*, and this number is estimated to rise as more *E. coli* are sequenced (31-34). Only 2100 genes make up the conserved core *E. coli* genome (33). Therefore, most of the *E. coli* genome is highly variable between strains. *E. coli* can acquire genetic elements by horizontal gene transfer that encode fitness and virulence factors, which account for this variability of pathogenic strains compared to commensal (30). Consequently, pathogenic bacteria have the largest genomes when compared to K12 commensal. The UPEC strain CFT073 which has 13 pathogenicity islands (PAIs) is one of the larger *E. coli* genomes sequenced to date (31).

E. coli can be clustered into phylogenetic groups based on their genetic similarity. Seven phylogroups have been identified: Group A, B1, B2, C, D1,

D2 and E. *E. coli* strains can be separated into these phylogroups based on Multi Locus Sequence Typing (MLST) where the sequences of 6-8 housekeeping genes are compared, and more recently by core genome sequence alignments (35, 36). There are limited phenotypic *E. coli* associations with different phylogenetic groups. For example, commensal strains mainly fall into phylogroups A and B2, and there is evidence to suggest a general trend towards increased prevalence of B2 commensals since the 1980s (28). Group A contains the K-12 lab strains such as MG1655. GroupB2, despite containing many commensal strains such as Nissle1917, also houses many ExPECs, including the well-characterised UPECs CFT073 and UTI89 (36). The majority of UPECs occupy phylogenetic group B2. *E. coli* that occupy group B2 and D have been termed 'aggressive' commensals, residing harmlessly in the gut however contain the most virulence genes, a characteristic of ExPECs (37, 38).

1.3.1 Colonisation of the urinary tract

For UPECs to establish infection in the bladder, they migrate from the GI tract into the urinary tract via the urethra (See Fig 1.1). Bacteria typically contaminate the periurethral area before they ascend into the bladder lumen via epithelial attachments (39). Within the bladder, UPECs bind to and invade the bladder epithelial cells (BECs), via appendages on the bacterial cell surface (40, 41). As intracellular pathogens UPECs are able to evade the immune response and escape into the cytosol of host cells, to proliferate and form biofilm-like intracellular bacterial communities (IBC) (42). Epithelial cells respond to the formation of IBC by activating epithelial shedding, however this exposes underlying naïve epithelial cells to bacteria (11, 42). UPECs utilise this mechanism to infect exposed underlying transitional cells to form quiescent intracellular reservoirs (QIR) that can remain viable for months. It has been proposed that these QIR can be reactivated when transition cells differentiate into umbrella cells, and UPECs can then be released back into the lumen to cause secondary UTI (43). Additionally, UPECs are able to utilise motility mechanisms to ascend the ureters and colonise the kidney causing pyelonephritis (26, 29, 44). During prolonged infections, UPECs can

translocate through the renal pelvis and cause bacteraemia (11) (see Fig 1.1).

As UPECs transition from the GI tract to the urinary tract they have to adapt their metabolism and utilise virulence factors to overcome the nutritional and immunological challenges. While specific virulence factors have been shown to promote colonisation of the urinary tract by *E. coli*, there is no conserved set of genes that is specific to UPECs (38). Recent work has clarified the metabolic requirements for UPEC colonisation of the urinary tract (12, 45). In the urinary tract, urine is the primary source of nutrients encounter by the bacteria, with a very complex composition (46, 47). Compared to other host-associated environments such as the gastrointestinal tract, urine is relatively nutrient poor, as arginine, methionine, valine, uracil, adenine, isoleucine and iron are in limited concentration, with a very low availability of sugars (1, 48). Despite the limited nutritional supply, UPECs have established ways to grow in this nutrient poor environment.(1, 49). A recent study has shown rapid UPEC growth in the urine following infection enhances survival in the urinary compared to other *E. coli* strains (50). This implied rapid metabolic adaptation to the urinary tract is a key phenotype for UPEC pathogenesis.

1.3.2 Adapting metabolism to the urinary tract

UPECs in the bladder have to adapt from the nutritionally rich environment of the gut and utilise the limited nutrients in the urine to colonise the urinary tract. Within the GI *E. coli* preferentially reside within the nutrient rich environment of the mucus lining (51). In this environment *E. coli* faces competition for nutrients from other commensals and invading pathogens. *E. coli* preferentially utilise the mono- and di-saccharides within the mucus lining of the GI tract and cannot grow on complex polysaccharides as they lack the necessary hydrolysis enzymes (52). To overcome competition from other bacteria, *E. coli* have been found to utilise up to 6 limiting sugars at once to support colonisation of the GI tract (52). From mutational studies, glycolysis and the Entner-Doudoroff (ED) pathway are key for colonisation advantage of the *E. coli* commensal MG1655 (53). It has been found that gluconate, broken down by the ED pathway, is the first nutrient used by *E. coli* in the mouse intestine, therefore it is to be expected that mutants in this pathway

would result in a colonisation defect (54, 55). Commensal *E. coli* MG1655 and EHEC strain EDL933 do not utilise the tricarboxylic acid (TCA) cycle and gluconeogenesis for colonisation in the streptomycin treated mouse intestine, an environment where there is no competition from other aerobic Enterobacteria (56). However, when the pathogenic strain EDL933 faces competition by commensal *E. coli* MG1655, it adapts its metabolism to use gluconeogenesis pathways rather than glycolysis and the ED pathway (56).

When UPECs enter the bladder they rapidly adapt to the changing environment by altering their metabolism to the high-osmolality, moderately oxygenated, iron-limited environment that contains mostly amino acids and small peptides (49). Within urine UPECs utilise the TCA cycle and gluconeogenesis to generate energy from carbon, rather than glycolysis and ED pathway. This is due to the limited supply of mono- and di-saccharides in urine, except in diabetes (47). In the prototypical UPEC strain CFT073, mutations in the *sdhB* and *pckA* genes, that encode enzymes for the TCA cycle and gluconeogenesis pathway significantly reduce fitness *in vivo* in a murine UTI model (12). However, these pathways are dispensable in UPEC when residing in the GI tract, in favour of the ED pathway and glycolysis, therefore highlighting UPECs ability to adapt to utilises nutrients available in the distinct environments (53).

Within the urinary tract, UPECs colonise different niches with differing nutrient availability by adapting its metabolism. During initial infection in the bladder, glycolysis is dispensable however as the infection ascends towards the kidneys, mutant UPECs deficient in the *tpiA* gene which is used in the glycolysis pathway have a colonisation defect in the mouse kidney (12). Additionally, when UPECs grow intracellularly they utilise sorbitol and β-galactosides (57). Genes involved in the metabolism of sorbitol (*srlA*) and β-galactosides (*lacZ*) were upregulated in wild type bacteria in a UTI mouse model and deficiencies in these genes leads to significantly smaller IBC compared to wild types (57).

During *in vitro* growth in human urine, UPECs upregulate *ddpA* and *oppA*, genes encoding periplasmic peptide substrate-binding proteins. Deficiencies in producing these proteins leads to colonisation defects of UPECs grown in human urine (12). Other mutations affecting gluconeogenesis and

oxaloacetate for the tricarboxylic acid (TCA) cycle had similar effects, This suggest that amino acids and peptides in the urine represent the primary carbon source for UPECs during UTI (12). Additionally, while UPECs can utilise acetate as a source of carbon, it has been observed that the prototypical UPEC CFT073 utilises amino acids to produce acetyl-phosphate and subsequently acetate, but does not need to utilise acetate during murine UTI (58). This suggests that UPEC are adapted to acetogenic growth rather than assimilation. Peptide transport, the TCA cycle and gluconeogenesis are all necessary for UPEC colonisation of the urinary tract and up regulation of amino acid catabolic enzymes during growth in urine show the importance of amino acids and peptides as a source of carbon in the urine (12, 45, 59).

D-serine is an abundant amino acid in urine, present at a concentration of 3-40µg/ml, much higher than intestinal content (60-62). D-serine can be metabolised and used as a carbon source by some bacteria, however in the absence of a specific tolerance locus, intracellular uptake of D-serine is toxic. D-serine has also been found to be an important signalling mechanism to trigger expression of virulence genes. Deletion of the *E. coli* D-serine deaminase (*dsdA*), results in a prolonged lag phase when grown in human urine. In a competitive murine model this deletion was hypothesised to cause a hyper-colonisation phenotype (58). However, the latter phenomenon has been shown to be due to a non-isogenic mutant strain showing genetic rearrangement (63).

Despite the high abundance of urea present in the urine that could provide a substantial nitrogen contribution, urine is thought to be a nitrogen limited environment for UPEC. This is because most *E. coli* lack the urease enzyme that hydrolyses urea to release ammonia (45). Nitrogen is instead produced through the catabolism of amino acids and the glutamine synthase and glutamate oxo-glutarate aminotransferase system (GS/GOGAT). *In vivo* expression studies show that *glnA*, that encodes an enzyme involved in the GS/GOGAT, is up regulated in *E. coli* collected from infected urine (59). This system is upregulated to assimilate nitrogen when it is limited (64). Global transcription studies in urinary tract infection have shown that the ethanolamine utilisation (*eut*) operon is upregulated in urinary tract infection (17, 46). Ethanolamine provides EHECs with a source of nitrogen in the

bovine intestinal tract (3). Upregulation of the *eut* operon in infected urine implies it may be used as a nitrogen source during UTIs. This will be discussed further below.

Table1.1 Summary of the metabolic pathways utilised in the intestine and the urinary tract.

Intestine (Commensal)	**Urinary tract (UPEC)**
Glycolysis	TCA cycle
Entner Doudoroff	Amino acid metabolism
	Gluconeogenesis
	Sorbitol metabolism (IBC)
	Galactoside metabolism (IBC)

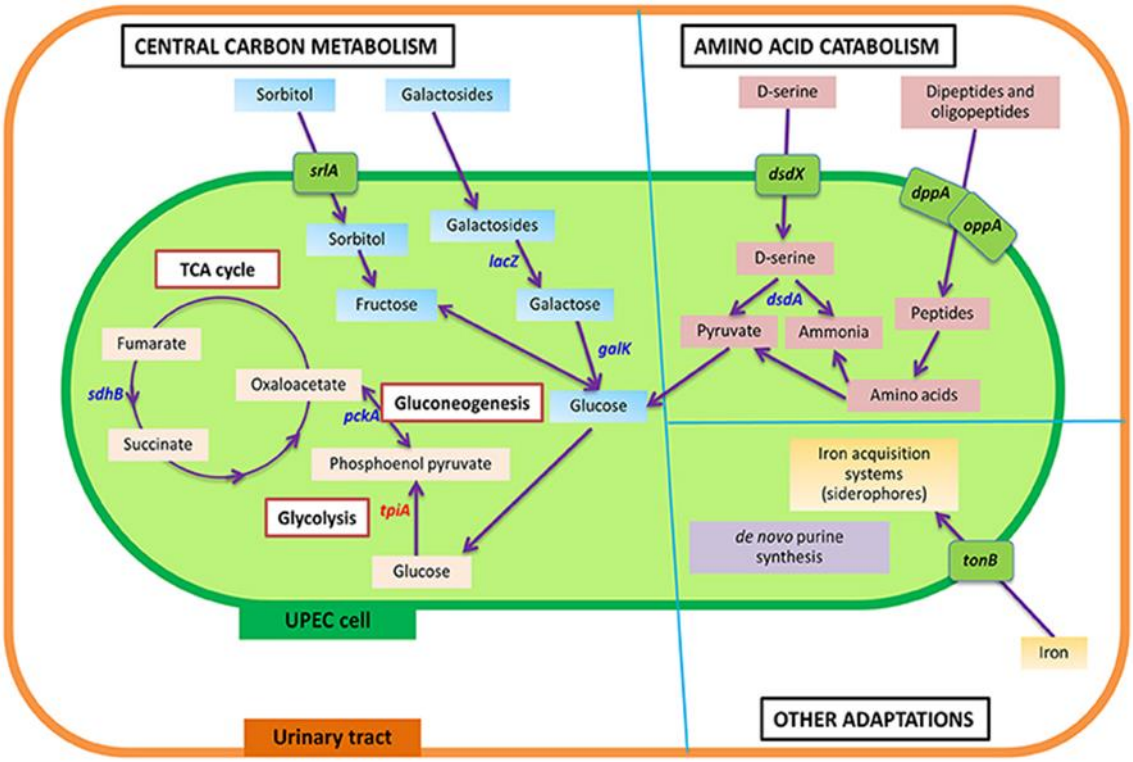

Figure 1.2 Metabolic pathways utilised by UPECs in the urinary tract. Genes in blue are important for UPEC fitness. *tpiA* in red is important for kidney colonisation. (1)

1.3.3 Metal acquisition in urine

Metal ions such as iron and zinc, are essential for bacterial metabolic functions and act as a co-factors for many enzymatic reactions. During host infection bacteria must acquire metal ions and utilise many sequestering systems to compete with the host for essential metals.

1.1.1.1 Iron

Urine is an iron-limited environment with on average 1.3µM iron (47). *E. coli* have evolved to sequester iron in iron-limited environments by producing iron binding molecules such as siderophores and haemophores to facilitate Fe^{3+} uptake in the urinary tract. During urinary tract infection iron acquisition operons are among the most highly upregulated genes in UPEC compared to growth *in vitro* (17, 59, 65, 66). *E. coli* encode four types of siderophores, low weight molecules that have a high affinity for ferric iron (Fe^{3+}): enterobactin, aerobactin, yersiniabactin and salmochelin (67). It has been observed that UPECs produce all siderophores when residing in the gut prior to colonisation of the urinary tract. However salmochelin and yersiniabactin are produced in higher quantities in the urine compared to the intestine suggesting they have a greater role in urovirulence (67). Single mutational studies have found that uptake of aerobactin and yersiniabactin has greater effect on urovirulence than enterobactin and salmochelin (68).

The primary iron regulator in UPEC is the iron sensing transcriptional repressor, Fur. In the presence of Fe^{2+} Fur binds to the *fur* box promotor region to prevent transcription of gene under its regulation. These include the siderophore operons, *entD*, *entE*, *entCEBA and iucABCD* which encode enterobactins and aerobactins respectively within UPECs (69). In iron limiting conditions Fur has low affinity for the *fur* box, therefore preventing repression of iron acquisition molecules (70).

In addition to siderophores, iron is sequestered from haem, an iron-containing porphyrin molecule, by secreted protein haemophores. Two outer membrane receptors ChuA and Hma mediate the uptake of iron from haem, and are both upregulated in iron limiting conditions in both human urine and

the mouse UTI model (71, 72). ChuA is assumed to be a favoured haem receptor as mutants in ChuA are outcompeted by Hma mutants, however absence of either of these receptors leads to a fitness defect in the mouse UTI model (72). Additionally ChuA plays a function in IBC formation by UPEC as ChuA is upregulated in IBC infected epithelial and lack of ChuA results in smaller IBC (66).

Iron-bound molecules are transported into bacterial cells by utilising the TonB-ExbB-ExbD complex. Proton motive force mediated by ExbB and ExbD activity energises TonB which provides the energy for the iron receptor on the surface to translocate iron-bound complexes into the periplasm (70, 73). ATP-binding cassettes then translocate the molecule into the cytoplasm. *In vivo* experiments have found that TonB mutants have fitness deficiency compare to the wild type in the mouse model (74).

The host immune system blocks UPEC uptake of siderophores by secreting lipocalin-2 (LCN-2). Neutrophils and epithelial cells secrete LCN-2 in response to TLR-mediated bacterial recognition (75). LCN-2 specifically binds iron-bound enterobactin to prevent binding to surface bacterial uptake receptors. However UPEC overcome this host defence by producing glycosylated enterobactin, termed salmochelin (67). Salmochelin production requires the *iroA* operon *iroBCDEN* which encodes glycosyltransferase (glucotransferase) *iroB*. Glycosylation of enterobactin prevents host LCN-2 recognition and binding, giving these bacteria a distinct advantage (76, 77).

1.1.1.2 Zinc

In addition to iron requirements, zinc is an essential metal for bacterial survival. There are two main uptake systems utilised by UPECs to import zinc. The first is the ABC transporter ZupACB and the second is the permease ZupT (70). The Znu transport system (ZupACB) is a zinc specific transporter while ZupT can also facilitate the import of Fe^{2+}, Mn^{2+} and Co. Mutational studies have found that the Znu transport system is the primary method of zinc uptake and that ZupT has a secondary role (78). While UPECs are able to colonise the urinary tract in the absence of ZupACB , numbers are severely reduced (78). It is known that during acute infections neutrophils produce calprotectin which binds zine and calcium ions, however

UPEC do not have increased virulence in calprotectin deficient mice (79). Therefore, calprotectin does not appear to have an obvious protective role against UPEC.

1.1.1.3 Copper

Copper ions and haem form the catalytic core of cytochrome *bo* terminal oxidase (*cyoABCD*) which is involved with aerobic respiration in bacterial cells (70). Copper however is biocidal to bacteria when in excess and there is a recent hypothesis that neutrophils or other aspects of the innate immune system use copper ions to kill bacteria (80). Cu^{+} can generate very toxic hydroxyl radicals which can damage iron-sulphur clusters in the cell and inactivate dehydratases, which are important in the synthesis of branched chain amino acids and other reactions (81). To counteract the toxic effect of copper, UPECs utilise copper efflux systems. There are three main systems in UPECs CopA, CueO and CusCFBA, which are expressed dependent on the severity of toxicity. CopA is active in low toxicity conditions, CueO is activated with CopA in moderately toxic conditions and finally the CusCFBA which is active during severe toxicity and low oxygen conditions (82-84). Within infected urine copper was measured at 287nM compared to 59nM in healthy urine, which supports the recent hypothesis that immune cells use copper ions to eliminate bacteria (80). In the study the *cus* system was highly upregulated in UPEC in infected urine compared to growth in sterile urine *in vitro*, and *in vivo cus* mutants had a colonisation deficiency in the murine model (17) demonstrating the importance of copper efflux in UTIs. In contrast, *cueO* deletion mutants had a colonisation advantage in mouse model by facilitating the influx of Fe^{2+}(85).

1.3.4 Colonisation factors

UPEC, like other bacteria have short filamentous organelles called fimbriae that allow the bacteria to adhere to various surfaces. UPEC carry significantly higher number of fimbriae genes in their genome compared to faecal and commensal strains, with the highly characterised CFT073 containing 12 fimbriae gene clusters in its genome (86). There are many types of fimbriae produced by UPEC including type 1, P, F1C, F9 and Auf. Type 1 and P fimbriae are the best characterised bacterial fimbriae (86).

Type 1 fimbriae encoded by the *fim* operon are conserved in *E. coli*. Within the urinary tract type 1 fimbriae mediate adhesion to BECs via the fimbriae binding protein FimH. FimH binds mannosylated glycoproteins, uroplakin (UP) Ia and IIIa on superficial facet cells and $\alpha_1\beta_3$ integrin found on the surface of the naïve transitional epithelial cells (40, 87). Adhesion of UPEC to the epithelial cell wall via FimH prevents the expulsion of bacteria by shear force stress created by urination (88). In addition, FimH mediates invasion of the bladder epithelium by UPEC to create intracellular bacterial communities (IBC). Binding to the BECs activates Rho GTPase, which initiates actin rearrangement within the epithelial cell and internalisation of the UPEC (41, 89, 90). Expression of type1 fimbriae in urine is tightly regulated by several global regulatory proteins controlling the orientation of an invertible element carrying the promoter region (9). This promoter is inverted to the 'ON' orientation in the presence of FimB recombinase and locked in the 'OFF' orientation in the presence of FimE recombinase.

Type 1 fimbriae are conserved in UPEC and are considered essential in the development of UTIs in murine and human investigations. The *fim* operon is highly expressed in UPEC isolated from the murine urinary tract and *fim* mutants do not colonise the mouse urinary tract (59, 91). However, it is notable that, when gene expression in bacteria isolated from infected human urine was analysed, components of the *fim* operon were detectable in less the 50% of the urine samples collected (46, 65).

P fimbriae or pyelonephritis-associated fimbriae are unique to uropathogenic *E. coli*, encoded on pathogenicity islands distributed amongst UPEC and most commonly associated with pyelonephritis strains (9). The adhesion PapG mediates binding to glycosphingolipids on renal epithelium. Expression of the P fimbriae is controlled by the methylation of the promotor region *papAB*. However, deoxyadenosine methylase which mediates the methylation of the promotor region, is competitively blocked by the leucine-responsive regulatory protein (Lrp), which binds to the promotor region preventing methylation and therefore transcription (9).

E. coli preferentially form one type of fimbriae at a time (92). Cross talk between fimbriae operons in a single strain of *E. coli* can lead to variable

expression of the different fimbriae (93). This is a process known as phase variation and can give rise to subpopulations of UPEC expressing functionally distinct fimbriae increasing the probability of adherence (94). Additionally mutational studies have found that in the absence of the preferred type 1 fimbriae and P fimbriae, UPEC express alternative fimbriae to retain colonisation of the urinary tract (94).

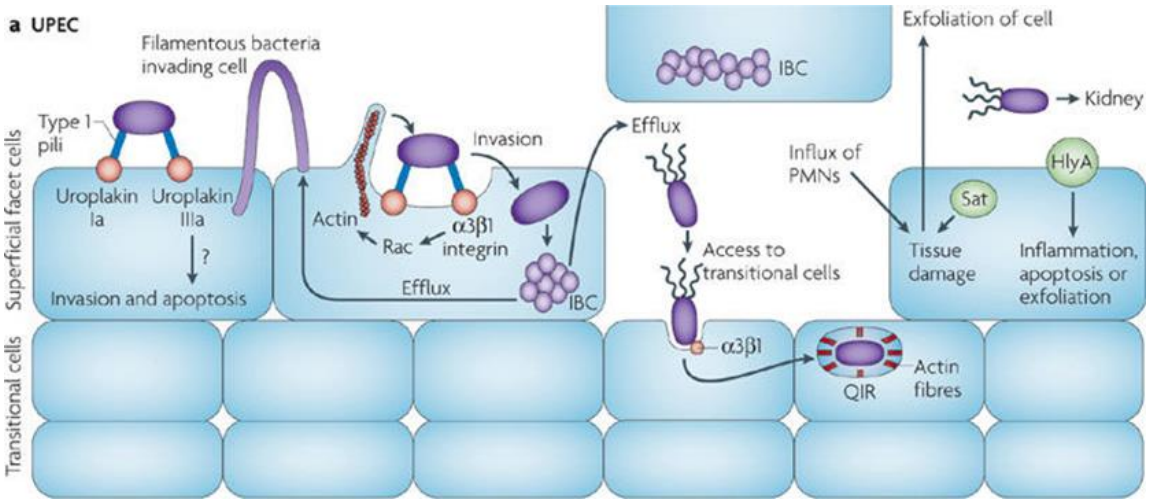

Figure 1.3 Pathogenic mechanism of Uropathogenic *E. coli* attachment and invasion of bladder epithelial cells. Type 1 pili mediate attachment to the superficial BEC via uroplaking Ia and IIIA. Invasion of the UPECs into epithelial cells is controlled by Rho GTPase activated actin rearrangement and once within the cells UPECs form intracellular bacteria communities (IBCs). Toxins released by UPECs in sublytic concentration can lead to cell apoptosis and exfoliation, exposing underlying epithelial cells to bacteria invasion. UPECs can form quiescent intracellular reservoir (QIRs) which are involved with recurrent infections. Adapted from Croxen and Finlay 2010 (29)**.**

1.3.5 Motility

Flagella are appendages produced by *E. coli* and other bacteria to facilitate motility. Transcriptome studies have shown that *fliC*, a major flagellin protein is not expressed during acute cystitis (17, 59, 65). However GFP-tagged FliC is highly expressed in the ureter in the mouse model (44). This suggests flagella are important for the progression of UPEC into the kidneys, and is confirmed by a mutational study found that *fliC* mutants successfully colonise the bladder however they do not ascend to the kidneys (95). Within the kidney flagella also mediate the invasion of UPEC into the renal epithelium (96). As the need to bind to epithelial cells and move in the urinary tract are conflicting it has been suggested that there is interplay between fimbriae and flagella operons. Lane et al. found that expression of the *fim* operon decreases the expression of flagella, while overexpression of the flagella gene *flhDC* in UPECs does not prevent expression of type 1 fimbriae (97). This suggests that expression of the *fim* operon expresses a unidirectional repression on flagella-mediated motility in UPEC. Further investigations have found that 'X' genes located in fimbriae operons, in particular *papX* and *focX*, repress the expression of the flagella regulator *flhDC* (98).

1.3.6 Toxins

Some secreted toxins that cause tissue damage and inflammation are encoded by UPEC. Well characterised examples include α-haemolysin (HlyA), cytotoxic necrotising factor-1 (CNF-1), secreted auto-transporter toxin (Sat) and vacuolating transporter protein (Vat) (11, 26).

HlyA toxin is encoded by around 50% of all UPEC and expression of the toxin is associated with increased clinical severity (26). HlyA at high concentration integrates into the cholesterol environments in the host cell membrane in a Ca^{2+} dependent process, to create pores in the cell membrane (11). Pore formation promotes lysis of cells, releasing iron and nutrients. Upregulation of *hlyA* in IBC suggest that HlyA is important for intracellular survival (66). In addition to its cytolytic activity, when present in

sub-lytic concentrations, HlyA is involved with communication between host and pathogen by modulating signalling pathways within the host cell. Sub-lytic concentrations of HlyA can modulate the immune response such as suppressing the pro-survival signal pathways, NF-kB and Akt, which increases cell apoptosis and epithelial shedding (99, 100).

CNF-1 is encoded by approximately one third of UPEC isolates (26). Once secreted by the bacteria CNF-1 enters the host cells via endocytic vesicles (101). Within the host cells CNF-1 disrupts Rho GTPases signalling by constitutive activation. This disrupts the cytoskeleton leading to formation of actin stress fibres, lamellapodia, filopodia and induction of membrane ruffling, which increases bacteria uptake (26). In addition to these morphological changes, CNF-1 disrupts immune pathways and increases epithelial cell shedding. Absence of CNF-1 has been associated with decreased fitness in the murine UTI model therefore highlighting the importance of CNF-1 in UPEC infection (102).

1.4 Host Defences Against UTIs

Despite the bladder's close proximity to the densely populated GI tract, the bladder remains mostly infection free. The anatomy and physiology of the bladder prevent the pathogenic colonisation of the urinary tract. The bladder is lined by a mucus membrane, comprised of a layers of epithelial cells covered with a thin lining of glycosaminoglycan forming a barrier over the epithelial cell and deters bacteria attaching to the apical surface of the epithelium (103, 104).

Urine held within the bladder provides a potential growth medium for bacteria in the bladder (50). However, the shear force of urine flow expels bacteria before they can establish colonisation. UPEC have adapted to circumvent the effects of shear force through epithelial attachment. Both type1 and P fimbriae can utilise the shear force of urination to strengthen their attachment to the bladder epithelium surface and generate resistance to detachment from the force needed to unravel their typical helical structure (88).

1.4.1 Epithelial response

If bacteria persist in the bladder they encounter the innate immune response mediated by epithelial cells. 90% of the apical surface of the epithelium is covered in urothelial plaques, proteinaceous scallop-shaped membrane plaques assembled from uroplakins (UPs). These plaques, create a physical barrier, which discourages the attachment and invasion of most bacteria (105). UPEC however utilise UP Ia/IIIa as receptor for type 1 fimbriae to facilitate colonisation (87).

Invading pathogens are recognised by pattern receptor receptors (PRR) on the epithelial cell such as toll like receptors (TLR) TLR-4, TLR-5 and TLR- 11. Recognition of lipopolysaccharides (LPS) and flagella on the bacteria surface mediate the secretion of cytokines and chemokines such as interleukin-6(IL-6), IL-1β and IL-8 from the epithelium (106, 107). These are the first cytokines detected in the urine after infection and activate an influx of immune cells to eliminate the offending pathogen. Antimicrobial peptides

(AMPs) are also secreted by the epithelium which can directly target the bacteria and eliminate them from the urine (108, 109). The mRNA of human cathelicidin, LL-37, is detected in the urine within 5 minutes of BEC stimulation with UPEC, and deficiency in LL-37 secretion has been associated with increased UPEC load in the murine urine (108). β-defensin, another AMP is primarily secreted from kidney epithelial cells (109). Secretion of both AMPs contributes to cytokine production and subsequent neutrophil recruitment to the bladder (110).

As part of the function of the bladder, it has to expand and contract depending on the volume of urine contained. The cells in contact with urine are called umbrella cells which cyclically change their surface area transforming from an inverted umbrella parasol shape in voided empty bladders to flat and squamous shaped in filled bladders (111). Fusiform vesicles assist with the recycling of the epithelial membrane, in particular there are large pools of the fusiform RAB27b in the umbrella cell epithelium (112). When urine enters the bladder the fusiform vesicles exocytose into the umbrella cell membrane in a cAMP dependent manner to provide the extra membrane for bladder distension and as the bladder empties, intracellular fusiform vesicles form by internalising the RAB27b membrane (112, 113). UPEC have exploited this pathway to gain entry into the epithelial cells (113). TLR-4 receptors within the fusiform vesicle detect the invading bacteria and proceed to expel the bacteria (114). Over 80% of bacteria are expelled from the epithelium after 24 hours but the remaining bacteria are able to multiple and form intracellular communities (113). When the bladder epithelium become overburdened with bacteria the epithelial cells undergo cell death and shedding of epithelial occurs to eliminate bacteria from the bladder (42, 115). Shedding the apical layer of the epithelium however exposes the underlying naïve cells to the bacteria remaining in the urine (42).

1.4.2 Neutrophils, mast cells and macrophages

Neutrophils are the first immune cells recruited to the bladder after bacteria have been detected in the bladder and the presence of white cells in the urine is a hallmark for urinary infection. In response to IL-8 and TNFα secretion from the epithelium, and TNFα secretion from mast cells (see

below) neutrophils migrate through the epithelium (116, 117). The secretion of matrix metalloprotease-9 (MMP-9) by the neutrophils facilitates their ability to penetrate the basement membrane (118). Neutrophils have been found to be present in the bladder within 2 hours of infection and peak at around 6 hours post infection (119). They play an important role in bacterial clearance and deficiency in neutrophil recruitment increases susceptibility to UTI and decreases ability to clear infection in mice (120). Neutrophils clear infection by engulfing and degrading the bacteria intracellularly. To facilitate this mechanism, neutrophils secrete pentraxin 3 (PTX3), which acts as an opsonin to coat the invading bacteria (121). The release of neutrophils however can have detrimental effects in the urinary tract, as the release of reactive oxygen species and other cytotoxic products including cyclooxygenase 2 (COX2) causes inflammatory damage to the bladder tissue and could predispose the bladder to persistent infection (122).

In addition to neutrophils, mast cells and macrophages are important cellular defences in the bladder. Mast cells are the most prominent resident innate immunity cell in the urinary tract, and reside in the lamina propria of the bladder. Within the first hour of infection, histamine and other proinflammatory molecular normally located in the granules of mast cells are detected in the urine (123). TNFα is one of the pro-inflammatory molecules secreted by mast cells and aids in recruitment of neutrophils to the bladder. When mast cells are deficient, bacterial clearance is limited (117). In addition to promoting inflammation, mast cells are important in establishing homeostasis and tissue recovery. It was recently reported that several hours into an immune response, mast cells abruptly express the immunosuppressive cytokine IL-10 (117). This coincides with epithelial shedding, and therefore the need to replenish the epithelial layer, a process that cannot happen during active inflammation. Expression of IL-10 however can result in the premature resolution of inflammation which can leave a residual bacterial community and cause subsequent infections(117).

Macrophages also play a critical role in the neutrophil response in the bladder. A sub population of macrophages reside in the mucosal lining of the bladder. Upon infection macrophage produce cytokines to drive an inflammatory response. In particular the resident macrophages (mainly

LY6C) secrete CXCL-1 and CXCL-2 to recruit neutrophils and LY6C+ macrophages into the bladder. LY6C+ macrophages are essential for neutrophil migration through the basement membrane (118). TNFα secreted by recruited LY6C+, causes the resident macrophages to secrete CXCL2 which in turn activates the release of MMP-9 (124). Therefore, macrophages aids in the control of the neutrophil response in the bladder.

1.4.3 Bladder microbiome

Until the advancement of culture-independent methods to detect bacteria, the healthy urinary tract was believed to be sterile. Studies as early as 2004 identified non-cultured bacteria in individuals who had no previous episode of urinary tract infection (125). Clean- catch urines from asymptomatic healthy women have been found to contain more than 45 genera across 11 different phyla (126). There is much variation in bacteria genera described for the urinary microbiome, however *Lactobacillus* and *Streptococcus* have been the most frequently genera reported in the urinary microbiome (127). These species have been associated with protective functions.

The urinary microbiome has been observed to vary depending on sex and age (128, 129). Lewis et al., found that *Jonquetella*, *Proteiniphilum*, *Saccharofermentans* and *Parvimonas* were only present in individuals over the age of 70, however there are species in the urinary microbiome that are present independent of age (128). In regard to differences between sex, women were found to have predominately *Lactobacillus* species, while *Corynebacterium* were the predominant species in men (129). However cautious interpretation of this data is required due to the likely contamination of urine from female patients from the resident microflora of the urogenital tract in clean-catch specimens.

In the gut, the resident microbiome protects the host from infection (130). Therefore it could be hypothesised that a bladder-resident microbiome could provide the same protection, especially with the identification of *Lactobacillus*, a genus that is considered beneficial in both the intestine and the vagina (131). However, evidence for a function of resident urinary microbiome in protection against UTI is currently lacking.

1.5 Ethanolamine Utilisation

Ethanolamine is an amino alcohol that is present in mammalian and bacterial cell membranes in the form of phosphatidylethanolamine (PE) (132, 133). PE is the most abundant phospholipid in prokaryotic cells and the second most abundant phospholipid in eukaryotic cells after phosphatidylcholine (132). Phosphodiesterases break down PE to release glycerol and ethanolamine that can then be utilised by bacteria and *E. coli* encodes phosphodiesterases required for the breakdown of PE to ethanolamine (134, 135).

The animal gut is an abundant source of ethanolamine due to the high turnover of enterocytes (25% per day), bacterial presence and the host diet (136). A concentration of over 2mM of ethanolamine was measured in bovine intestinal content and between 0.5mM and 1mM of ethanolamine has been detected per gram of homogenised colon (3, 4). Recent metabolome studies have detected ethanolamine in serum at a concentration of 2µM and in the urine at a mean concentration of 37.0 µM/mM creatinine in urine from 20 healthy adult subjects (approximately 500 µM) (47, 137). Ethanolamine can be used by bacteria as a valuable source of nitrogen and carbon, and within the intestine the ability to metabolise ethanolamine has been found to provide pathogenic bacteria with a competitive advantage (3, 4).

1.5.1 Ethanolamine utilisation operon

The best documented route for ethanolamine utilisation by bacteria is via activation of the ethanolamine utilisation (*eut*) operon. The *eut* operon was first identified as a 17-gene operon in *Salmonella enterica* Serovar Typhimurium (*S.* Typhimurium) (5). Comparative genomic analysis has now revealed that a form of the *eut* operon is conserved in 100s of species of bacteria across the phyla Proteobacteria and Firmicutes (138). The gene content of these operons however differs with some species only containing a ‘short operon’, encoding core enzymes while other species contain a ‘long operon’ which in addition encodes structural genes for bacterial microcompartments. All taxa containing a form of the *eut* operon conserve *eutB* and *eutC,* which together comprise the two subunits of the ethanolamine ammonia lyase enzyme, suggesting that these genes formed the earliest version of the operon (139).

E. coli and *S.* Typhimurium, encode a 17-gene *eut* operon (5)(Fig 1.4). In addition to the enzymes required for ethanolamine metabolism, the operon encodes regulatory proteins, structural proteins that form a bacterial microcompartment (BMC) and substrate transport proteins (5). This form of the *eut* operon is under the control of the regulatory protein EutR. Studies in *S*. Typhimurium have found that all of the *eut* genes are under the control of one upstream promotor P1, which is activated by the binding of EutR with the cofactors ethanolamine and adenosyl cobalamin (AdoCbl) (7, 13, 140). *eutR* is located at the distal end of the *eut* operon and is preceded by the low-level constitutive promotor P2 (13, 141). The location of *eutR* in the operon creates a positive feedback loop increasing the amount of *eutR* (141). Biochemical studies have found that EutR binds to P1 in the absence of ethanolamine and AdoCbl, however it is only with these co-factors that the operon is expressed (7). It has been found when EutR is present in high levels, that the operon can be activated in the presence of only one co-factor (141). In addition to EutR the ethanolamine ammonia lysase requires AdoCbl for activity (see below), therefore autoregulation of the *eut* operon EutR to effectively compete with the ethanolamine ammonia lysase for AdoCbl and maintain expression of the operon (140).

Table1.2 Function of genes in the ethanolamine utilisation operon

Gene	Function	
eutR	Transcriptional Regulator	(141)
eutB	Ethanolamine ammonia lyase large subunit	(139)
eutC	Ethanolamine ammonia lyase small subunit	(139)
eutE	Aldehyde oxidoreductase	(2)
eutD	Phosphotransacetylase	(5)
eutG	Alcohol dehydrogenase	(2)
eutJ	Putative chaperone protein	(5)
eutT	Corrinoid cobalamin adenosyltransferase	(5)
eutH	Transport protein	(2)
eutA	Reactivating factor	(5)
eutQ	Ethanolamine utilisation protein	(5)
eutP	Ethanolamine utilisation protein	(5)
eutM	BMC shell protein	(5)
eutN	BMC shell protein	(5)
eutK	BMC shell protein	(5)
eutL	BMC shell protein	(5)
eutS	BMC shell protein	(5)

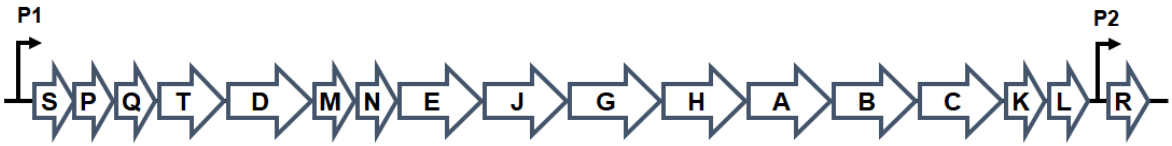

Figure 1.4 Organisation of *eut* operon in *E. coli.* 15Kb operon (not to scale).

1.5.2 Metabolism

Ethanolamine is metabolised in a two-step enzymatic reaction to produce ammonia, acetyl coenzyme A (Co-A) and acetate (13, 142, 143) (Fig 1.5). Ethanolamine is hydrolysed by the ethanolamine ammonia lyase enzyme (EAL) encoded by *eutB* and *eutC* to produce ammonia and acetaldehyde (144). This reaction is dependent on the cofactor AdoCbl (143) which is produced from the adenosylation of cobalamin (B_{12}) by EutT, a cobalamin adenosyl transferase (145). The breakdown of ethanolamine by the EAL irreversibly cleaves the C-Co bond in the co-factor AdoCbl inactivating the enzyme. EutA is a reactivating factor which removes the damaged co-factor from the enzyme allowing a new AdoCbl molecule to bind (146).

Acetaldehyde is converted to acetyl-CoA by the acetaldehyde dehydrogenase, EutE (5, 13). Acetyl-CoA can be used in a number of metabolic reactions including the TCA cycle, the glyoxylate cycle or lipid biosynthesis. Some Acetyl-CoA is converted by EutD into acetyl-phosphate before going on to form acetate via the acetate kinase enzyme (147, 148). There is some dispute in the necessity of EutD in the utilisation of ethanolamine as a carbon source (15, 148). It is agreed that EutD is needed to recycle Co-A and generate acetate which can be recaptured when bacteria required energy. Penrod and Roth however attribute the necessity of EutD, to prevent build-up of acetyl-coA and acetaldehyde (15), while Starai et al. believe that the conversion of acetaldehyde to ethanol by the action of EutG can prevent toxic build-up of acetyl-coA and acetaldehyde (148).

EutG, an alcohol dehydrogenase, converts acetaldehyde to ethanol. Stojiljkovic et al. have demonstrated that EutG is needed by most bacteria to utilise ethanolamine as a carbon source and in some cases as a nitrogen source (2). As mentioned above it has been suggested that EutG is used as a mechanism to prevent the toxic build-up of acetaldehyde (2, 133). Additionally, EutG can convert acetaldehyde to ethanol to maintain a redox balance by recycling NADH to NAD^+. However as this can also be achieved through respiration it is not assumed to be an essential role of EutG in most conditions (5).

Other accessory proteins that are involved with ethanolamine metabolism include EutH, a transporter protein that translocates ethanolamine across the bacterial membrane in acidic pH (149). The function of proteins encoded by *eutJ*, *eutP* and *eutQ* are less clear. Mutational studies have found that EutJ is needed to utilise ethanolamine as a carbon source but is dispensable for utilisation as a nitrogen source. It has been postulated by Stojiljkovic et al. that EutJ is a chaperone for EutE and EutG (2). In *S.* Typhimurium EutP and EutQ have recently been shown to have acetate kinase activity, which is required for the growth of *S.* Typhimurium in anaerobic conditions (150).

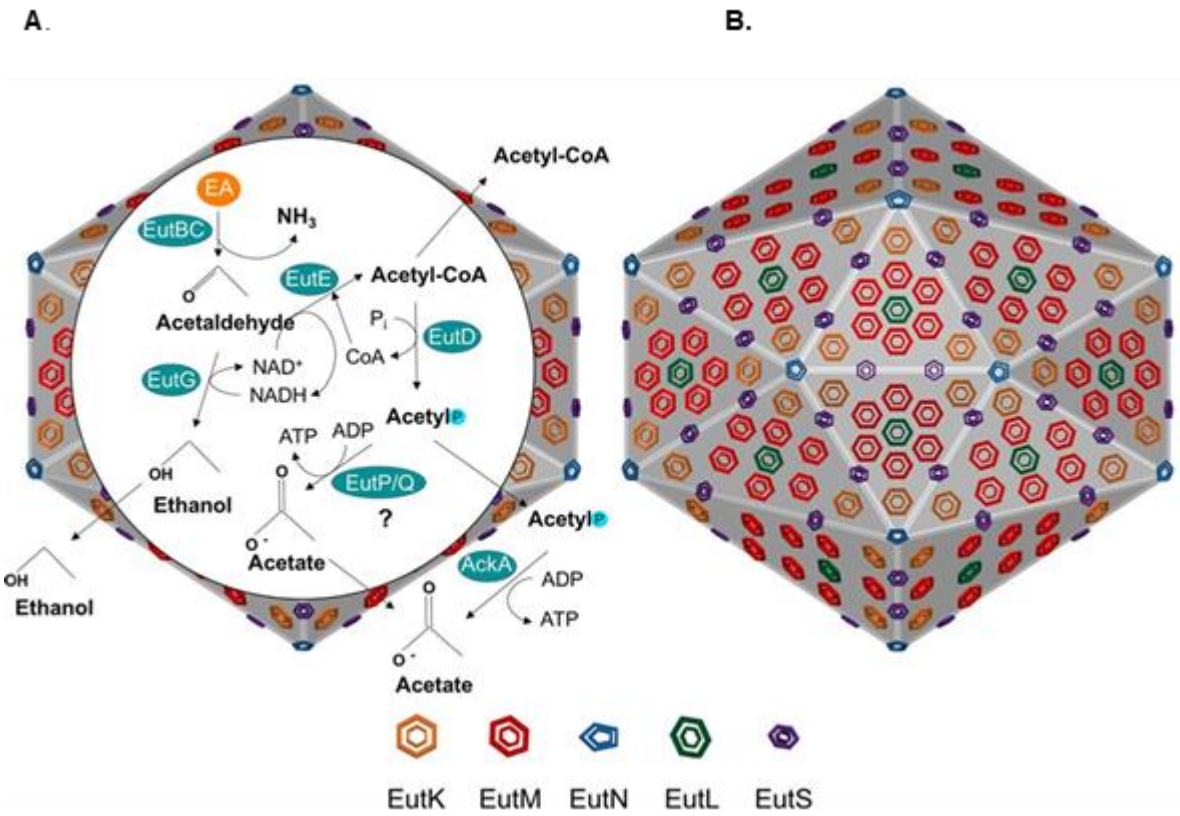

Figure 1.5 Schematic representation of the Eut metabolosome or bacterial microcompartment A. metabolism of ethanolamine within the microcompartment **B.** arrangement of shell protein in the *eut* bacterial microcompartment. (151)

1.5.3 Bacterial microcompartments

Ethanolamine metabolism in *E. coli* and other *Enterobacteriaceae* occurs within proteinaceous organelle-like structures called bacterial microcompartments (BMC) in the cytoplasm (5). These structures are around 100-200nm in diameter and form distinct polygonal shapes (152). They were first observed by Drews and Niklowitz in the 1950s in cyanobacteria using electron microscopy (153). Twenty years after BMCs were first identified in cyanobacteria it was found these proteinaceous structures were filled with RuBisCO and play an important role in carbon fixation, and were then known as carboxysomes (154). Since their initial discovery, homologues of carboxysome structural proteins have been identified in diverse operons in bacteria, and at least 23 different type of BMCs are known to facilitate anabolic reactions (e.g. carboxysomes) and different catabolic processes (metabolosomes) (155). These include catabolism of 1-2 propanediol (*pdu* operon) and ethanolamine (*eut* operon) (2, 154, 156, 157). Unlike carboxysomes, metabolosomes are not constitutively expressed and are only assembled in the presence of their specific substrate (13, 156).

The basic structure of BMC is conserved across all types of BMC where a thin enclosing shell is composed of small protein subunits. Protein crystal structures have allowed the classification of the protein subunits belong to three categories of shell proteins first identified in carboxysomes in 1994 (158). Subsequently they have been identified in the genome of many bacteria such as in the *pdu* operon and *eut* operon of *Salmonella* sp and the *eut* operon of *E. coli* (5, 138, 156). BMC shell proteins are on average 90 amino acids in length and mainly form cyclic hexamers which assemble together to form the basic structure of the BMC (157). The three types of BMC shell proteins that have been identified and are essential for functional shell assembly are: BMC-H, which are the most numerous, contain one copy of the Pfam domain PF00936 and form cyclical hexamers; BMC-T which contains two copies of PF00936 (tandem domain) and form trimers (pseudohexamers); and a BMC-P, the least abundant, which contains the domain PF03319 and form cyclic pentamers (159, 160). BMC-H and BMC-T

form molecular sheets through antiparallel association of lysine residues conserved across all PF00936 domains. BMC can form in the absence of BMC-P which have been hypothesised to close the BMC at the vertices of a polygonal structure, however these structures are presumed to be highly porous (161). BMC-P pentamer proteins, also known as BMC vertex proteins (BVP), are positioned at the vertices of the BMC and guide the formation of the typical icosahedral configuration of carboxysomes. Electron microscopy has found that *pdu* BMC form polyhedral shapes *in vivo* but these are not obviously icosahedral. A small recombinant very regular microcompartment shell has been completely crystallised and the interrelationships of the different BMC proteins are precisely known for this structure (162). Individually cloned BMC-H and BMC-T proteins have the ability to form long tube like structures (163). Less is known about the structure of the *eut* microcompartment, however they are assumed to form polyhedral shapes similar to the *pdu* BMC as the operon also encodes a BMC-P pentamer protein (5). Identification of five BMC protein resembling carboxymsome shell proteins were identified in the *eut* operon of *S*. Typhimurium (5). These are, EutS, -M, -N, -L and –K. EutN forms a pentameric structure with other the BMC proteins in the *eut* MCP. Despite being identified genetically there are few images of *eut* BMC particularly in *E. coli* (164, 165)

While the presence of the BMC and reactions that occur within BMCs have been identified, the role of the protein shell is less clear. In metabolosomes such as the *pdu* BMC and *eut* BMC, it has been postulated the structure of the BMC protects the bacteria from the toxic aldehyde intermediates produced in the metabolism of 1, 2-propendiol and ethanolamine (2, 166). By enclosing them in a protein shell, it drives the production of non-toxic compounds through the action of downstream enzymes such as aldehyde dehydrogenase *eutE* and alcohol dehydrogenase *eutG* in the *eut* BMC (14). An alternate hypothesis for the function of BMC implies that the BMC functions to prevent the loss of these volatile aldehyde intermediates from the cell (15). By retaining the aldehyde intermediates, metabolism can be driven forward to produce acetyl-CoA or produce acetate which can be recaptured later. When the formation of the *eut* BMC is disrupted in *S.* Typhimurium,

ethanolamine cannot be utilised as a carbon source, and high excretion of acetaldehyde is detected (15).

1.5.4 Ethanolamine utilisation and pathogenicity

The *eut* operon is widely distributed in bacterial species with many of them residing in the mammalian gastrointestinal tract (138). These include the pathogenic and commensal bacteria in the genera *Listeria, Salmonella*, and *Clostridium*, pathogenic and commensal strains of *Escherichia coli* and the commensal strains of the genus *Enterococcus* (138). Genome analysis and literature mining however has associated the metabolism of ethanolamine with gastroenteritis (138, 167). This has been supported by enteric colonisation studies detecting expression of the *eut* operon in animal models (168, 169).

As ethanolamine can be broken down to be used as a source of nitrogen or carbon, it is hypothesised that ethanolamine provides *eut*-operon containing bacteria with a nutritional advantage. Bertin et al. measured 2.2mM ethanolamine in the bovine GI tract and found that EHEC strain O157:H7, a zoonotic pathogen which has been associated with large food poisoning outbreaks, utilises ethanolamine as a nitrogen source. This provided a competitive advantage over commensal bacteria in bovine intestinal content *in vitro* (3). Mutational studies have found that *Listeria monocytogenes* deficient in key enzymes in the metabolism of ethanolamine have reduced colonisation of host models (168, 170). Additionally, *S.* Typhimurium can utilise ethanolamine to provide a colonisation advantage in the gut during acute infection. This however is dependent on the presence of the final electron acceptor tetrathionate that is produced during inflammation in the gut to allow ethanolamine to be respired (4, 171, 172). Surprisingly, in the *Clostridium difficile* hamster model, the ability to metabolise ethanolamine does not enhance colonisation of the gut, but provides a protective role for the host, delaying the progression of disease, compared to mutants in *eutA* (173). While ethanolamine has been predicted to be utilised by pathogens providing them with a source of ethanolamine, a recent study has found that commensal *E. coli* can also utilise ethanolamine and that metabolising ethanolamine provides the commensals with a competitive advantage over

pathogenic *E. coli* O157:H7(174). However this competitive advantage was seen in minimal media, while O157:H7 held a competitive advantage over commensals when grown in bovine intestinal rumen, therefore further investigation in complex media would be needed (3).

There is evidence to suggest that ethanolamine has a role in pathogenesis beyond metabolism. In a study in *S.* Typhimurium, there was a colonisation defect in *eutB* mutants in the murine infection model, however this deficiency was more severe in *eutR* mutants and reduced the progression of the disease in this model (16). *S.* Typhimurium is a facultative intracellular pathogen that invades macrophage as part of its colonisation. The ability to survive within macrophages depends on the expression of type three secretion systems (T3SS) which are encoded on Pathogenicity Island- 2 (SPI-2)(175). Anderson et al. has found that EutR regulates the expression of SPI-2 by directly binding to the SPI-2 regulator *ssrB* (16). Like *S*. Typhimurium, the *eut* operon acts as a signalling molecule in EHEC. In EHEC, ethanolamine has been implicated in the expression of the LEE operon, which is responsible for the attaching and effacing lesions in the colon characteristic of EHEC infection (7). Ethanolamine and B_{12} dependent transcription of *eutR* activates the LEE operon by binding directly to the *ler* regulator (7). Additionally, ethanolamine activates the expression of *qse* (sensor kinase), *stx2A* (shiga toxin) and multiple fimbriae operons (6, 8). The signalling phenotype observed here can occur in the presence of micromolar concentration of ethanolamine that do not activate the *eut* operon. It has therefore been proposed by Kendall et al. that there is a secondary sensor activated in response to micromolar concentrations of ethanolamine (6).

More recently, the ethanolamine metabolism has been identified in UTIs. Human metabolome studies have measured ethanolamine in the urine of small numbers of healthy volunteers at concentration between 0.38 and 0.47mM (47). RNA-seq analysis has detected expression of the *eut* operon *in vivo* in urine from patients with UTI (17, 46). One study found that the *eut* operon is upregulated *in vivo* compared to *in vitro* growth in sterile urine, suggesting host factors influence the upregulation of the operon (17). In the same study wild type UPEC had a colonisation advantage over their *eut* mutant in a mouse UTI infection model. More recently the expression of the

eut operon has been shown to assist UPEC by subverting the innate immune response in the bladder in a mouse models(10). *eut* mutants had a colonisation reduction in wild type UTI mouse model, while there was no difference in colonisation in immunocompromised mice, however the mechanism unknown. This new research suggests that the *eut* operon promotes fitness of UPEC during UTIs.

1.6 Objectives of this Study

The overall objective of this work is to investigate the role of ethanolamine utilisation in urinary tract infection. While there is evidence to suggest that ethanolamine contributes to pathogenesis in the gut, a link between ethanolamine utilisation and urinary tract infections has only begun to be investigated. It is hypothesised that ethanolamine utilisation by UPEC enhances pathogenicity by providing a competitive growth advantage in the nutritionally limited environment of the urinary tract, and that ethanolamine sensing regulates key virulence factors in UTI. This thesis will address this hypothesis by:

1. Characterising UPEC in infected urine to assess whether they display evidence of *eut* operon induction or biochemical evidence of ethanolamine utilisation.
2. Investigating the ability of clinical UPEC isolates to metabolise ethanolamine in an *in vitro* urine model.
3. Investigating whether ethanolamine regulates virulence factors in UPEC as has been seen in EHECs.

Chapter 2 Materials and Methods

2.1 Human Urine Collection and Clinical Sample Culture

Human urines were selected from samples sent for culture at the Cork University Hospital (CUH), Department of Microbiology, in 7 collections over a 2-year period. Urines were collected on the same day as arrival at CUH microbiology laboratory and selected for raised white count and bacteria as determined by routine microscopy analysis. Clear urines with no visible white cells were collected as controls. The protocol was approved by the Clinical Research Ethics Committee of the Cork Teaching Hospitals ref ECM 4 (c) 12/08/14.

Urines were transported to University College Cork (UCC) before further analysis. On arrival at UCC 200µl of urine were centrifuged by cytospin onto a microscope slide. The cells were then fixed and stained using Shandon Kwik-Diff stain following manufacturer instructions (Thermofisher). Cells were centrifuged out of urine by differential centrifugation. First urines were centrifuged at 800xg for 10mins, before the supernatant underwent a second centrifugation at 4000xg for 10mins to harvest bacteria cells. The cell pellets were resuspended in RNA Lysis buffer (Zymo Research) and stored at -80°C until RNA extraction. The resulting urine supernatant was filtered at 0.2µm to remove any remaining bacteria and stored at -80°C until use.

Bacteria were isolated from urine by CUH diagnostic laboratory staff using routine culture on CLED media. Pure colonies cultured on Columbia blood agar were identified by MALDI-TOF using a Microflex LT mass spectrometer (Bruker Daltonik) and the MALDI Biotyper software package (version 3.0). Antimicrobial sensitivity was determined by the VITEK® 2.0 system (Biomérieux) using EUCAST breakpoints. Bacterial strains were transported to UCC on agar slopes and stored at -80°C using cryobeads (FisherScientific).

2.2 Human Cytokine detection

Filtered urine collected from CUH were analysed for cytokines quantification using Meso Scale Discovery (MSD) V-PLEX proinflammatory panel I and Cytokine Panel II (MSD, Rockville, MD) enzyme-linked immunosorbent assays (ELISAs). These assays were to quantify the following cytokines:

interferon γ (IFN-γ), interleukin (IL) 10, IL-13, IL-1β, IL-4, IL6, IL-8, IL-5, IL17A and tumour necrosis factor-α (TNF-α). Assays were performed following manufacturer's instructions and measured using MESO QuickPlex SQ120. Calibrator's samples were run in duplicate in parallel to the urines and used to form a standard curve. The concentration of cytokines in the urine were extrapolated from the standard curve. Values which fell below the limits of detection were excluded from statistical analysis.

2.3 Genome Sequencing

DNA was extracted from UPEC isolated from infected urine. DNA was extracted using DNeasy Blood and Tissue Kit (Qiagen) using manufacturer's instructions. RNA was removed from the samples by incubation of sample with 20µl RNaseA treatment for 2mins at room temperature (Sigma-Aldrich). Sequencing of the DNA was performed by MicrobesNG (Birmingham, UK) as follows. DNA libraries were prepared using Nextera XT Library Prep Kit (Illumina, San Diego, USA) following the manufacturer's protocol. The following modification were made: DNA quantity was increase from 1ng to 2 ng and PCR elongation time was increase from 30s to 1 min. The library preparation was carried out on a Hamilton Microlab STAR automated liquid handling system. Prepared libraries were sequenced on the Illumina HiSeq using a 250bp paired end protocol.

2.4 Bioinformatics

Sequenced reads from UPEC DNA were further analysed by MicrobeNG (Birmingham, UK). The reads were trimmed using Trimmomatic 0.30 with a sliding window quality cut off of Q15 (176), were assembled using SPAdes version 3.7 (177), and contigs were annotated using Prokka 1.11 (178).

Bioinformatics analysis on assembled reads was carried out with the help of Professor Michael B. Prentice. Phylogenetic trees were generated from contig sequences with Parsnp (Harvest tool suite (179)) and edited with interactive tree of life(180). Parsnp produces a core genome alignment and identifies SNPs for tree generation by FastTrees (181). Alignment with 32 reference genomes known to be representative of six *E. coli* phylogroups was used for phylogroup assignment (182). Gene presence in genomes was taken as >75% identity in BLASTN search over the full reference gene.

2.5 Bacterial Strains and Growth Conditions

A list of the bacteria used in this study can be found in Table 1. Bacteria were routinely grown aerobically in LB broth (Table 2.2), Modified minimal media (Table 2.3), and Artificial Urine Medium (Table 2.4). For solid media LB broth was supplemented with 1.5% Bacteriological Agar (Merck Millipore). Where appropriate antibiotics were added to media at the following concentrations: Ampicillin (Amp) 100µg ml^{-1}; Chloramphenicol (Cm) 20µg ml^{-1}; Kanamycin (Km) 50µg ml^{-1}. Ethanolamine hydrochloride (Sigma-Aldrich) was added at concentration specified in the text. Vitamin B_{12} (Sigma-Aldrich) was added to a final concentration of 200nM when ethanolamine hydrochloride (Sigma-Aldrich) was added to media.

Experiments were routinely set up by inoculating 5ml LB (plus antibiotic were appropriate) with 1 colony and incubated overnight at 30°C. Following incubation bacteria were washed in 1xPBS by centrifugation at 4000xg for 10mins. Growth media was then inoculated to a starting OD_{600nm} of 0.05.

Table 2.1. Strains used in this study.

Name	Description	Source
E. coli JW2430-1	F-, *Δ(araD-araB)567*, *ΔlacZ4787*(::rrnB-3), *λ*$^-$, *ΔeutR766::kan*, *rph-1*, *Δ(rhaD-rhaB)568*, *hsdR514*	KEIO Library (183)
E. coli JW2434-1	F-, *Δ(araD-araB)567*, *ΔlacZ4787*(::rrnB-3), *λ*$^-$, *ΔeutB770::kan*, *rph-1*, *Δ(rhaD-rhaB)568*, *hsdR514*	KEIO Library (183)
E. coli JW2439-1	F-, *Δ(araD-araB)567*, *ΔlacZ4787*(::rrnB-3), *λ*$^-$, *ΔeutE775::kan*, *rph-1*, *Δ(rhaD-rhaB)568*, *hsdR514*	KEIO Library (183)
UPEC U1	Clinical cystitis isolate	CUH, Ireland
UPEC U2	Clinical cystitis isolate	CUH, Ireland
UPEC U3	Clinical cystitis isolate	CUH, Ireland
UPEC U4	Clinical cystitis isolate	CUH, Ireland
UPEC U5	Clinical cystitis isolate	CUH, Ireland
UPEC U6	Clinical cystitis isolate	CUH, Ireland
UPEC U7	Clinical cystitis isolate	CUH, Ireland
UPEC U8	Clinical cystitis isolate	CUH, Ireland
UPEC U9	Clinical cystitis isolate	CUH, Ireland
UPEC U10	Clinical cystitis isolate	CUH, Ireland
UPEC U11	Clinical cystitis isolate	CUH, Ireland
UPEC U12	Clinical cystitis isolate	CUH, Ireland
UPEC U13	Clinical cystitis isolate	CUH, Ireland
UPEC U14	Clinical cystitis isolate	CUH, Ireland
UPEC U15	Clinical cystitis isolate	CUH, Ireland
UPEC U16	Clinical cystitis isolate	CUH, Ireland
UPEC U17	Clinical cystitis isolate	CUH, Ireland
UPEC U18	Clinical cystitis isolate	CUH, Ireland
UPEC U19	Clinical cystitis isolate	CUH, Ireland
UPEC U20	Clinical cystitis isolate	CUH, Ireland

UPEC U21	Clinical cystitis isolate	CUH, Ireland
UPEC U22	Clinical cystitis isolate	CUH, Ireland
UPEC U23	Clinical cystitis isolate	CUH, Ireland
UPEC U24	Clinical cystitis isolate	CUH, Ireland
UPEC U25	Clinical cystitis isolate	CUH, Ireland
UPEC U26	Clinical cystitis isolate	CUH, Ireland
UPEC U27	Clinical cystitis isolate	CUH, Ireland
UPEC U28	Clinical cystitis isolate	CUH, Ireland
UPEC U29	Clinical cystitis isolate	CUH, Ireland
UPEC U30	Clinical cystitis isolate	CUH, Ireland
UPEC U31	Clinical cystitis isolate	CUH, Ireland
UPEC U32	Clinical cystitis isolate	CUH, Ireland
UPEC U33	Clinical cystitis isolate	CUH, Ireland
UPEC U34	Clinical cystitis isolate	CUH, Ireland
UPEC U35	Clinical cystitis isolate	CUH, Ireland
UPEC U36	Clinical cystitis isolate	CUH, Ireland
UPEC U37	Clinical cystitis isolate	CUH, Ireland
UPEC U38	Clinical cystitis isolate	CUH, Ireland
UPEC U57	Clinical cystitis isolate	CUH, Ireland
UPEC U58	Clinical cystitis isolate	CUH, Ireland
UPEC U61	Clinical cystitis isolate	CUH, Ireland
UPEC U66	Clinical cystitis isolate	CUH, Ireland
UPEC U67	Clinical cystitis isolate	CUH, Ireland
UPEC U68	Clinical cystitis isolate	CUH, Ireland
UPEC U69	Clinical cystitis isolate	CUH, Ireland
UPEC U71	Clinical cystitis isolate	CUH, Ireland
UPEC U74	Clinical cystitis isolate	CUH, Ireland
UPEC U76	Clinical cystitis isolate	CUH, Ireland
UPEC U79	Clinical cystitis isolate	CUH, Ireland
U1Δe*utR*::Km	P1:JW2430-1→UPEC U1	This thesis
U1Δe*utB*::Km	P1:JW2434-1→UPEC U1	This thesis

U1Δe*utE*::Km	P1:JW2439-1→UPEC U1	This thesis
MG1655	K12: F- λ- *ilvG*- *rfb*-50 *rph*-1	Lab stock
HM605	Clinical Isolate from colonic mucosal biopsy	Dr Barry Campbell (184)

Table 2. 2 LB Broth Recipe

	Concentration
Peptone	$10gL^{-1}$
Yeast extract	$5gL^{-1}$
Sodium Chloride	$5gL^{-1}$

Table 2. 3 Modified M9 Salts Recipe (3). Media was filter sterilised (0.2µM).

	Concentration
Potassium dihydrogen phosphate	22mM
Disodium phosphate	48mM
Sodium Chloride	8.5mM
Calcium Chloride	0.6mM
Magnesium Sulphate	1mM
Thiamine (vitamin B1)	0.03mM
Trace Metals (0.1µM $ZnSO_4$; 0.045µM $FeSO_4$; 0.2µM $Na_2Se_2O_3$; 0.2µM Na_2MoO_4; 2µM $MnSO_4$; 0.1µM $CuSO_4$; 3µM $CoCl_2$; 0.1µM $NiSO_4$)	$2ml\ L^{-1}$

Table 2. 4 Artificial urine medium recipe (AUM) (185). pH was adjusted to 6.5. Media was filter sterilised (0.2µM).

	Concentration
Peptone from Casein	1g L^{-1}
Yeast extract	0.005g L^{-1}
Lactic acid	1.1mM
Citric acid	2mM
Sodium bicarbonate	25mM
Urea	170mM
Uric acid	0.4mM
Creatinine	7mM
Calcium chloride.$2H_20$	2.5mM
Sodium chloride	90mM
Iron II sulphate.$7H_2O$	0.005mM
Magnesium sulphate.$7H_2O$	2mM
Sodium sulphate. $10H_2O$	10mM
Potassium dihydrogen phosphate	7mM
Di-potassium hydrogen phosphate	7mM
Ammonium chloride	25mM

2.6 Screening for Ethanolamine utilisation

2.6.1 Automated

UPEC were screened for their ability to utilise ethanolamine as a nitrogen or carbon source in a modified minimal media previously used by Bertin et al. 2011 (3). To determine utilisation of ethanolamine as a sole nitrogen source, ethanolamine hydrochloride (concentration specified in text) (Sigma-Aldrich) and 20mM glycerol (Sigma-Aldrich) was added to modified M9 media (Table 2.3). To determine utilisation of ethanolamine as a sole carbon source, ethanolamine hydrochloride (concentration specified in text) (Sigma-Aldrich) and 20mM ammonia chloride (Sigma-Aldrich) was added to modify M9 media (Table 2.3). 96 well plates were filled with 200µl of culture grown in triplicate. The plate was incubated at 37°C using an ION Biotek plate read and OD_{600nm} readings were measured using an ION plate reader over a 36-48hour period. Growth curves were analysed by GrowthRates (Bellingham Research Institute) to determine Max_{OD} (186).

2.6.2 Manual

UPEC were grown aerobically in 35mls of Modified Minimal Media (ethanolamine as nitrogen source) or AUM at 37°C to measure growth. OD_{600nm} reading were taken ever 2-4 hours and growth was measured over 32hours. When CFU was measured culture were diluted 10-fold and spotted onto LB agar (with appropriate antibiotics). Plates were incubated at 37°C and CFU ml^{-1} was calculated. During growth samples were collected for HPLC (Section 2.9) and gene expression analysis (Section 2.10).

2.7 P1 Transduction

Knock out mutantiond in the *eut* operon were introduced into UPEC strain U1 using the generalised P1 transduction method described in (187). The method utilises P1cml bacteriophage and bacterial strains JW2430-1, JW2434-1 and JW2439-1 from the KEIO library (183) as donor strain for gene deletion.

2.7.1 Prepare the lysogen

50µl of P1cml lysate (induced from *E. coli* ZK2686) was incubated with a colony of the donor strain suspended in 50µl LB (JW2430-1, JW2434-1 or JW2439-1) and 5µl of 1M $CaCl_2$. The mixture was incubated statically at 30°C for 30mins. The entire mixture was plated onto Km and Cm LB agar to select for the lysogen and incubated at 37°C.

2.7.2 Preparing the lysate

Lysate was prepared from a lysogen colony with desired knockout genotype. 2ml of LB broth was inoculated with one lysogen colony and incubated overnight at 30°C. The next day the culture was used to inoculate 5ml of LB broth to give a starting OD_{600nm} of 0.02 and grown shaking at 30°C until OD_{600nm}=0.1-0.2. The culture was heat shocked at 42°C for 20mins shaking at 180rpm. The culture was moved to 37°C incubator until total lysis was observed. Chloroform (final concentration 2% v/v) was added to the lysate and vortexed before the mixture was centrifuged to remove cell debris. The lysate was filter sterilised using a 0.2µm filter and stored at 4°C until used.

2.7.3 Transduction

Overnight culture were prepared as described (Section 2.5) and incubated at 37°C. The next day the cells were pelleted by centrifugation at 4000xg for 10mins and suspended in 5ml Transduction Buffer (10mM $MgSO_4$, 5mM $CaCl_2$). A mixture of 100µl of U1 suspended in Transduction Buffer and either 10µl, 100µl or 200µl lysate were incubated at 37°C for 30mins. A cell free and a lysate free control were set up in parallel. After this incubation 200 µl of 1M sodium citrate was added to the mixture and incubated for a further hour

at 37°C. The cells were pelleted in 1.5ml Eppendorf tubes by centrifugation at 12,000 x g in a microcentrifuge and the supernatant was removed. The cells were then washed in 100µl LB broth with 20mM sodium citrate before suspension in 100µl LB broth with 20mM sodium citrate. The mixture was spread plated onto Km LB agar containing 20mM sodium citrate and incubated at 37°C overnight. Colonies were purified by restreaking onto Km LB agar with 20mM sodium citrate. Insertion of the Kanamycin cassette was confirmed by colony PCR (Section 2.7.4) and whole genome sequencing (MicrobesNG, Birmingham, UK) (Section 2.3).

2.7.4 Colony PCR

Colony PCR were used to confirm successful transduction of UPEC strains. Single colonies were suspended in 50µl molecular grade H_2O and 0.5µl of suspended colony was used as the DNA template in a 25µl PCR reaction. A colony of corresponding KEIO strain and a colony of wild type strains were used as positive and negative controls respectively along with H_2O. Each PCR reaction contained 5µl 5XGreen GoTaq® reaction buffer (Promega), 0.5µl 10mM dNTPs(NEB), 1 µl 20mM Primer 1, 1 µl 20mM Primer 2, 0.125µl GoTaq G2 DNA polymerase (Promega), 0.5µl DNA template and H_2O molecular grade up to 25µl. PCR conditions were as followed: 95°C for 5mins; 30 cycles of (95°C for 30s, primer specific annealing temperature for 30s, 72°C for 1mins per kb);75°C for 5mins. 5µl of the resulting PCR product were run on a 1% agarose gel to determine successful transformation. Primers used for colony PCR are listed in Table 2.5.

2.7.5 DNA gel electrophoresis

DNA electrophoresis was carried out on a 1% (w/v) agarose gel in 1x Tris-Acetate-Ethylenediaminetetraacetic acid (EDTA) buffer. Ethidium bromide (Sigma-Aldrich) was added to the gel to achieve a final concentration of 0.5mg ml^{-1}. Where loading dye (NEB) was needed it was added to a final concentration of 1X. Quick-Load purple 1kb DNA ladder (NZY Tech) was added to each gel. Gels were electrophoresed at 100V for 30mins and DNA bands were viewed under UV light.

Table 2.5 Primers used for colony PCR. Primers were designed using Primer3 and synthesised by Sigma-Aldrich.

Name	Sequence 5'-3'	Source
KD13_K1	CAGTCATAGCCGAATAGCCT	Baba et al. (183)
KD13_K2	CGGTGCCCTGAATGAACTGC	Baba et al. (183)
eutR_L	TTGTTGGCGCTGTTAACATC	This study
eutR_R	GGCGGGCTGTTCTTTGATGA	This study
eutB_L3	TACCCTTTCGCTCTCTGGCAG	This study
eutB_R3	AGTGATCGGCCAGGAAACGCA	This study
eutE_L	ATTGTCGATGAGGTGGTGTC	This study
eutE_R	TGGTTACACAGCGTTGCC	This study
eutRin_L	TCGTTCTGGTTTGGCATTCC	This study
eutRin_R	GACGGCTTCTCGGAAAACAG	This study
eutBin_L	ATGTGCTGAGCGATGAAACC	This study
eutBin_R	CCCATGATGTAGTTGCAGCC	This study
eutEin_L	ATTGCTGCCATTCGTGAAGC	This study
eutEin_R	ATGTTCTGCGGTGGTTTCCA	This study
cpz_pl65_R	CGGGCAATGTGATTGTTG	This study

2.8 Complementation of knockout mutants

The ASKA *E. coli* library is a complete set of cloned individual genes (188). The genes are cloned into the plasmid pCA24N and is under the control of the PT5- lac promotor. Introducing the plasmids into the knock out mutants allows for the expression of the deleted gene in the presence of Isopropyl β-D-1-thiogalactopyranoside (IPTG).

2.8.1 Plasmid extraction

Plasmids were extracted from the ASKA *E. coli* library of ORF clones. The plasmids were extracted from the donor cell using the GeneJet Plasmid MiniPrep kit (Thermo Scientific) following manufacturer's instructions. To confirm the plasmid extraction, 5µl of plasmid DNA was run on a 1% (w/v) agarose gel.

2.8.2 Preparing electrocompetent cells

Overnight cultures were diluted 1:500 in 100ml LB broth and incubated at 37°C until OD_{600nm} reached 0.4-0.7. Cells were pelleted by centrifuged at 4000xg for 10mins at 4°C. The supernatant was removed, and the bacterial pellet was suspended in 100ml of ice cold sterile MilliQ water. Bacteria were pelleted as above, and the pellet was suspended in 50mls ice cold sterile MilliQ water. The bacteria were pelleted as above, and cells were in suspended in 1.6ml ice cold 20% (v/v) glycerol. Bacteria were pelleted for a final time before the resulting pelleted was suspended in 150µl of ice cold 20% (v/v) glycerol. The bacterial suspensions were stored in 50µl aliquots at -80°C until required.

2.8.3 Electroporation

Each mutant was complemented by the electroporation of the strain with pCA24N and either pCA24N::*eutB*, pCA24N::*eutE* or pCA24N::*eutR*. Electrocompetent cells and plasmids were defrosted on ice and 2µl of plasmid was added to the 50µl of competent cells. The mixture was transferred to a 2mm electro cuvette and pulsed on setting Ec2 (2.5kV) of

BioRad micro-pulsar. Immediately after electroporation 950µl of pre-warmed LB was added to the cells and the culture was incubated shaking at 37°C to recover for 1-2hrs. The culture was then plated on LB plates containing appropriate antibiotics. Colony PCR confirmed the presence of the plasmid.

2.9 High Performance Liquid Chromatography

High performance liquid chromatography (HPLC) was used for the detection and measurement of metabolites in urine and bacterial media supernatant. Media was removed from cultures (2.6.2) and filter sterilised through a 0.2µm syringe top filter. Samples were frozen at -80°C until used.

2.9.1 Ethanolamine detection

Ethanolamine was measured by gradient HPLC using an Agilent 1250 Infinity HPLC system after derivatisation with o-phthaldialdehyde (OPA) using a method adapted from Sturms et al. (189). The mobile phase consisted of Buffer A [10% methanol (Sigma-Aldrich) -90% 10mM Na_3PO_4 (pH7.3) (Sigma-Aldrich)], and Buffer B [80% Methanol- 20% 10mM Na_3PO_4 (pH7.3)]. Samples were prepared using an in-loop derivatization reaction where 6µl of sample were taken up followed by 6µl 10mg/ml OPA and 3-mercaptopropionic acid in 0.4M boric acid (Agilent Technologies) and incubated at room temperature for 3 minutes. The samples were injected into a 4.6 by 100mm, 2.7µm pore Infinity Lab Poroshell HPH-C18 column (Agilent Technologies) and eluted with 5ml linear gradient from 50% Buffer B to 100% Buffer B followed by 5mls of 100% Buffer B at as constant flow rate of 1ml min^{-1}. The excitation was detected at 224nm. A standard curve was created before each sequence run. Identification of the peak and quantification was determined by comparison to retention time and standard curve.

2.9.2 Acetate and ethanol detection

Acetate and ethanol were measured by HPLC using an Agilent 1200HPLC system with a refractive index detector. 10µl of sample was injected into a REZEX 8µm 8%H, Organic Acid Column 300x7.8mM (Phenomenex, USA) and eluted with 15ml of 0.01M H_2SO_4 at a flow rate of 0.6ml min^{-1}. The column was maintained at 65°C for the duration of the experiments. Substrate identification was determined by comparison of retention time to pure compound and concentrations were quantified by comparison to known standards.

2.10 Gene expression

2.10.1 RNA extraction and DNase digestion

Bacteria cultures from experimentation in section 2.6.2 were collected from media at specific time points by centrifugation at 4000xg for 10mins at 4°C. Bacteria were suspended in 1ml RNALater (ThermoScientific) and incubate at 4°C overnight. Bacteria were pelleted from the solution by centrifugation as above, and the supernatant removed. Bacterial pellets were stored at -80°C until RNA was extracted.

RNA was extracted from bacterial pellets using the Zymo Fungal/Bacterial Mini Prep kit following manufacturer's instructions. On column DNAse was performed using Zymo DNase treatment. After extraction, if residual genomic DNA was detected by PCR of *adk*, samples were treated with TURBO DNA-free (Ambion) DNAse I treatment. The RNA was quantified using the Nanodrop 1000 spectrophotometer.

2.10.2 cDNA synthesis

cDNA was synthesised by reverse transcription carried out in nuclease free 96well plates. RNA was diluted using molecular grade H_2O (Sigma-Aldrich) to a final concentration from of 100ng μl^{-1} in a 10µl volume. The RNA was mixed with: cDNA reaction was set up 4ul 5x Reverse transcription Buffer (Roche); 3ul Random Hexamer Primer (Roche); 2ul 20mM dNTPs mix; and 1ul Reverse transcriptase/RNase Inhibitor to give a total volume of 20µl. The reaction mixture was incubated in a thermocycler in the following condition: 10mins at 25°C; 30mins 55°C; 5mins at 85°C; hold at 4°C. The cDNA was then diluted to 100µl and stored at -20°C until use.

2.10.3 Quantitative Polymerase Chain Reaction (qPCR)

The Universal Probe Library (Roche- based on Primer3) was utilised to design primers for quantitative PCR. The primers designed and used in this study are listed in Table 2.6. Amplification reactions were a mix of: 3µl of cDNA; 7µl TaqMan Probe Master Buffer (Roche); 1µl 20mM primer mix (L+R primers); 0.1µl of 10mM probe (Roche); and 0.9 µl molecular grade H_2O to a

make a final volume of 10 µl. When the probe was not available a SYBR Green master mix was used which included: 3 µl cDNA, 5 µl 2xSYBR Green I Master buffer (Roche); 1µl 20mM primer mix (L+R primers) and 1µl molecular grade H_2O to a final volume of 10 µl. All reactions were performed using a 384 well plate on the LightCycler®480 System (Roche) with Molecular grade water included as a negative control. Thermal cycling condition were as follows: 50°C for 2mins, 95°C for 10 mins followed by 45 cycles for 95°C for 10s, 60°C for 45 and 72°C for 1. Relative gene expression was calculate using the 2-ΔΔCt (190). Fold changes in mRNA of target gene was quantified relative to the geometric mean of the housekeeper genes *gyrA* and *rrsB* for bacteria gene expression.

Table 2.5 qPCR Primers used in this study. Primers synthesised by Sigma Aldrich.

Name	Sequence 5'-3'	
EC_gyrA_L	GCAGGATCGCAGTGATAGC	This study
EC_gyrA_R	GTCGTCCGATCGTCAACC	This study
EC_rrsA_pL5_L	GACGATCCCTAGCTGGTCTG	This study
EC_rrsA_pL5_R	CGTAGGAGTCTGGACCGTGT	This study
EC_eutB_pL_34_L	CGCGGAGTTCAACCGTAT	This study
EC_eutB_pL_34_R	CAGAGCCTTGTCCGGTTTC	This study
EC_eutR_pL_74_L	TGTCTATGAACATGCTTTAACGATT	This study
EC_eutR_pL_74_R	CGGATGCAGCTGATCGTA	This study
EC_eutS_pL_153_L	CACACTGGCGCATCTCAT	This study
EC_eutS_pL_153_R	CCGGGAGTTAGCGTCATAAT	This study
EC_fimH_pL_68_FL	ATTGATGCGGGTCATACCA	This study
EC_fimH_pL_68_R	ACGTTTGTTGCGCTACCC	This study
EC_fimE_pL40_L	TGACCGGACTGACGCTATATTT	This study
EC_fimE_pL40_R	ATACCGGCATCGCGAATA	This study
EC_fliC_pL28_L	CGGTAACCTGACGAAAAACC	This study
EC_fliC_pL28_R	CCGTTGAAAATACCGTCCAA	This study
EC_flhD_pL67_L	CAAGATTCCCGCGTTGAC	This study
EC_flhD_pL67_R	GCAAGCGTGTTGAGACAT	This study

2.11 Competition Assay

The Competitive Index of wild type strains compared to mutants was investigated as previously described (3). Wild type and deletion mutant cultures were prepared up by inoculating 5mls of LB broth with a single colony of bacteria and incubated overnight at 30°C. The following day the bacteria were pelleted by centrifugation at 4000xg for 10mins and washed in 1xPBS. Artificial urine media was inoculated with approximately equal concentrations of wild type and mutant bacteria to a starting OD_{600nm}=0.1. Parallel culture were set up with 0mM, 0.5mM or 10mM ethanolamine and 200nM B_{12} added. The bacterial cultures were incubated at 37°C with shaking. After 24 hours growth the OD_{600nm} was measured and bacteria were inoculated into fresh AUM with corresponding concentration of ethanolamine to give a starting OD_{600nm} of 0.05. These cultures were incubated at 37°C with shaking. At each time point co-cultures were serially diluted 10-fold and spotted onto LB and LB Km agar. Agar plates were incubated at overnight 37°C. The CFU ml^{-1} of the mutant strains was calculated from the Km selective agar and the CFU ml^{-1} of the wild type bacteria was calculated by subtracting the CFU ml^{-1} of mutant bacteria from the CFU ml^{-1} of bacteria grown on the LB agar. These values were used in the following equation to determine the competitive index at each time point:

$$CI = \frac{eut\ mutant\ CFU\ recovered/Wild\ Type\ CFU\ recovered}{eut\ mutant\ CFU\ inoculum/Wild\ type\ CFU\ inoculum}$$

A competitive index below 1 indicates that the wild type was outcompeting the mutant strain at that time point. The CI at time zero is by definition 1.

2.12 Transmission Electron Microscopy

Bacteria pellets were prepared for sectioning and imaging by transmission electron microscopy. After growth in AUM with or without 10mM ethanolamine, bacteria cells were pelleted by centrifugation for 10 mins at 4,000xg, to give a pellet no larger than 500µl in volume. The supernatant was removed, and the cells were incubated in 2ml of 2.5% glutaraldehyde (Flukka) diluted in 0.1M Sodium cacodylate pH 6.8 (CAB) (bioWORLD). After incubation overnight at 4°C, the bacteria were pelleted by centrifugation as above and the pellet was suspended in 2ml of 2.5% glutaraldehyde diluted in CAB before being sent to University of Kent, Canterbury, UK for embedding, sectioning and imaging by Dr Mingzhi Liang.

The bacteria were stained for 1 hour in 1 ml of 1% osmium tetroxide (w/v) (250µl 4% osmium tetroxide; 250 µl MiliQ H_2O; 500 µl CAB). The pellets were washing in 2ml MiliQ H_2O for 10 minutes twice before the pellets were dehydrated. Pellets were dehydrated through an ethanol (EtOH) gradient as follows: 50% EtOH (v/v) x 10mins; 70% EtOH x 10min; 90% EtOH x 10mins; 100% EtOH x 10mins three times and then the bacterial pellets were washed twice in propylene oxide for 10mins. The pellets were embedded into resuspended in 1.5% ml propylene oxide: LV resin at 1:1 for 30 min followed by incubation 2 × 1.5 h in 100% freshly made agar LV resin. The pellets were resuspended in 1ml of 100% LV resin and transferred to a conical bottom flask. The bacterial pellet was centrifuged at 900xg for 5mins and was left to incubate at 60°C for 24hours.

Bacteria were sectioned to 65nm with a diamond knife on a MT-6000-XL ultramicrotome. Sections were collected on 400 mesh copper grids and stained with 4.5% (w/v) uranyl acetate in 1% acetic acid (v/v) for 45mins and Reynolds lead citrate for 7mins at room temperature. Sections were then observed on a Jeol 1230 transmission electron microscope operated at an accelerating voltage of 80kV and imaged with a Gatan MultiScan 791 digital camera.

2.13 Haemagglutination

Haemagglutination assay were performed as previously described (38, 191, 192). 5mls of LB was inoculated with a single colony of bacteria were grown statically at 37°C overnight. The next day the bacteria were normalised to OD_{600nm}=1 and 1ml of culture was centrifuged at 8000xg for 3 mins. The pellet was suspended in 1xPBS (Sigma-Aldrich) or 4% mannose (Sigma-Aldrich) in PBS and incubated at room temperature for 10mins. The suspensions was diluted 2-fold in 96-well round bottom plates using PBS until 2^{-6} dilution with control wells of PBS and 4% mannose. Guinea Pig Erythrocytes (TCS Bioscience) were prepared by washing in PBS before making a 5% solution in PBS. Equal volume of the erythrocyte suspension was added to each well and the plates were left to incubate overnight at 4°C. Haemagglutination titre was determined by recording the maximum dilution before the formation of an erythrocyte button.

2.14 Yeast Agglutination

Bacterial culture prepared for haemagglutination assay in section 1.16 were tested for type 1 fimbriae production using yeast agglutinations. A 0.5% baker yeast *Saccharomyces cerevisiae* solution was made up and 25µl of culture was mixed with 25ul of yeast solution in a flat bottom 96 well plate. The mixture was incubated shaking for 10mins at room temperature before agglutination was determined. Agglutination was measured as + or -.

2.15 Cell Culture.

The human bladder cell carcinoma cell line HT1376 (ATCC CRL-1472) was maintained in High Glucose Dulbecco Modified Eagle Media (DMEM)(Sigma-Aldrich) supplement with 10% Foetal Bovine serum (FBS) (Gibco), 200mM L-Glutamine (Sigma-Aldrich) and 100U ampicillin, 100µg streptomycin ml^{-1} (Sigma-Aldrich). When the cells reached 90% confluency the cells were passaged using 0.25% trypsin-EDTA (Sigma-Aldrich).The cells were maintained in a cell incubator at 37°C and in 5% CO_2. All work involving epithelial cells were carried out in a Class II Laminar Flow cabinet.

2.15.1 Epithelial cell Co-culture.

Cells were seeded into 24 well-plates in DMEM supplemented with 10% Foetal Bovine Serum (Gibco) and 200mM L-Glutamine (Sigma-Aldrich) and grown until 90% confluency achieved. On the day of infection, cells in the control wells were counted using 0.4% Trypan Blue (Sigma-Aldrich) and used to determine the Multiplicity of Infection (MOI) 1:10. Overnight bacterial cultures were washed 2x in PBS and OD_{600nm} reading were used to estimate CFU (OD_{600nm} 1=$7.5x10^8$ CFU ml^{-1}). Low-glucose DMEM (Sigma-Aldrich) supplemented with 10% FSB was inoculated with bacteria to obtain a MOI of 10 and where appropriate was supplemented with 10mM Ethanolamine-Hydrochloride (Sigma-Aldrich) and 200nM B_{12}. Cells were washed with PBS before 1ml of the inoculated bacteria was added to the cells. The cells were inoculated in triplicate.

2.15.2 Bacterial invasion assay

The bacteria and epithelial cells were incubated for 4hrs before the supernatant was removed and the cells were washed 3x with PBS. The cells were then incubated for a further hour with 50µg ml^{-1} Gentamicin (Sigma-Aldrich) before cells were washed 3x in PBS and lysed in 300µl 0.1% Triton X-100. All the lysate was plated onto 3 LB plates and incubated at 37°C overnight. Colonies were counted and the total CFU of invasive bacteria was calculated.

2.15.3 Adherence assay

The bacteria and epithelial cells were incubated for 3hrs. After this time the supernatant was collected, and the cells were washed 3x in PBS. The cells were lysed in 100µl 0.1% Triton X-100 and diluted 10-fold in PBS. Dilutions were spotted (20 µl) on to the LB agar in triplicate and the plates were incubated at 37°C overnight. The following day colonies were counted and CFU ml^{-1} was calculated.

2.16 Statistical Analysis

Statistical analysis was carried out using GraphPad prism 5.03 software. Student T-test and Mann Whitney U tests (non-parametric) was carried to compare two groups. A one-way ANOVA, with Tukey post-test or Kruskal Wallis, with Dunn's multiple comparison (non-parametric) was used to compare 3 or more groups. Correlations were measured and significance was tested using Pearson rank or Spearman's Rank (non-parametric). Significance was assumed when $p \leq 0.05$.

Chapter 3 Investigation into Ethanolamine metabolism in infected patient urines

3.1 Abstract

Urinary tract infections (UTIs) are a common bacterial infection worldwide (18). The majority of UTIs are caused by *E. coli* (11). Putative virulence factors in the genome of uropathogenic *E. coli* (UPEC) has been linked to the colonisation of the urinary tract, however these are not conserved between UPEC in different studies (193). Host-mediated induction of core bacterial pathways however has been associated with colonisation in murine models (38). Transcriptome analysis has found that host induction of ethanolamine metabolism occurs in UPEC infection of humans and it confers a colonisation advantage *in vivo* in the mouse UTI model (17). Additionally, ethanolamine metabolism has been associated with bladder colonisation by subverting the innate immune system in the murine model (10).

In this study, infected urines were collected from Cork University Hospital. Bacterial isolates from urine were identified by MALDI-TOF and the genomes of UPEC isolates were sequenced. UPEC genome sequences were analysed for the presence of virulence factors. The presence of the ethanolamine utilisation operon was conserved across all strains, while putative urovirulence factors were concentrated in phylogroup B2 strains. Gene expression analysis confirmed the up regulation of the *eut* operon in infected urine, and ethanolamine was present at a mean concertation of 0.57mM. Typical breakdown products of ethanolamine metabolism were also present in urine. There was no significant correlation between cytokine expression and ethanolamine concentration detected in the urine. In conclusion, in this Chapter the presence of ethanolamine was detected in infected urine and evidence for the upregulation of the *eut* operon in *E. coli* infected urine.

3.2 Introduction

The urinary tract is a common site for bacterial infection and it is estimated that 150 million episodes occur globally per year (18). Urinary tract infections (UTIs) cause significant morbidity in women with 50% of women expected to experience at least one UTI in their life time (20). As a result, there is a significant financial burden on the healthcare system, with an estimated US$6 billion spent per year in treatment and management of UTIs worldwide (1).

E. coli are responsible for the majority of UTI, accounting for approximately 75% of all UTIs diagnosed, and over 80% of uncomplicated UTIs (11). *E. coli* that cause UTIs generally reside in the gut harmlessly, however they can migrate to other environments such as the urinary tract and the blood-stream, where they cause infection (193). *E. coli* that cause infection outside the intestines are known as extra-intestinal pathogenic *E. coli* (ExPECs), with uropathogenic *E. coli* (UPEC) being a specific term for *E. coli* that cause UTI (193).

UPEC cause uncomplicated UTIs by migrating from the gut to contaminate the periurethral area (194). This is followed by colonisation of the urethra and ascend into the bladder, via the urethra, where UPEC utilise adaptive mechanisms, or virulence factors to cause infection. The UPEC can ascend to the upper urinary tract and the kidney causing localised damage and in a small number of cases can enter the blood stream to cause bacteraemia (11).

The genome of *E. coli* is highly variable with the size ranging from 4.3Mbp to 5.3Mbp (195). The wide variation in *E. coli* genome size reflect presence of pathogenicity factors, with laboratory adapted K-12 *E. coli* having on average smaller genomes than pathogenic *E. coli* (30). ExPECs generally have the largest genomes, such as the prototypical UPEC CFT073 which has one of the largest *E. coli* genomes sequenced to date with 8-11% more open reading frames than most other *E. coli* strains (31). The large size of these genomes is due to the presence of multiple putative pathogenic genes and Pathogenicity Island (26). However, unlike other *E. coli* pathotypes, ExPECs lack a set of conserved genes related to pathogenesis (38). *E. coli* are

classified into phylogenetic groups (A, B1, B2,C ,D1, D2, E) based on genetic similarity and different *E. coli* pathotypes have been found to cluster into similar phylogroups (196). ExPECs typically belong to B2 and the majority of UTIs in USA and Europe are caused by UPEC in group B2 (197, 198). Other phylogenetic groups, A, B1, D2 account for between 25 and 50% of all cystitis strains (199). All commonly studies UPEC strains such as CFT073 and UTI89 are B2 strains, while UPEC in other phylogroups haven't been studied in detail (86).

A recent study has shown that B2 strains encode more putative urovirulence factors (PUFs), than other phylogenetic groups, regardless of pathotype (38). These PUFs include adhesins, toxins, iron accumulation system and invasins (193). Adhesins, such as type 1 fimbriae are crucial for initial colonisation of the urinary tract(91). Type 1 fimbriae however are conserved across all *E. coli* and are associated with the successful colonisation of UPEC in the murine bladder (91). Interestingly, adhesion via type 1 fimbriae also mediates the invasion of bladder epithelium to form intracellular communities, where bacteria can evade the host immune system (90). In addition to traditional virulence factors, metabolic loci have been proposed to be important for the colonisation of the urinary tract. D-serine, the most abundant amino acid in urine is preferentially used by *E. coli* in the urine to provide growth enhancement (58, 200).

Despite the presence of various virulence factors in UPEC, murine model studies have failed to detect an association between the numbers of putative urovirulence genes present in individual strains and a pathogenic phenotype (38). Instead the regulation of core bacterial processes in response to environmental cues, such as the host environment, is more predictive of virulence in the murine urinary tract (38). In a separate study, the copper tolerance pathway (*cus*), and ethanolamine utilisation (*eut*) operon were upregulated in infected urine collected from patients compared to the same bacteria grown in urine *in vitro*. Mutational studies found that these host inducted pathways provided a competitive colonisation advantage in a mouse model (17).

Ethanolamine is found naturally in the body as part of the phospholipid phosphatidylethanolamine (132). Breakdown of this phospholipid from cell membranes releases ethanolamine that can be metabolised by bacteria (136). Within the gastrointestinal (GI) tract, for example the bovine intestinal tract, where there is high turnover of epithelium, ethanolamine is present at a concentration of 2.2mM and provides a competitive growth advantage for enterohaemorrhagic *E. coli* (EHEC) (3). Within the normal urinary tract epithelial turnover is 5-60 fold slower than the gut (up 200 days), and therefore in health would not provide a large source of ethanolamine (201). However, excretion of ethanolamine in urine has been reported in healthy urine (47). A characteristic of UTI is the presence of numerous inflammatory and bladder epithelial cells (BECs) in urine which could provide an alternative source of ethanolamine (202). Host recognition of bacteria in the urinary tract mediate the release of proinflammatory cytokines such as Interleukin (IL) 6 and IL-8 by the epithelium recruiting masses of neutrophils to the bladder (106, 120). Additionally, the invasion of epithelium by *E. coli* mediates epithelial sloughing (42).

In this study infected urines from Cork University Hospital (CUH), were assessed for the presence of ethanolamine, evidence of ethanolamine metabolism by invading bacteria, and a correlation between the host and inflammatory response and ethanolamine metabolism. Genomic analysis of *E. coli* isolates for phylogeny and the presence of putative virulence factors was also performed.

3.3 Results

3.3.1 *E. coli* infection account for the majority of clinically infected urine samples collected in this study.

It has previously been reported that *E. coli* accounts for approximately 75% of UTIs (1). 103 infected urines were collected and cultured with speciation of isolates at CUH Microbiology laboratory. 61 of the 103 urines collected were infected with *E. coli*, which equates to around 55% (Fig 3.1).

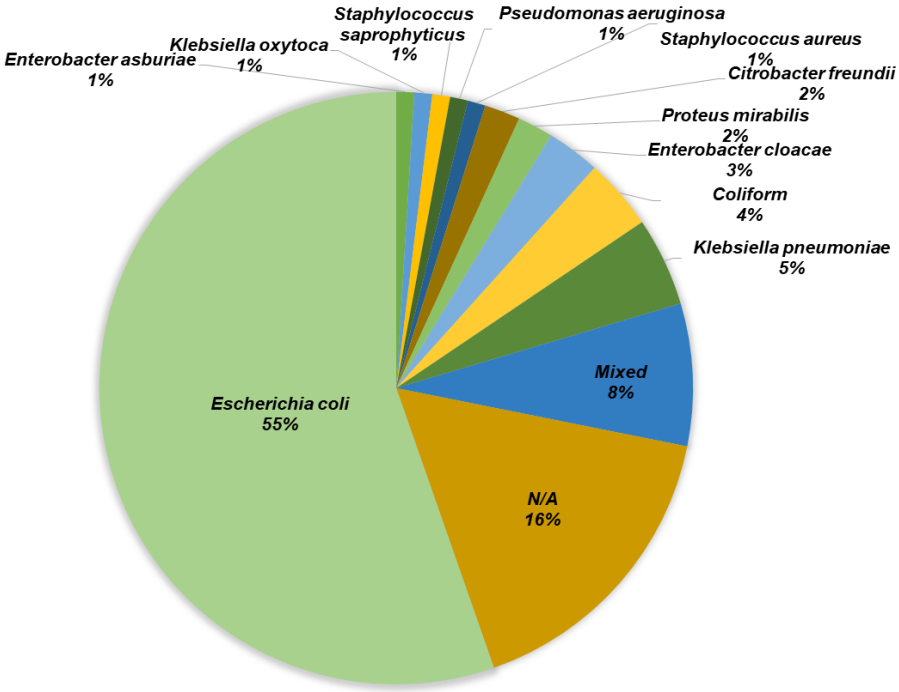

Figure 3.1 The majority of urines were infected with *E. coli*. N=103

3.3.2 Genomic Analysis of UPECs

The genomes of UPEC isolated from infected urines were sequenced by MicrobesNG using Illumina HiSeq 2500 2x250bp paired-end reads as described in Chapter 2. The 47 UPEC genomes were aligned with 32 reference *E. coli* genomes representative of six different phylogroups using parsnp (Fig 3.2)(179, 182). The sequenced UPEC occupied all 6 phylogenetic groups however the largest single group was B2 with 47% of the UPECs. This is followed by D2 with 23%, A with 15%, B1 with 9%, D1 with 4% and finally E with 2%. This distribution matches observation of other samples of UPECs (38).

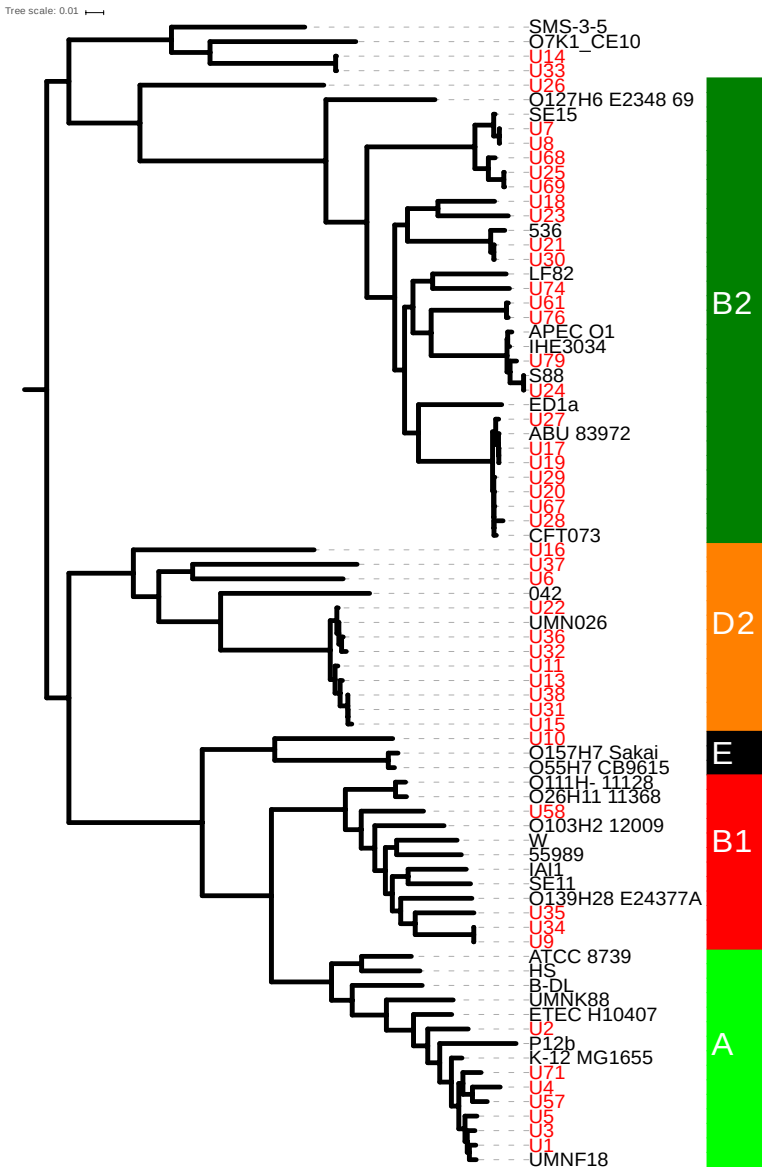

Figure 3.2 Phylogenetic analysis of uropathogenic *E. coli* strains (UPEC). Core genome alignment of 47 UPEC (red) with 32 reference strains representative of six *E. coli* phylogroups (black). Phylogenetic assignments shown in the vertical bar on the right. N=79. Professor Michael B Prentice

The genomes of the UPECs were analysed for the presence of 31 putative virulence factors (PUFs) which have previously been found to be associated with the UPECS compared to other *E. coli* strains (38). Presence of PUF was determined by BLASTN. All 31 putative virulence factors were detected in the 47 UPECs, with a range of 2 to 25 PUFs per strain. Those UPECs that fall into phylogroup B2 had significantly higher PUFs than non-B2 strains (Fig 3.3b) ($p<0.001$, Mann-Whitney U). Antibiotic resistance phenotypes were also analysed for phylogenetic relationships. The majority (59.6%) of *E. coli* strains were resistant to one or more antibiotic, however no phylogenetic relationship with number of antibiotic resistances was discernible (Fig 3.3c). Hierarchical clustering found that strains clustered based on B2/non-B2 phylogeny associated in relation to PUF presence but not antibiotic resistance genes presence (Fig 3.3a).

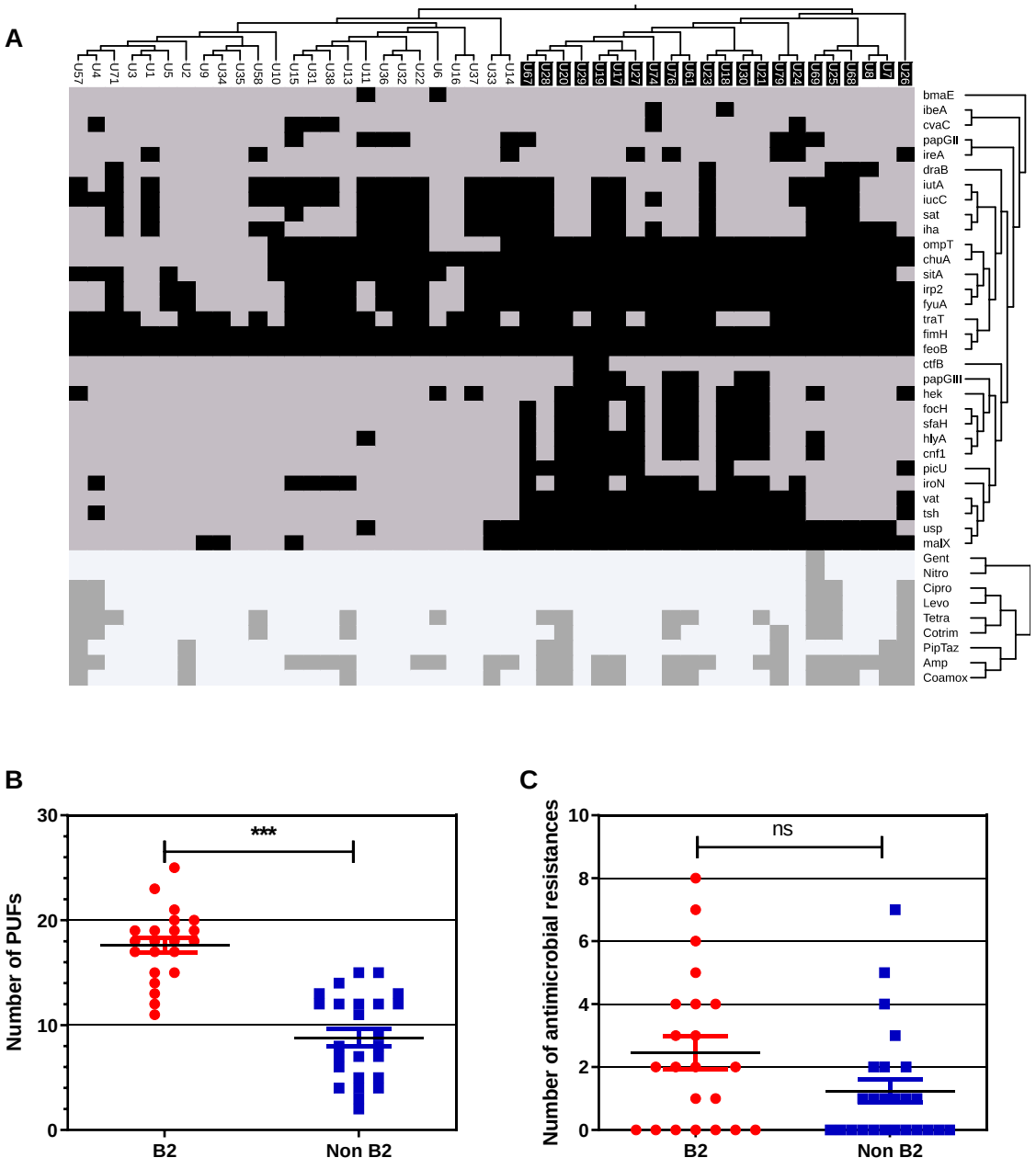

Figure 3.3 Carriage of Putative urovirulence factors (PUFs) is associated with phylogenetic group B2. A Heat map of presence of 31 previously described PUF (y axis) in UPEC. Two dimensional hierarchical clustering shows PUF co-occurrence by strain (upper y-axis dendrogram) and PUF association with phylogeny (x-axis dendrogram). UPEC highlighted in black are B2. Clade B2 strains are indicated by white names on a black background (x-axis labels). Lower diagram shows hierarchical clustering of resistance (dark grey squares) and sensitivity (pale grey squares) to nine different antimicrobials (lower y-axis dendrogram) by strain phylogeny. Abbreviations as follows: Gent, Gentamicin; Nitro, Nitrofurantoin; Cipro, Ciprofloxacin; Levo, Levofloxacin; Tetra, Tetracycline; Cotrim, Cotrimoxazole; PipTaz, Piperacillin/tazobactam; Amp, Ampicillin; Coamox , Amoxicillin/clavulanic acid. **B** Comparison of PUF scores between B2 and non-B2 UPECs. **C** Comparison of number of antibiotic resistances between B2 and non-B2 UPECs. Mann-Whitney U test *** $p<0.0001$. N=47

In addition to the putative virulence factors mentioned above, metabolism has been found to play a role in UPEC pathogenesis. D-serine metabolism has been linked to colonisation advantage in a murine model (203). The D-serine tolerance locus (*dsdCXA*) which is responsible for the breakdown of D-serine was present in 57% of the UPECs. B2 strains were more likely to possess a complete *dsdCXA* locus than non-B2 strains with 77% of B2 having a *dsdCXA* locus compared to 40% in non-B2 UPECs (Table 3.1). In contrast to the *dsd* locus, the ethanolamine utilisation operon (*eut*) operon that controls the metabolism of ethanolamine in *E. coli* was conserved across all the 47 UPEC strains. In one strain U71 the operon was interrupted by the presence the prophage insertion between *eutA* and *eutB* (Fig 3.4). This insertion site is also occupied by a prophage in the K12 strain MG1655 (204).

Table 3.1 Frequency of D-serine tolerance locus (*dsdCXA*) and *eut* operon in UPEC strains based on phylogenetic group.

		Frequency	Percentage of all UPECS
dsdCXA	A	7	100.0%
	B1	0	0.0%
	B2	17	77.3%
	D1	2	100.0%
	D2	1	9.1%
	E	0	0.0%
	All UPECs	27	57.4%
eut	A	7	100.0%
	B1	4	100.0%
	B2	22	100.0%
	D1	2	100.0%
	D2	11	100.0%
	E	1	100.0%
	All UPECs	47	100.0%

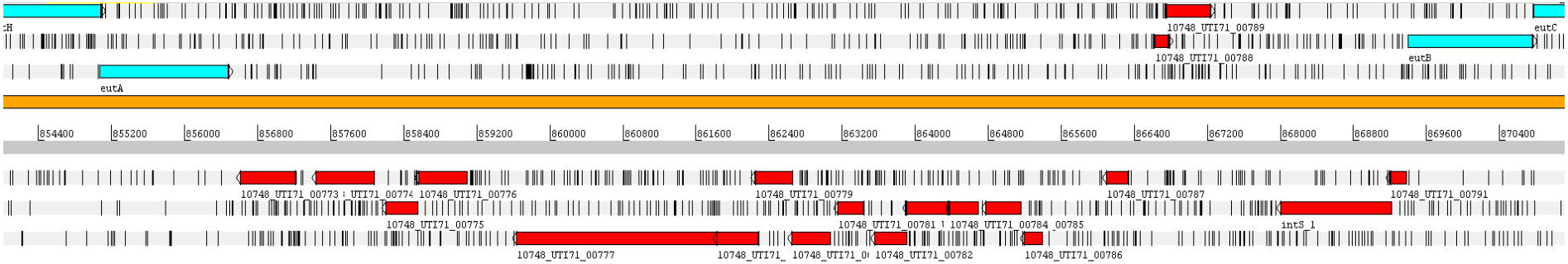

Figure 3.4 Presence of prophage between *eutA* and *eutB* in U71. Gene of the *eut* operon are in blue; gene of the prophage in red.

3.3.3 Free ethanolamine is detectable in Urine

To assess whether ethanolamine metabolism is important for bacteria colonisation and survival in the urine, collected urines were filtered and stored for detection of ethanolamine. HPLC was used to measure the concentration of ethanolamine in urine as previously described (Chapter 2) (189). The average concentration of free ethanolamine was measured in 64 of the urines collected. The average concentration of ethanolamine in infected urine was 0.548mM while the concentration on non-infected urine was 0.653mM. Comparing the two groups did not show a significant difference in the level of ethanolamine (Fig 3.5a) (Mann-Whitney U test). There was likewise no significant difference detected between UPEC and non-UPEC infected urines when the levels of ethanolamine were compared (Mann-Whitney U test) (Fig 3.5b). The mean concentration of ethanolamine in all urines was 0.567mM.

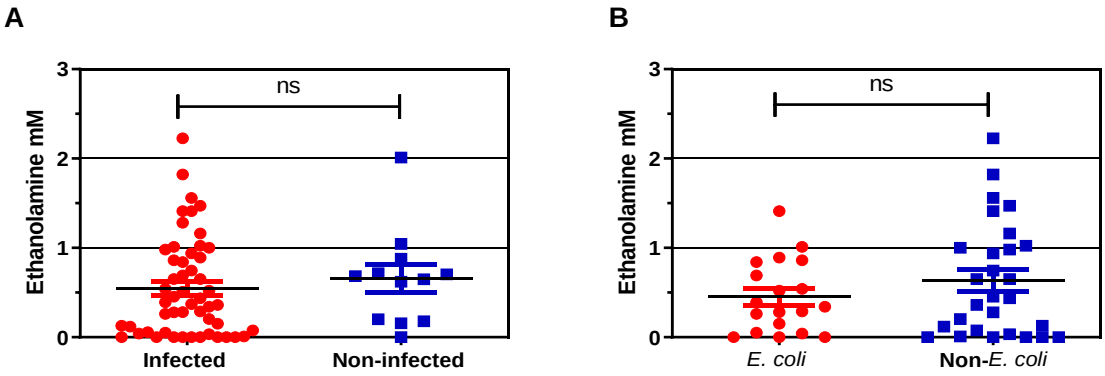

Figure 3.5 Ethanolamine concentration in urine is not associated with presence of infection. Ethanolamine concentration in urine was measured using HPLC. **A**. Concentration of ethanolamine in infected urines (n=52) vs non-infected urines (n=12). **B** Concentration of ethanolamine in *E. coli* infected urines (n=19) vs non-*E. coli* infected urines (n=28). Mann Whitney-U test.

3.3.4 Evidence for ethanolamine metabolism

As ethanolamine was detected in the urine at an average concentration of 0.57mM, UPECs were assessed for expression of the *eut* operon in urine. RNA was extracted from 24 bacteria pellets from infected urines, of which 18 were identified as *E. coli*, and 6 were mixed cultures, with one strain being *E. coli*. The expression of the *eut* operon was then measured using qRT-PCR. To determine whether ethanolamine was sensed in the urine, expression of the regulator *eutR* was measured. In 62.5% of the samples *eutR* expression was detected at an average 2.3-fold expression relative to *gyrA* (Fig 3.6a). Next, expression of *eutB* which encodes the major subunit of the ethanolamine ammonia-lyase enzyme which is responsible for the first stage of ethanolamine metabolism was measured. In 88% of the RNA samples, *eutB* was detected with an average 3.1-fold expression relative to *gyrA* (Fig. 3.6). The final gene measured for relative expression was *eutS*, which encodes a protein subunit the *eut* bacterial microcompartment, a proteinaceous structure that encloses the ethanolamine metabolic pathway. *eutS* was detected in 68% of the samples with 2.4-fold expression relative to *gyrA* (Fig 3.6).

To determine if the expression of the *eut* operon is linked to the concentration of ethanolamine in the urines, correlations between relative expression and ethanolamine concentration were measured. There were weak correlations between *eutR* ($r=0.423$) and *eutS* ($r=0.309$) expression compared to ethanolamine concentration (Fig 3.6) and these correlations were not statistically significant (Spearmans Rank). In contrast a strong positive correlation between expression of *eutB* and ethanolamine concentration was present ($r=0.815$, $p<0.001$, Spearmans Rank) (Fig 3.6). This provided evidence that infecting UPEC were actively responding to the concentration of ethanolamine in urine.

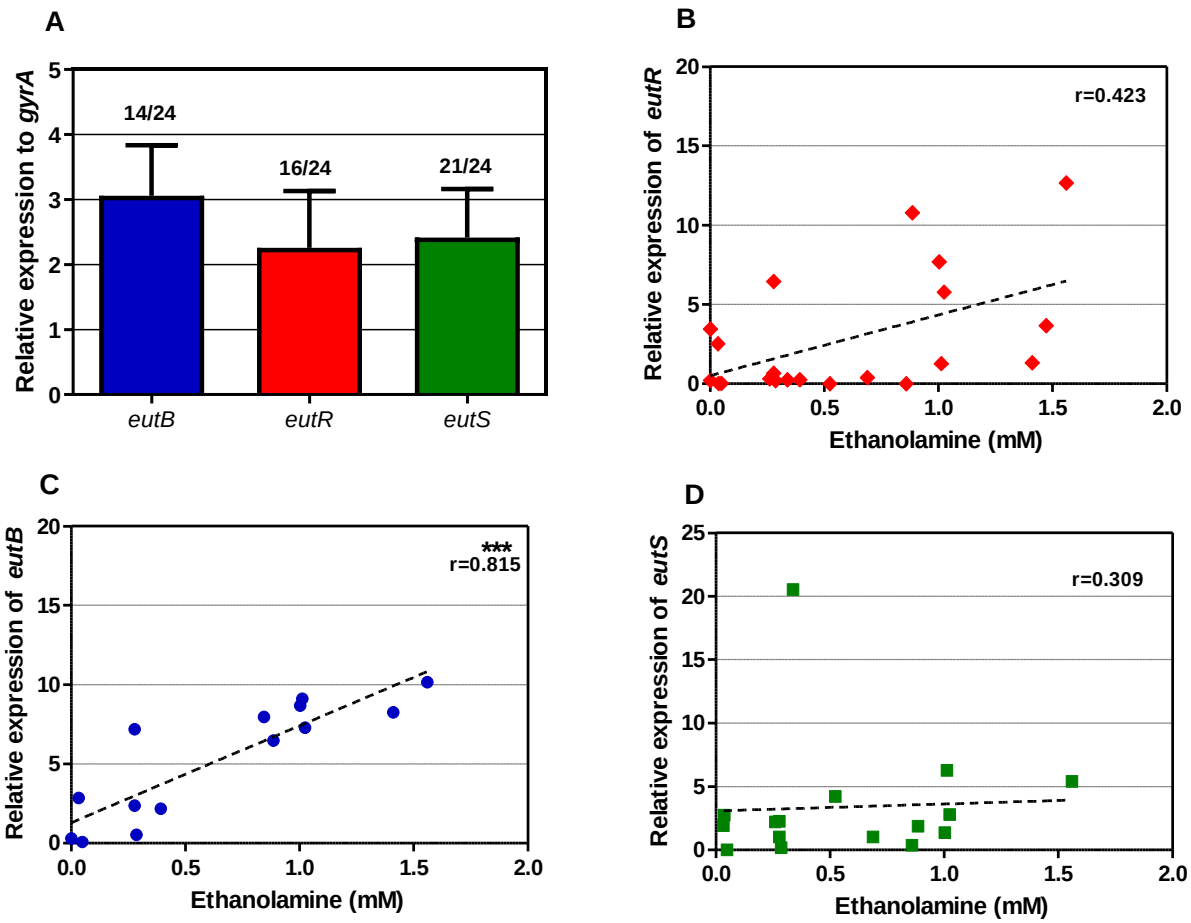

Figure 3.6 *eut* operon expression in detected in *E.coli* infected urine. A qRT-PCR of *eut* operon expression relative to *gyrA*. Proportion of *E. coli* where expression was detected **B** Correlation between relative expression of *eutR* and ethanolamine concentration in urine. **C** Correlation between relative expression of *eutB* and ethanolamine concentration in urine. **D** Correlation between relative expression of *eutS* and ethanolamine concentration in urine. *** p<0.001 n=24

Next, acetate concentration in urine was measured by HPLC. Acetate is a product of ethanolamine metabolism and the catabolism of some amino acids by bacteria (205, 206). As such, the level of acetate in urine has recently been identified as a biomarker for UTI status (207). In this study, acetate levels were first compared between infected urine (18.3mM) and non-infected urine (14.7mM), to determine if bacterial metabolism contributed to acetate excretion. There was no significant difference measured between these two groups (Mann-Whitney U) (Fig.3.7a). A comparison was made between the level of acetate measured in *E. coli* (16.6mM) and non-*E. coli* (14.7mM) infected urine, to determine whether acetate excretion was species specific. However, there was no significant difference between these two groups (Mann-Whitney U) (Fig.3.7 b).

To determine if the acetate was produced in the urine due to ethanolamine metabolism, the concentration of ethanolamine detected in urine was correlated with the concentration of acetate detected in urine. There was very weak non-significant correlation between acetate and ethanolamine concentration in all urines (r=0.168, Spearmans Rank) (Fig 3.7c). Additionally, there was very weak non-significant correlation between acetate and ethanolamine in *E. coli* infected urine (r=0.207, Spearmans Rank) (Fig 3.7 d). Finally, the correlation was measured between acetate level and expression of the *eutR* and *eutB* (Fig 3.7 e, f). There was weak, non-significant correlation between acetate and *eutR* or *eutB* (r=0.162, r=0.157, respectively, Spearmans Rank). From this evidence it is concluded that acetate levels in the urine were not related to ethanolamine metabolism.

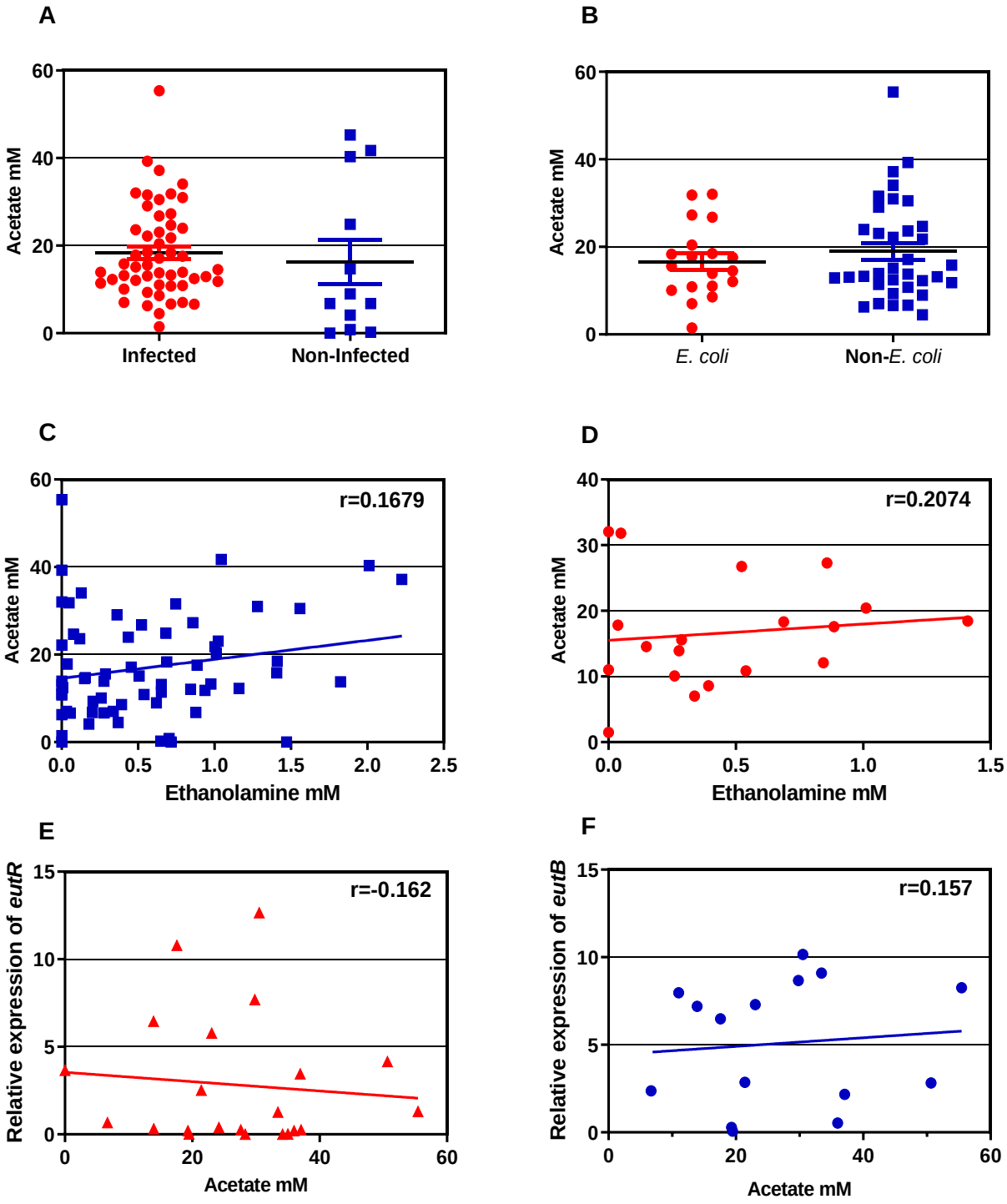

Figure. 3.7 Detection of breakdown products in infected urine. **A**. Acetate concentration of infected urines (n=52) vs non infected urines (n=12). **B** Acetate concentration of *E. coli* infected urines (n=19) vs non-*E. coli* infected urines (n=28). Mann Whitney-U test. **C** Correlation between acetate and ethanolamine in *E. coli* infected urine (n=19) **D** Correlation between acetate and ethanolamine in all collected urines (n=64). **E** The correlation between *eutR* gene expression and acetate levels. **F** The correlation between *eutB* gene expression and acetate levels. Correlation was measured by Spearman Rank.

3.3.5 Bacteria in the urine are associated with eukaryotic cells.

Cells from whole urines collected from patients with suspected UTIs were transferred onto microscope slides by Cytospin and stained with the Kwik-Diff™ staining protocol. Within the infected urines there were large numbers of eukaryotic cells, identified as epithelial cells and immune cells. Bacteria within these urine samples were strongly associated with the eukaryotic cells (Fig 3.8), with transmission electron microscopy confirming association of bacteria with eukaryotic cells. These results are coupled with the detection of *fimA* RNA in *E. coli* infected urines. FimA is a major subunit of type 1 fimbriae, which facilitated *E. coli* attachment to bladder cell epithelial (91). *fimA* RNA was detected in 56% of *E. coli* infected urines analysed by RT-PCR with an average 10-fold higher expression relative to *gyrA.*

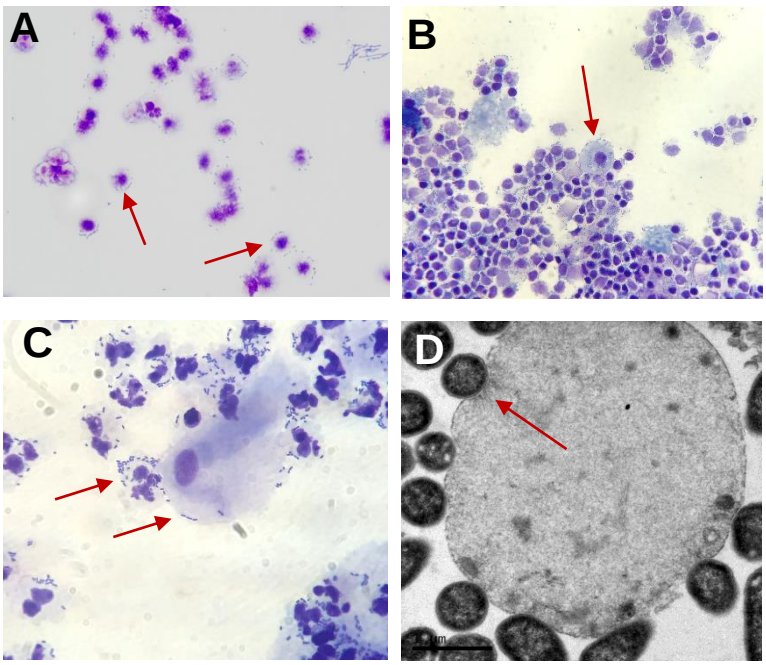

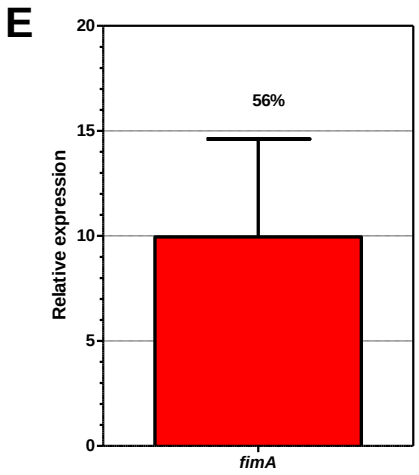

Figure 3.8 Bacteria associated with eukaryotic cells in infected urine. Whole infected urines from CUH was centrifuged onto slide and strained with QwikDiff. **A** (40x), **B** (40x) and **C** (100x). **D** Bacterial pellets were imaged under Electron microscopy (courtesy of Dr M Liang University of Kent). **E** Expression of *fimA* in bacteria RNA (Fig. 3.3) relative to *gyrA* (n=24). Percentage of *E. coli* where gene expression was measured is indicated.

3.3.6 Influx of immune cells does not correlate to ethanolamine concentration

Examining infected urine under the microscope, it is evident that there is an influx of immune and epithelial cells (Fig 3.8). As ethanolamine is a major component of the phospholipid bilayer of eukaryotic cells it can be hypothesised that there is a link between urinary tract inflammation and ethanolamine accessible for bacteria (132). The host response was investigated by measuring cytokine and proinflammatory markers by MSD ELISA. Of 10 cytokines and proinflammatory markers tested, three (IL-8, IL-1β and IL-6) were detected in more than a half of the 64 urine supernatants tested, with 81%, 81% and 62.5% positive samples respectively. There was a significant increase in IL-1β ($p=0.0048$, Mann Whitney U) and IL-8 ($p<0.001$, Mann Whitney U) in infected urines compared to non-infected urine. There was no significant difference in IL-6 expression, however the mean level in infected urine was 44.45pg ml^{-1} compared to 23.39pg ml^{-1} in control urine, therefore there was elevation of IL-6 during infection. When looking at the infected urine there was no significant difference in interleukin concentration between *E. coli* infected urine and non-*E. coli* infected urine.

To explore the idea that ethanolamine comes from the breakdown of inflammatory cells the expression of cytokines was correlated against the level of ethanolamine detected in the urine. There was no significant correlation between cytokine expression and ethanolamine concentration. Therefore, it can be concluded that ethanolamine concentration in the urine is not influenced by inflammatory cells.

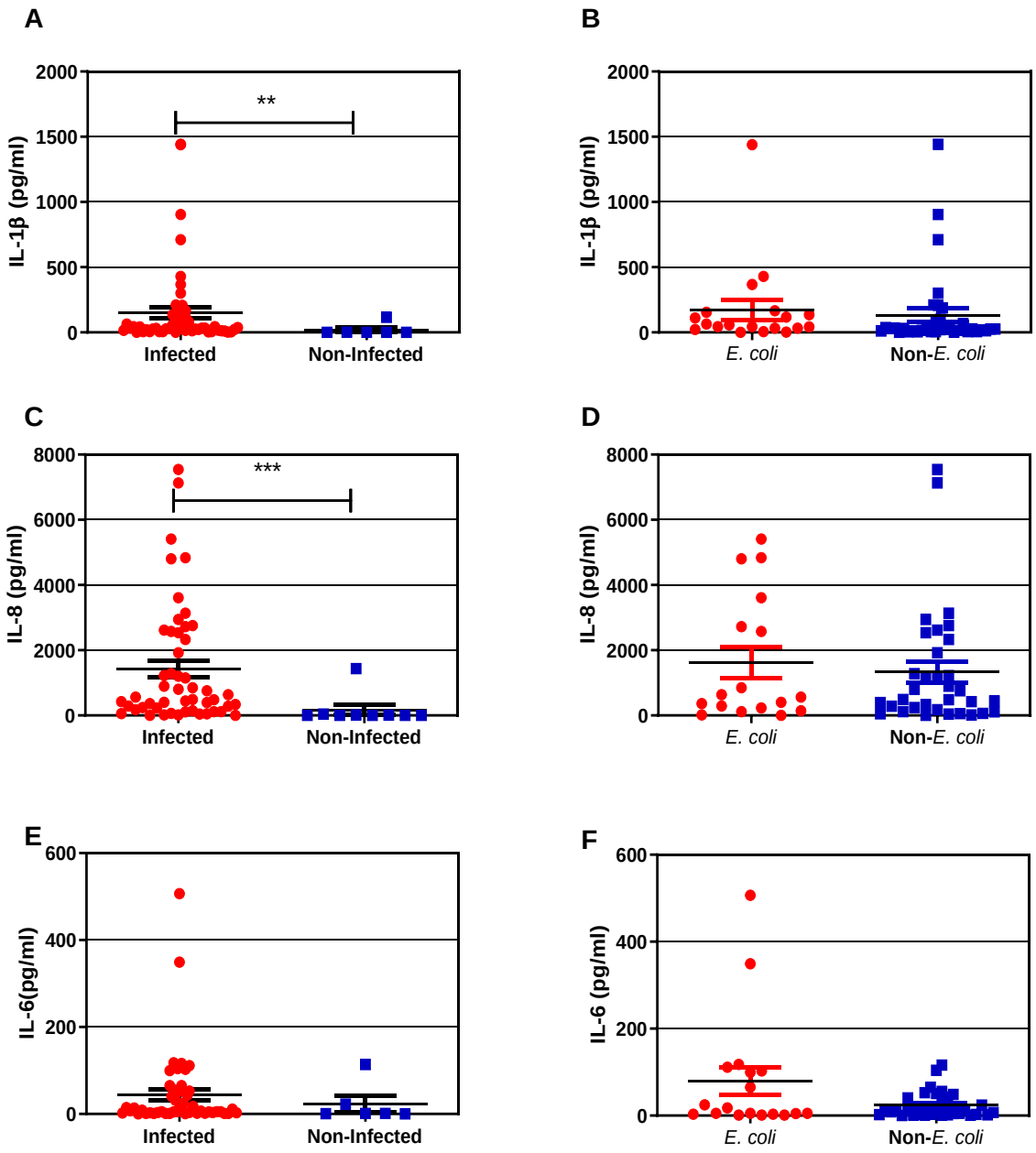

Figure 3.9 Pro-inflammatory cytokines detected in infected urine. Detectable level of: **A** IL-1β **C** IL-8 **E** IL-6 in infected urine (n=52) compared to non-infected (n=12). Detectable level of **B** IL-1β **D** IL-8 **F** IL-6 in *E. coli* infected urine (n=19) and non-*E. coli* infected urine (n=28). Compared by Mann Whitney-U ** p≤0.01 *** p<0.001

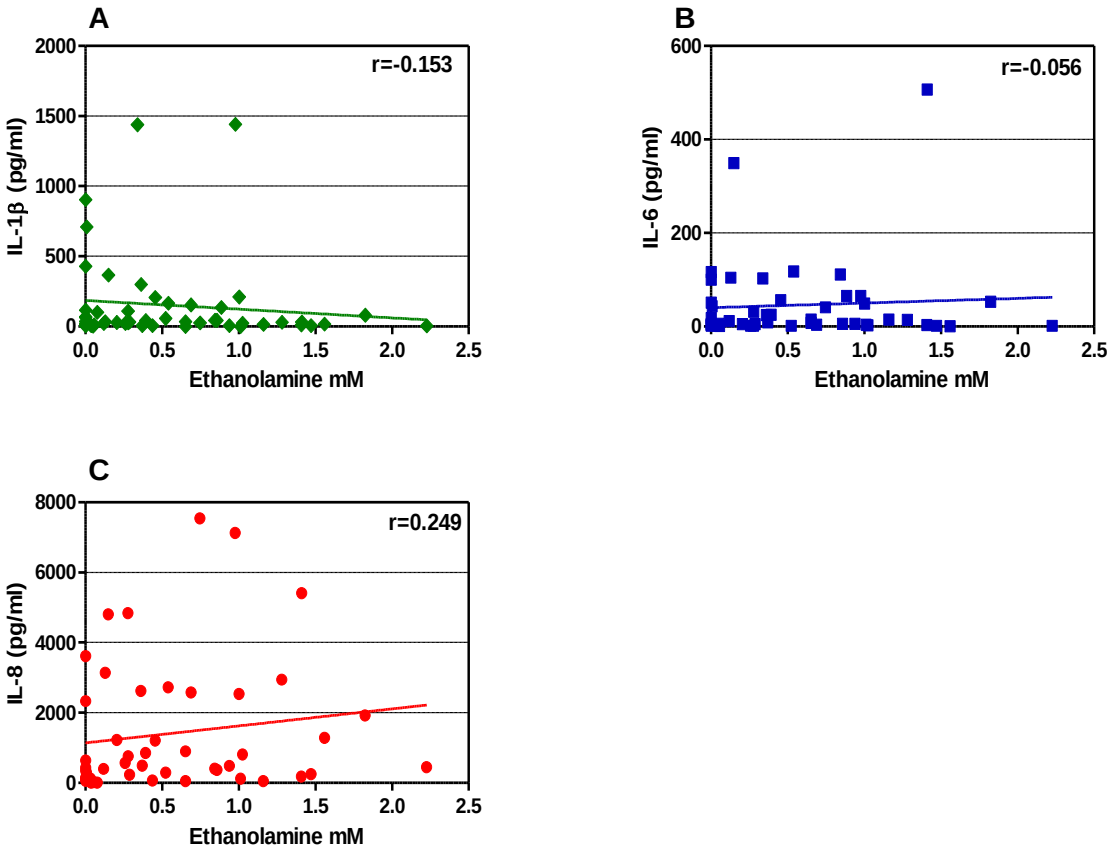

Fig 3.10 Expression of pro-inflammatory cytokines does not correlate to ethanolamine concentration. Correlation of detectable level of **A** IL-1β, **B** IL-6 and **C** IL-8 and ethanolamine in all urines (n=64). Correlation by Spearman's Rank.

3.4 Discussion

This study sought to characterise infected urines that were collected from CUH. The most prevalent bacteria isolated from infected urines was *E. coli* at 55% (Fig 3.1). However, this is lower than the published prevalence of 75% (11). The 55% stated could be a low estimation for our urines as *E. coli* identified in mixed cultures isolated from infected urines were not included in this statistic and 16% of clinically infected urines did not yield isolates, probably because specimens were anonymised and not controlled for antimicrobial therapy.

Analysing the genomes of the *E. coli* strains isolated from urine, the UPEC in this study were phylogenetically similar to previously published observations of urinary tract infection, where the majority of UPEC fall into phylogroups B2 and D2 (38). In this sample there is a lower proportion of B2 strains (46%) (Fig. 3.2) than in urosepsis and urinary tract infection studies from the USA (67%-69%) (38, 198, 208), with a similar proportion to Slovenia (50%) (209), and more than China (19%)(199).

While other pathotypes of *E. coli* have associated virulence genes, there is a lack of core virulence factors that determine pathogenicity in UPEC. 31 putative urovirulence factors (PUF) have been identified by comparison of UPEC with *E. coli* isolated from other sites (208). In this study, PUF were strongly associated with phylogroup B2 strains, (Fig. 3.2) consistent with previous findings from a set of UTI isolates from the USA (38). However the study from the USA showed that the PUF were strongly associated with phylogroup B2, rather than uropathogenic strains, with similar levels of PUF identified in B2 UPEC and B2 strains not associated with UTIs (38). Additionally it was found that PUF profile does not correlate with virulence in animal models of UTI (38). In fact, PUF may be more important to the colonisation of the gut, as B2 strains are the most prevalent *E. coli* in the GI tract (210). Similarly, it was found that the metabolic loci proposed to promote growth in urine such as *dsdCXA* were also associated with phylogroup B2 rather than UPECs in general (Fig 3.3). In contrast, the *eut* operon is not associated with phylogenetic group but conserved within all UPEC (Fig 3.3).

The *eut* operon, is a 17-gene operon that facilitates the metabolism of ethanolamine to produced ammonia, acetyl Co-A and acetate that can be utilised by the bacteria as nitrogen and energy (further detail of ethanolamine metabolism is given in Chapter 1 and Chapter 4) (5). The *eut* operon is part of the core genome of *E. coli* however in some K-12 strains of *E. coli* the prophage CPZ-55 is located within the *eut* operon in an the opposite orientation to its transcription thus preventing the metabolism of ethanolamine (Appendix 4.5, Chapter 4) (204, 211, 212). In this sample of UPECs all strains contain a complete *eut* operon however one strain, U71, has a novel prophage insertion between *eutA* and *eutB* in the same location as CPZ-55 in MG1655 and BW23115 (Fig 3.4).

In this study similar concentrations of ethanolamine were measured in infected urine (0.57mM) and non-infected urine controls (mean 0.65mM) (Fig 3.5). This is consistent with previous reports on a smaller numbers of urine from healthy controls using different methodology such as NMR (0.38mM) and LC/MS (0.47mM) rather than HPLC (47, 213). Within the bovine intestine ethanolamine was measured at 2.2mM. Metabolising ethanolamine at this concentration provided enterohaemorrhagic *E. coli* with a competitive advantage *in vitro* (3). In comparison, D-serine which is regarded as an abundant substrate for *E. coli* metabolism in human urine has been reported at a mean concentration of 0.38mM (1, 62).

There is evidence that ethanolamine in infected urine was sensed by *E. coli* with induction of the *eut* operon regulator *eutR,* and is also being metabolised, with induction of the ethanolamine deaminase component *eutB* correlated with measured ethanolamine levels in urine (Fig 3.6 b, c). Additionally, acetate, a breakdown product of ethanolamine was detected in urine (Fig 3.7). Acetate levels however were not significantly correlated to ethanolamine concentration or expression of the *eut* operon (Fig 3.7e). As acetate is also produced from the metabolism of amino acids and peptides, which are thought to be the main source of carbon for bacterial growth in urine, there are multiple potential sources for the acetate detected (49, 58). More recently acetate has being suggested as biomarker for bacteria growth

in urine (207). The acetate levels measured in this study however are considerably higher than those measured in recent publication which describe concentrations of between 0.017mM and 0.135mM detected in healthy urine, increasing to 1.15mM in infected urine (47, 207) (Fig. 3.7). In this study the level of acetate in urine is measured by HPLC while the previous studies use NMR (47, 207). Therefore, the discrepancy in acetate could be due to method sensitivity, however another detection method would be needed to confirm the acetate levels in these urines in this study.

Ethanolamine is found naturally in the body in the form of phosphatidylethanolamine (PE). PE is the most abundant phospholipid in prokaryotic cells and the second most abundant phospholipid in eukaryotic cell (132). Within the GI tract available ethanolamine is assumed to derive from the breakdown of phospholipid from the rapid turnover of the epithelium and dietary phospholipid (134). There is a constant supply of ethanolamine in urine in both heath and infection (Fig 3.5), and the source in health seem unlikely to be cell turnover in the urinary tract, because this occurs at a relatively slow rate compared to the gastrointestinal tract. During UTIs there is an influx of inflammatory cells in response to pathogen pattern receptor activation (106) (Fig 3.8). The turnover of inflammatory cells, or the shedding of epithelial cells provoked by infection could provide a source of ethanolamine (42). However, there was no correlation between expression of IL-8, IL-6 and IL-1β, which are responsible for the influx of neutrophils, and concentration of ethanolamine detected in urine (Fig 3.10). As there is similarity in ethanolamine concentration between healthy and infected urine in this cohort, it can be predicted that ethanolamine is excreted through the kidney.

There is however evidence of association of bacteria with host cell membrane in the urinary tract (Fig 3.8). Studies with enteropathogenic *E. coli* and enterohaemorrhagic *E. coli* has found that they preferentially bind to PE, over phosphatidylcholine and phosphatidylserine (214). Associated of bacteria with epithelial cells induce apoptosis which correlates with an increase in PE on the outer membrane facilitating increased binding to PE (215). More work however would be needed to see if this occurs with UPEC

in the urinary tract and whether bacterial binding of PE facilitated local ethanolamine metabolism without increasing urinary ethanolamine.

In conclusion, this study has shown a consistent presence of ethanolamine has been detected in urine and provided evidence of ethanolamine metabolism in the urinary tract. The *eut* operon is conserved across all UPECs isolated in this study and is upregulated in this sample of infected urines. The upregulation detected in UPECs significantly correlated to the level of ethanolamine detected in urine (Fig 3.6). Published global expression analysis has provided evidence that while expression of the *eut* operon is dependent on host interactions, cytokine directed recruitment of inflammatory cells does not appear to contribute to *eut* expression in this study (17). Other host factors such as turnover of epithelial cells in response to bacterial infection could facilitate ethanolamine metabolism in the urine (42).

Chapter 4 An Investigation into the metabolism of ethanolamine by Uropathogenic *E. coli*

4.1 Abstract

Ethanolamine is an amino alcohol present in abundance in cell membranes as phosphatidylethanolamine. Ethanolamine can be metabolised by *Escherichia coli* and *Salmonella spp*. as a source of carbon and nitrogen (13, 143). The mechanism to metabolise ethanolamine by these Enterobacteria is encoded in the ethanolamine utilisation (*eut*) operon which is conserved across *E. coli* and *Salmonella* strains, however ethanolamine is not a preferred nutrient for growth (5). In the gastrointestinal (GI) tract, ethanolamine metabolism has been found to promote Enterohaemorrhagic *E. coli* (EHEC) and *Salmonella typhimurium* overgrowth to promote gastrointestinal infection (3, 4). Extra-intestinal *E. coli* that naturally resides in the GI tract can colonise the bladder to cause urinary tract infections. While it is clear that ethanolamine is present from food and cell breakdown in the nutrient rich gut, until recently its presence in the relatively nutrient poor environment of urine was underappreciated. Ethanolamine has been measured in our study and others at average concentrations of 0.57mM in urine (Chapter 3 and (47)) and expression of the *E. coli eut* operon was detected in RNA from infected urine (Chapter 3 and(17)).

In this study, uropathogenic *E. coli* (UPEC) isolated from infected urines were evaluated for their ability to utilise ethanolamine. The majority of the isolated UPECs were able to utilise ethanolamine as a nitrogen source in modified M9 minimal media (Mod M9). Four isolates that demonstrated growth enhancement with ethanolamine in Mod M9 were grown using an *in vitro* urine model using artificial urine medium (AUM) (185) and confirmed a similar growth advantage. Subsequently, knock-out mutants in the *eut* operon were created. These strains were unable to utilise ethanolamine *in vitro* and were out-competed by their wild-type parental strain in AUM. UPECs were also able to metabolise physiological levels of ethanolamine to promote a biologically significant growth advantage. This study found that ethanolamine in the urinary tract is a reliable nutrient source for *E. coli* via microcompartment-mediated metabolism.

4.2 Introduction

Urinary tract infections (UTIs) are caused by bacteria ascending the urethra and migrating to the bladder where they replicate and colonise to cause infection (11). Seventy-five percent of non-complicated UTIs are caused by UPECs, a type of extra-intestinal *E.coli* (ExPEC), which reside harmlessly in the gut (1). Within the gut UPECs reside in the nutrient rich mucus lining, in contrast to the nutrient-limited environment of the urinary tract (51). Recent studies have found that UPECs undergo rapid growth in the urinary tract, compared to commensal strains and asymptomatic bacterial colonising strains. This suggests that rapid metabolic adaptation and proliferation in the urinary tract is a key part of UPEC pathogenesis (50).

Urine is the main source of nutrients for extracellular bacteria in the urinary tract. It is a complex mixture of amino acids, short peptides, and limited iron availability with moderate oxygenation (47). Competition studies in a mouse model of UTI has investigated UPEC requirements for central carbon metabolism in the urinary tract. Mutations that interrupt gluconeogenesis (*pckA*) and the TCA cycle (*sdhB*) have been shown to reduce fitness of UPEC in mouse models of bladder and kidney infection (12). This is in contrast to the nutrient-rich intestine where glycolysis (*pgi*) or the Entner-Douderoff (*edd*) pathway are required for colonisation fitness (55). In addition, deletion of the peptide transport proteins (*dppA* or *oppA*) also reduces fitness of UPEC in this model, suggesting that peptides and amino acids are crucial sources of carbon in the urinary tract (12). Genes involved with amino acid metabolism are upregulated during growth in urine including the D-serine deaminase (*dsd*) operon which regulates the metabolism of D-serine (59, 62). D-serine, one of the most abundant amino acids in the urine present in urine, is broken down to pyruvate and ammonia, and can be utilised by *E.coli* as a sole source of carbon and nitrogen (216).

Ethanolamine is an amino alcohol commonly found in the phospholipid layer of eukaryotic and prokaryotic cell membranes in the form of phosphotidylethanolamine (PE) (132). Ethanolamine can be broken down by bacteria to be used as a source of carbon or nitrogen (2, 3, 13, 144). EHEC, *Salmonella spp.* and *Listeria spp.* utilise the abundance of ethanolamine in

the gut to out-compete commensal bacteria (3, 4). As metabolising ethanolamine provides a competitive advantage to pathogenic bacteria, it has been linked to pathogenesis in gastrointestinal infections (3, 4, 167).

Metabolism of ethanolamine is controlled in *E. coli* by a conserved 17-gene ethanolamine utilisation operon (*eut* operon) described first in *Salmonella enterica* (5). In brief, the operon is controlled by the positive regulator *eutR*, which is activated in the presence of ethanolamine and cobalamin (141). Ethanolamine is broken down to ammonia, ethanol and acetyl-coenzyme A (acetyl-CoA) which can enter the TCA and glyoxylate cycle or can be utilised for lipid biosynthesis (151). During the first reaction ethanolamine is broken down to acetaldehyde by the ethanolamine ammonia lyase (EutBC) releasing ammonia, a convenient source of nitrogen for bacteria (143). Acetaldehyde is then converted to acetyl-CoA by the action of acetaldehyde dehydrogenase (EutE) and coenzyme A (CoA) in an NAD+ dependant reaction (13). NAD is subsequently oxidised for this by the action of the alcohol dehydrogenase EutG which converts acetaldehyde to ethanol consuming NADH in the process. Under energy limiting conditions acetyl Co-A is converted into acetyl-phosphate by phosphotransacetylase (EutD) and ultimately to acetate with generation of ATP either by microcompartment-associated acetate kinases EutP and EutQ or cytoplasmic acetate kinase AckA (147, 150, 206). Acetate is excreted but can be recaptured when it is needed (148, 205).

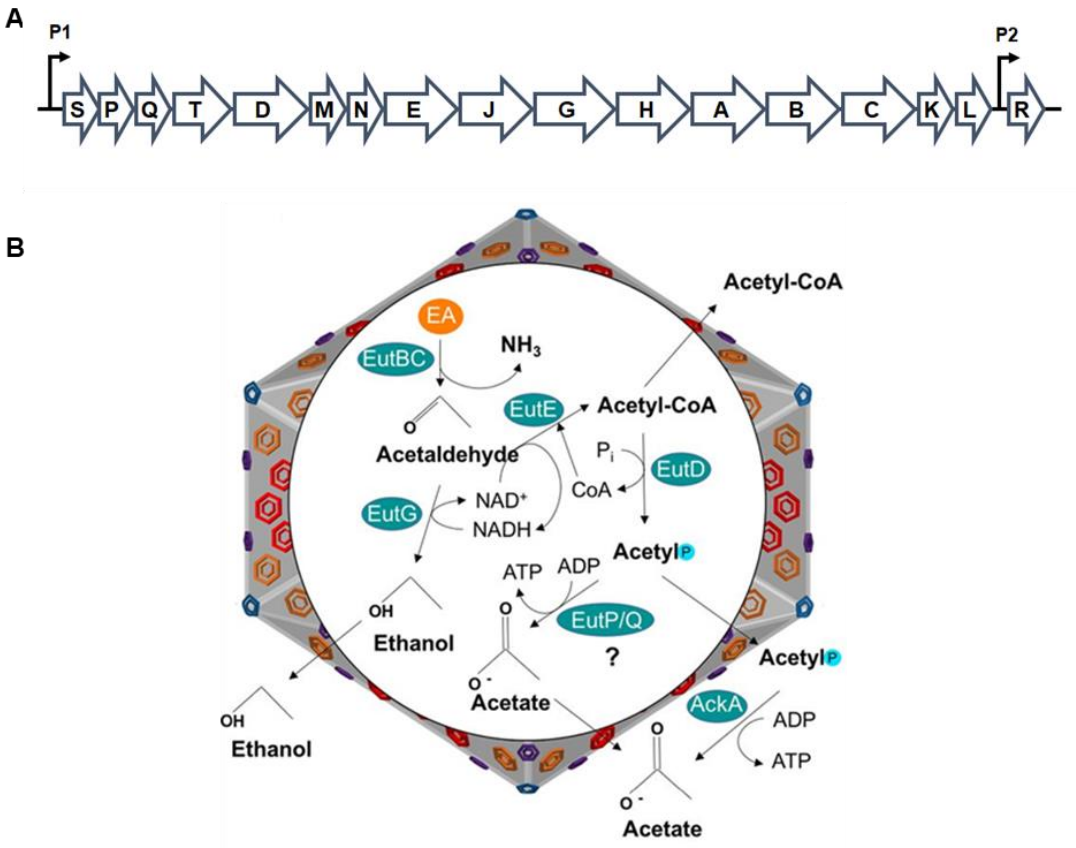

Figure 4.1 A. Configuration of the eut operon in *E. coli.* **B.** Schematic of ethanolamine metabolism in *E. coli.* Ethanolamine breakdown is carried out in microcompartments in the cytoplasm (151).

The enzymatic reactions for ethanolamine degradation are physically encased by a proteinaceous structure called a bacterial microcompartment (BMC). The structural proteins that form the thin shell of the Eut BMC are encoded by five of the 17 genes of the *eut* operon (Fig 4.1a) (5). These structures have been found in many phyla of bacteria however the functional role of the MCP structure has not been fully elucidated despite various hypotheses presented (14, 15). This is discussed in more detail in Chapter 1.

Induction of the *eut* operon has been identified in the urinary tract. An *in vivo* mRNA screen found that the *eut* operon was upregulated in human urine of active UTI (see Chapter 3). Competition assays revealed reduced fitness of the Eut operon knockouts compared to wild type in a mouse UTI model (17). In support of these findings, a recent study has found that the *eut* operon is

important for the avoidance of the innate immune response in the urine leading to the successful colonisation of the bladder (10). While *eut* operon function has been found to be important for UPEC colonisation of the bladder there is little evidence on whether ethanolamine is used as a nutritional source in the urine, as previously shown in the gut (3).

In Chapter 3, UPEC strains were characterised as having a conserved *eut* operon as a part of their core genome, however only 57% of the strains had an intact D-serine metabolism operon (Chapter 3). Additionally, ethanolamine was detected in urine from 64 patients at a mean concentration of 0.57mM (Chapter 3), consistent with findings from a urine metabolome study conducted on 22 healthy volunteers (47). This is higher than any individual amino acid present in the urine (47). In this study, UPEC isolated from infected urines were assessed for their ability to utilise ethanolamine as a nitrogen or carbon source. An *in vitro* model using an artificial urine medium was developed to determine if there is a growth advantage for UPEC in urine-simulated conditions when ethanolamine is added. Biochemical assays were used to identify if any advantage observed was accompanied by the metabolism of ethanolamine. Finally, this chapter investigates whether ethanolamine provides a nutritional competitive advantage for UPEC *in vitro*.

4.3 Results

4.3.1 Clinical UPEC strains can utilise ethanolamine as a sole nitrogen source but not a carbon source in minimal media.

The ability of the isolated clinical UPEC's to utilise ethanolamine as a carbon and nitrogen source was investigated by growing the clinical isolates in modified M9 minimal media (Mod M9) supplemented with 10mM ethanolamine. As previous studies have determined that *E. coli* can favourably utilise ethanolamine as a nitrogen source (3, 13), the UPEC isolates were screened for utilisation of ethanolamine as a sole nitrogen source in Mod M9 with glycerol as a carbon source. It was found that the 92% of the 48 UPECs isolated were able to utilise ethanolamine as a nitrogen source (Appendix 4.1). The growth increment conferred by addition of ethanolamine differed between the strains, and the increase in Maximum optical density at 600nm (OD_{600nm}) between cultures with ethanolamine and without ethanolamine was used as a measure of effective ethanolamine utilisation (Fig 4.2a). U1, U13, U17 and U38 were selected to investigate whether they could utilise ethanolamine as a sole carbon source considering they effectively utilised ethanolamine as a nitrogen source (Fig 4.2b). U1 and U17 could not utilise 10mM ethanolamine as the sole carbon source (Fig 4.2c). U13 and U38 showed a very slight increase in OD_{600nm} 30hrs after inoculation.

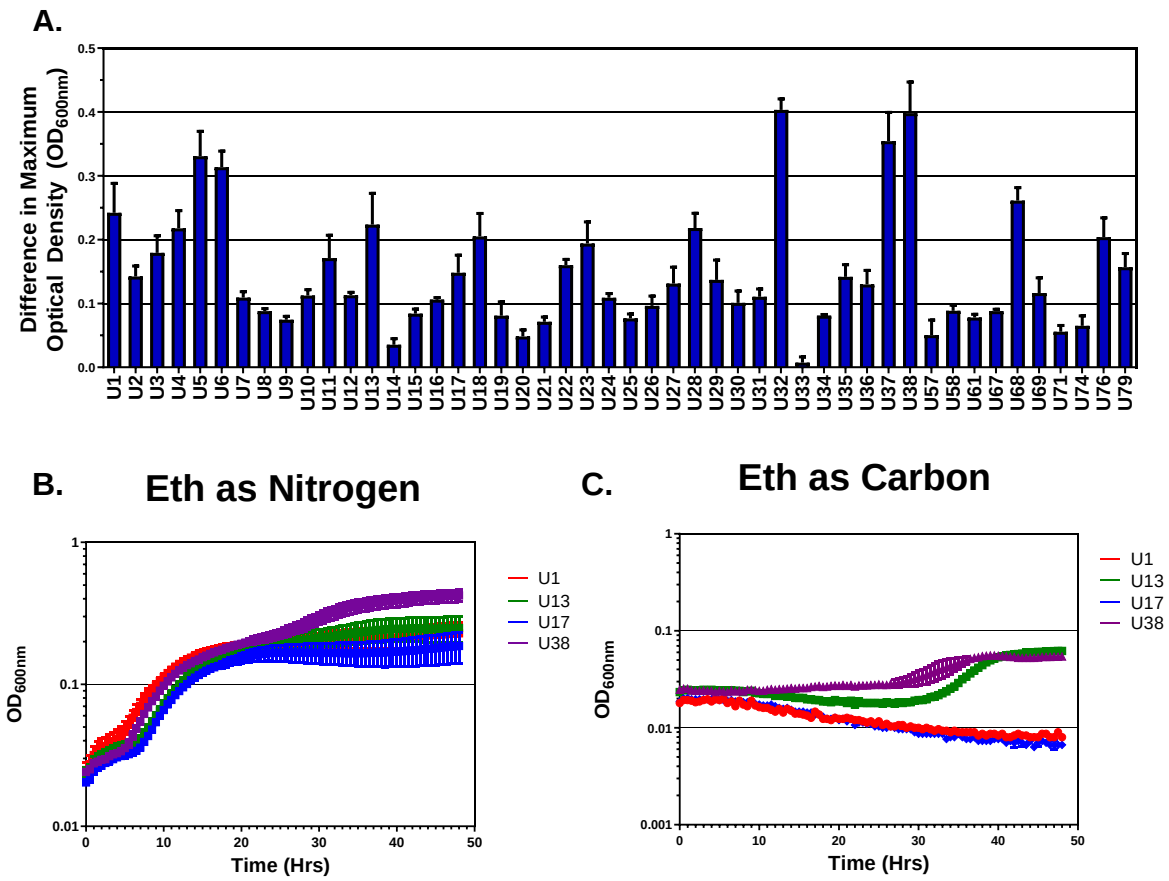

Figure 4.1 UPEC are able to utilise ethanolamine as a nitrogen source in modified M9 media but not as a carbon source. A Difference in Maximum optical density measured at 600nm (Max OD_{600nm}) in ammonia-free modified M9 media comparing the absence and addition of 10mM Ethanolamine. **B** Growth of selected UPECs in ammonia free modified M9 when 10mM ethanolamine is supplemented. **C** Growth of

4.3.2 Ethanolamine in Modified M9 and Artificial Urine Medium is metabolised by UPEC strains

UPECs were grown in Mod M9 and an artificial urine medium (AUM) which mimics the composition of urine (Chapter 2) (185). The four selected strains showed enhanced growth in both media when supplemented with 10mM ethanolamine (Fig 4.3) compared to the corresponding media without ethanolamine. Unlike Mod M9, AUM is able to support bacterial growth without the addition of ethanolamine. To investigate how ethanolamine is used in these growth conditions, the concentration of ethanolamine and its metabolic products acetate and ethanol were measured over time using HPLC analysis. The concentration of ethanolamine decreased over the 32Hr growth period at a rate of 0.67mM/hour when grown in Mod M9 and fell below 2mM after 16hrs incubation for all strains (Fig 4.4 a, c, e, g). Ethanolamine levels started to decrease as the bacteria left lag phase (8hrs) and enter exponential growth in tandem with acetate and ethanol production. Growth continued after all ethanolamine was consumed. In Mod M9 maximal acetate levels were approximately equimolar to the initial ethanolamine concentration and peaked for 3 of the 4 strains at 18hrs. Maximal ethanol levels likewise occurred at 28hrs but were approximately twice the initial molar concentration of ethanolamine. When the four UPEC strains were grown in AUM a shortened lag phase and increased rate of ethanolamine metabolism was noted than in ModM9 (Fig 4.4 b, d, f, h). Ethanolamine levels were almost completely diminished for three out of four strains by 12Hrs in AUM at a maximum rate of 1mM/hour. Ethanol levels reached their peak by 24hrs. Growth of the bacteria continued after ethanolamine was depleted. Unlike Mod M9, baseline levels of acetate were detected, and maximum levels were detected after 20hrs (Fig 4.4b, d, f, h).

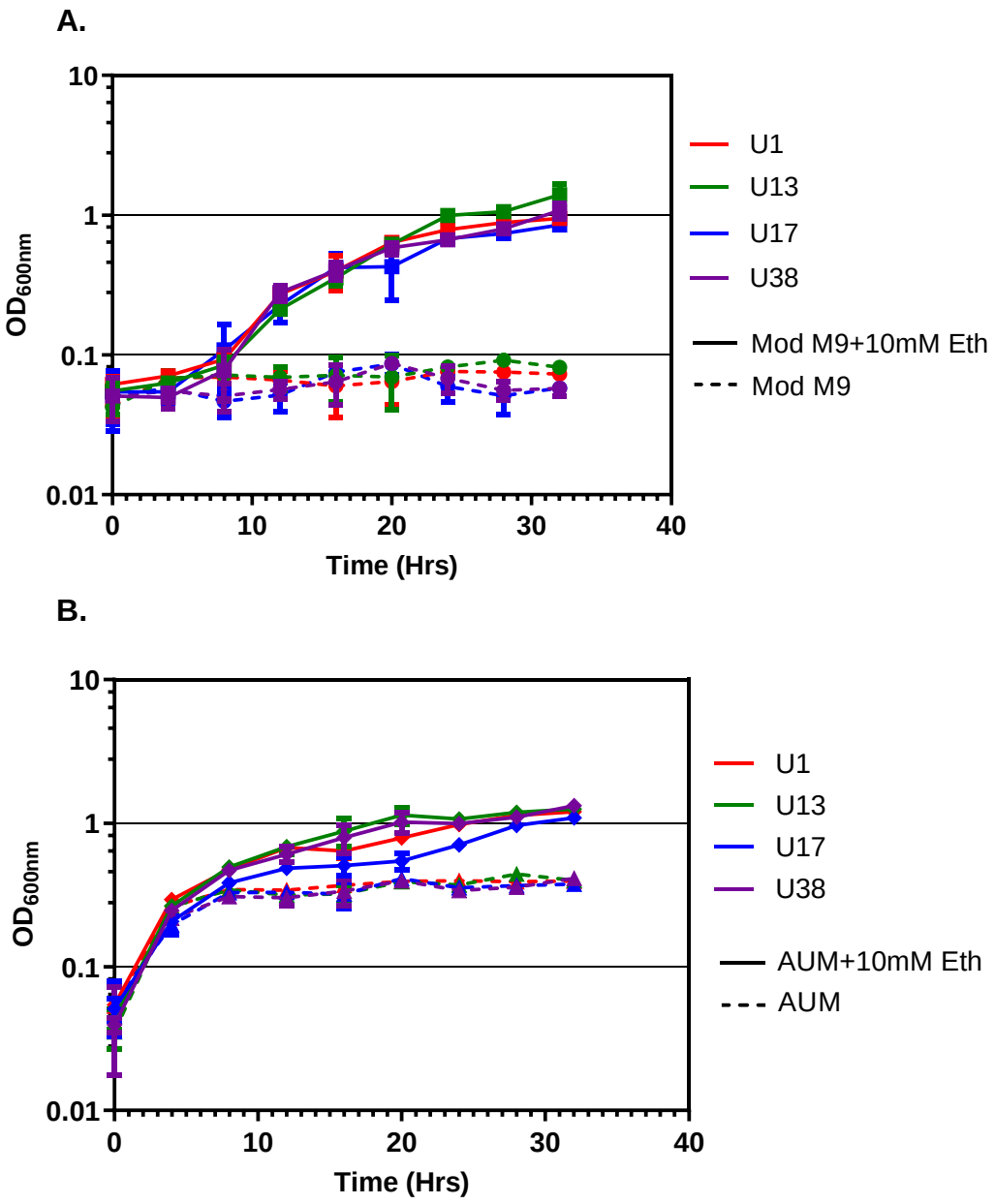

Figure 4.2 Ethanolamine promotes a growth advantage in Modified M9 and Artificial urine medium (AUM). Growth of selected UPEC in: **A.** Ammonia free modified M9 media (dashed line) and ammonia free modified M9 media with10mM Ethanolamine (solid line) **B.** AUM (dashed line) and AUM with 10mM Ethanolamine (solid line). Growth measured by optical density at 600nm (OD_{600nm}). Values are Mean ± SEM. N≥3.

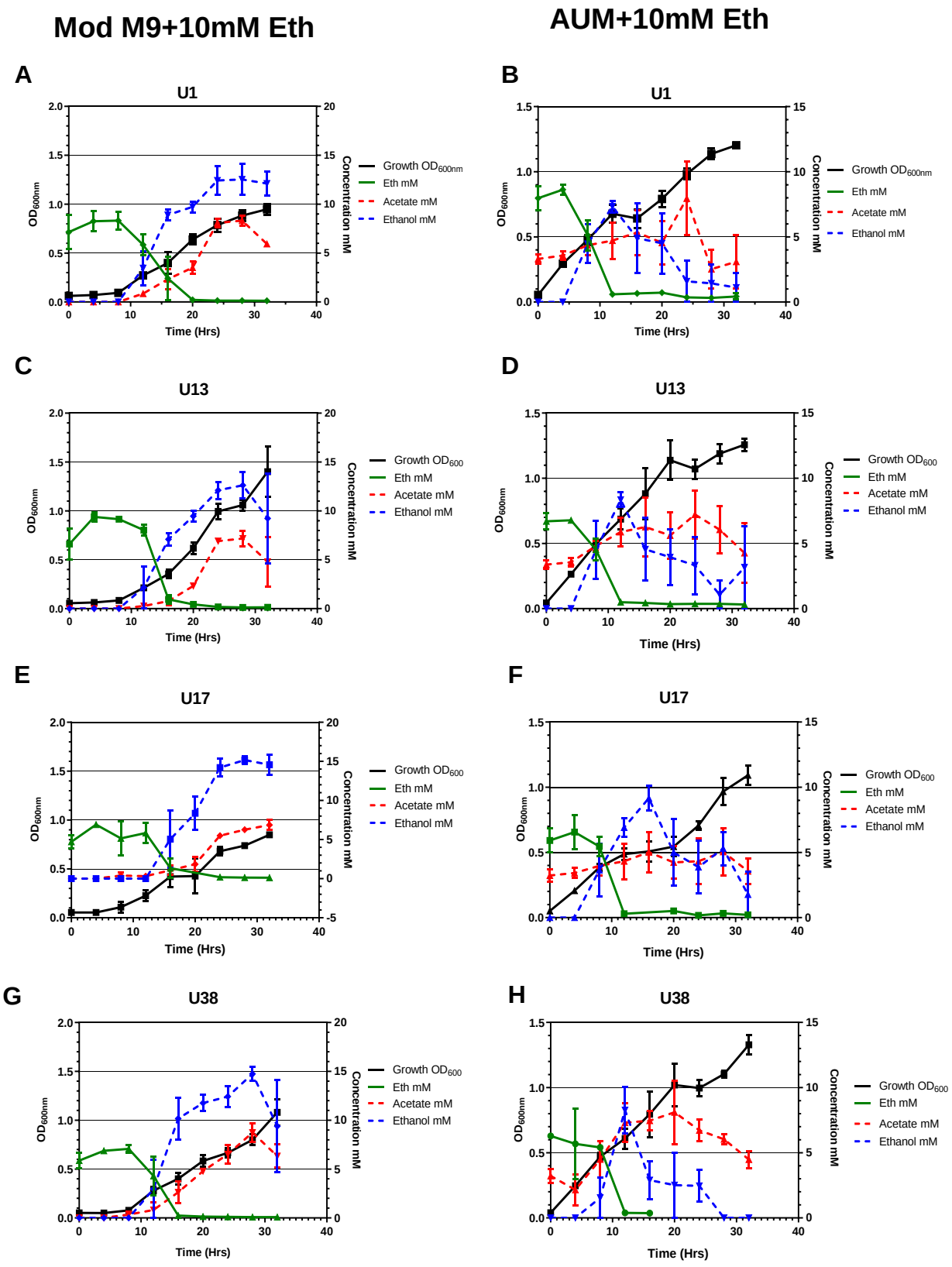

Figure 4.3 Ethanolamine is broken down by UPEC to release acetate and ethanol. A,C,E and G. Growth of UPEC's in modified M9 with 10mM ethanolamine (black) and concentration of ethanolamine (Eth)(green), acetate (red) and ethanol (blue) over the 32hrs. **B,D,F and H** Growth of UPEC's in AUM with 10mM ethanolamine (black) and concentration of ethanolamine (green), acetate (red) and ethanol (blue) over 32hrs . Values are Mean ± SEM. N=3.

4.3.3 Construction of *eut* mutants in clinical isolate strain U1

To assess the importance of ethanolamine metabolism in UPEC, in-frame knock-out mutants were created in U1 using P1cm1-directed transduction as described in Chapter 2. Strains from the KEIO collection of single gene knock-out mutants were used as donor strains to replace genes in wild-type U1 with a kanamycin cassette to create knock-out mutants by homologous recombination (183)(Fig 4.5a). Mutation was achieved in the *eut* operon regulator, *eutR*, the major subunit of the ethanolamine ammonia lyase enzyme, *eutB,* which facilitates the breakdown of ethanolamine to acetaldehyde and ammonia, and the acetaldehyde dehydrogenase, *eutE*, which is needed to generate acetyl-CoA from acetaldehyde. In each case a single kanamycin cassette insertion, flanked by Flp recognition site, replaced the expected gene and was confirmed by whole genome sequencing (183). However, in U1Δ*eutR* there was an additional prophage insertion between *eutA* and *eutB*. This prophage is identical to the prophage found in the K12 lab strain MG1655 with open reading frames in reverse orientation to the *eut* operon which prevents downstream transcription of the operon, and prevents utilisation of ethanolamine (Appendix 4.4) (141). To complement the single knock-out mutants, another *E. coli* library was utilised. The ASKA clones are a collection of individual genes ligated onto pCA24N under the control of the pTn5 lac-promotor that is activated by Isopropyl-β-D –thiogalactopyranoside (IPTG) (Fig 4.5c). The cognate plasmids were electroporated into the relevant knock out mutants and the presence of the plasmid was confirmed by colony PCR.

The strains were screened for loss of fitness by growth in LB prior to screening for loss of function. The single knock-out mutants did not display a fitness deficiency in LB compared to the wild-type. The complemented mutants did display a slight loss of fitness (Fig 4.5b). There is evidence of lethal over-expression of gene using the ASKA clones, therefore multiple concentrations of IPTG were tested for their ability to complement U1Δ*eutB* (188). Induction of the gene with 0.01mM IPTG restored the phenotype in Mod M9 with 10mM ethanolamine (Fig 4.5d). All strains were the assessed

for their ability to utilise ethanolamine by growth in Mod M9 with 10mM ethanolamine, with complemented strains being induced by 0.01mM IPTG (Fig 4.5e). The U1Δ*eutR* and U1Δ*eutB* both displayed a loss of growth phenotype compared to the wild type (Fig 4.5e). This phenotype was restored by complementation in U1Δ*eutB* and was not restored in U1Δ*eutR* as expected due to the presence of the prophage in the knock-out. However, the *eutE* mutant grew to an OD_{600nm} similar to the wild-type (Fig 4.5e). This confirms that the mutants are nonpolar as the transcription of the downstream genes *eutB* and *eutC* that encode the ethanolamine ammonia lyase enzyme, required for the breakdown of ethanolamine to acetaldehyde and ammonia, must be active to provide ammonia for the strain to grow on nitrogen limited Mod M9 with ethanolamine (142). In addition, the Δ*eutE* mutant and complemented strain had a faster growth rate compared to the wild type.

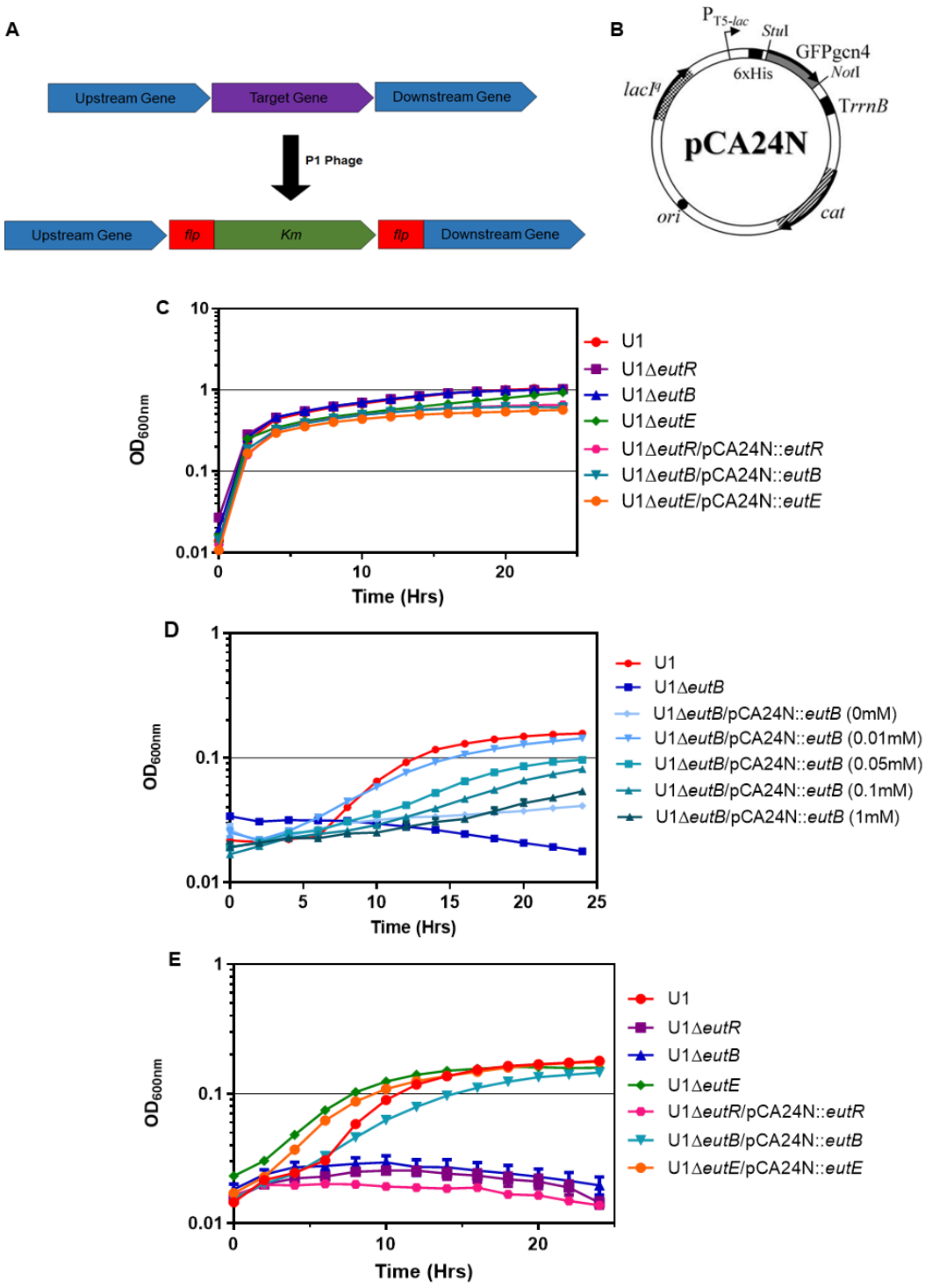

Figure 4.4 Construction of knock out mutants using P1 transduction. **A** Schematic of cassette insertion following P1 transduction. **B** Diagram of ASKA plasmid pCA24N (188). **C** Growth of U1, U1 mutants and complemented strains in LB over 36 hours. **D** Growth of U1ΔeutB+peutB with different concentration of IPTG. **E** Growth of U1, U1 mutants and complemented strains in Mod M9 with 10mM ethanolamine. Values are means ±SEM. N=3

4.3.4 *eutR* and *eutB* are essential for ethanolamine metabolism in Mod M9 and AUM

The function of *eutR*, *eutB* and *eutE* in ethanolamine metabolism was investigated by comparing substrate utilisation in the wild type and single gene knock-out mutants (Fig 4.6a). In Mod M9 medium, ethanolamine was consumed by U1 and U1Δ*eutE* strains with the concentration of ethanolamine decreasing over 24hrs (Fig 4.6b). This indicates that EutBC was functional in both U1 and U1Δ*eutE.* The breakdown of ethanolamine began between 8 and 12hrs in U1 and after 4hrs in U1Δ*eutE*, corresponding to exponential growth in the media (Fig 4.6b). After 24hrs ethanolamine was depleted in the media as the bacteria entered lag phase (Fig 4.6). U1Δ*eutB* and U1Δ*eutR* however were unable to consume ethanolamine (Fig 4.6b) and were unable to grow in Mod M9 with ethanolamine as a nitrogen source (Fig 4.6a).

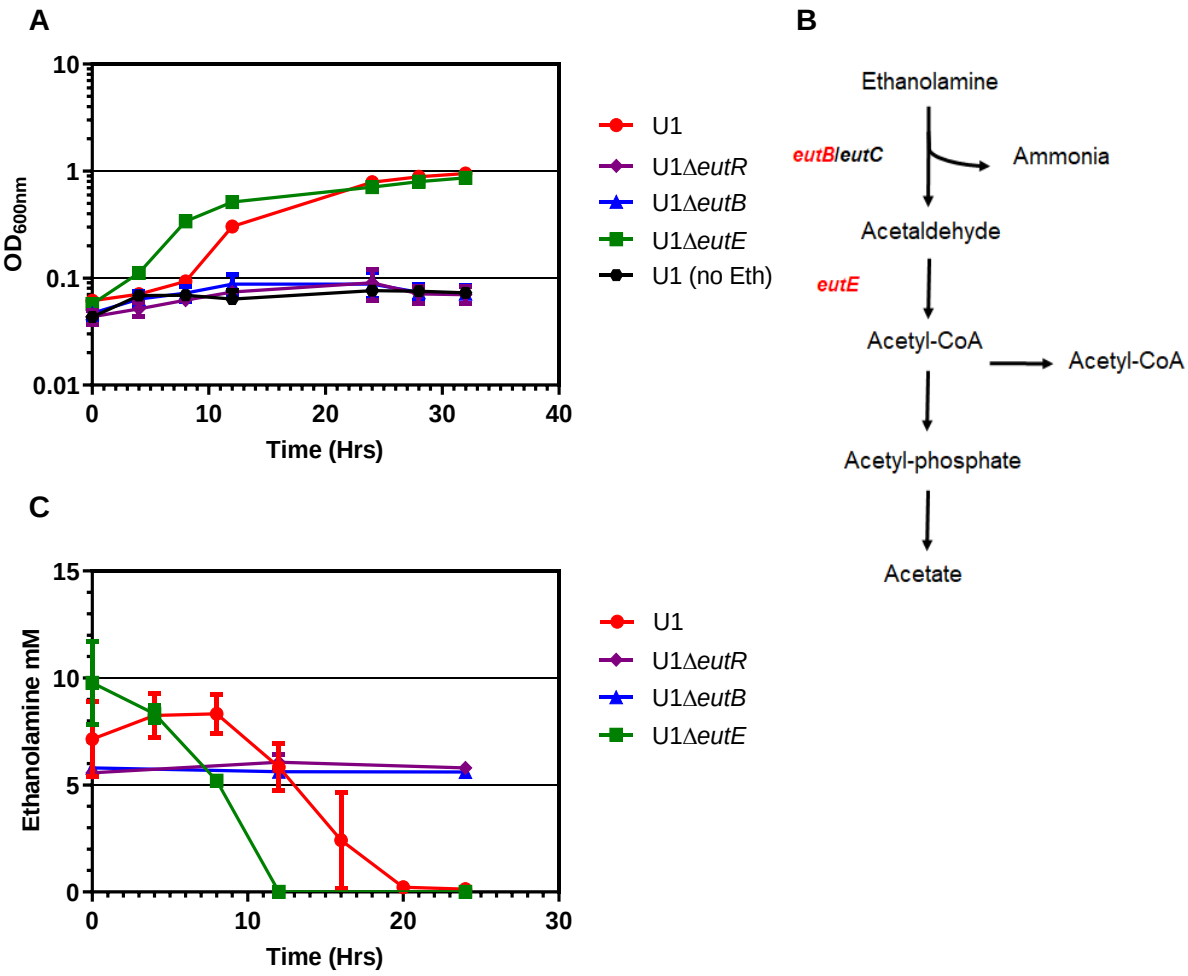

Figure 4.6 Ethanolamine is utilised as a nitrogen source in Mod M9. A. Growth of U1, U1Δ*eutR* U1Δ*eutB* and U1Δ*eutE* in modified M9 with 10mM ethanolamine. **B**. Schematic of ethanolamine metabolism pathways with genes knocked out highlighted in red. **C.** HPLC analysis of ethanolamine concentration in mod M9 with 10mM ethanolamine over 24 hrs. Values are Mean ± SEM. N=3.

The ability of the mutants, and complemented mutants to grow in AUM was compared to the wild type strain (Fig 4.7). When grown in AUM with 10mM ethanolamine all the strains had reduced growth compared to the wild type and match the maximum OD_{600nm} of the wild type when ethanolamine was not supplemented (Fig 4.7a). Interestingly, U1Δ*eutE*, which was not impaired for growth in Mod M9 medium with ethanolamine, was impaired compared to the wild-type in AUM plus ethanolamine (Fig 4.7a). The growth phenotype was restored to wild-type levels for all of the complemented mutants when the cognate ASKA plasmid was induced with 0.01mM IPTG. This included U1*eutR*/pCA24N::*eutR*, despite the prophage insertion (Fig 4.7a).

The ability of U1 and its corresponding mutants to utilise ethanolamine when supplemented in AUM was examined (Fig 4.7). The U1Δ*eutE* strain metabolised ethanolamine in AUM, however, unlike when grown in Mod M9, this did not translate to a growth phenotype similar to the wild type (Fig 4.7a). This suggests that ammonia produced from ethanolamine metabolism is not the primary cause of U1 growth enhancement when ethanolamine is added to AUM. Rather onward metabolism of acetaldehyde, derived from ethanolamine metabolism, is utilised for carbon or energy (Fig 4.1).

U1Δ*eutB* and U1Δ*eutR* did not metabolise ethanolamine, and growth of these strains was similar to U1 grown in AUM without ethanolamine (Fig 4.7a). Complementation of U1Δ*eutB* restored ethanolamine metabolism, while complemented U1Δ*eutR*/pCA24N::*eutR* showed very little utilisation of ethanolamine. A significant difference in the percentage of ethanolamine used at 24 hrs was found between the wild type and U1Δ*eutB*, U1Δ*eutR* and U1Δ*eutR*/pCA24N::*eutR* strains. Despite this, the growth phenotype was restored for U1Δ*eutR*/pCA24N::*eutR* as well as the Δ*eutB* mutations by complementation.

Colony PCR of U1Δ*eutR*/pCA24N::*eutR* after growth in AUM with 10mM ethanolamine confirms that the prophage insertion is present (Appendix 4.5). This data indicates that the restored growth phenotype observed in the U1Δ*eutR*/pCA24N::*eutR* is not primarily due to restoration of ethanolamine consumption. Instead growth could be restored by increased metabolism of

intermediates further down the ethanolamine degradation pathway such as acetaldehyde, or by EutR mediated regulation of an additional operon.

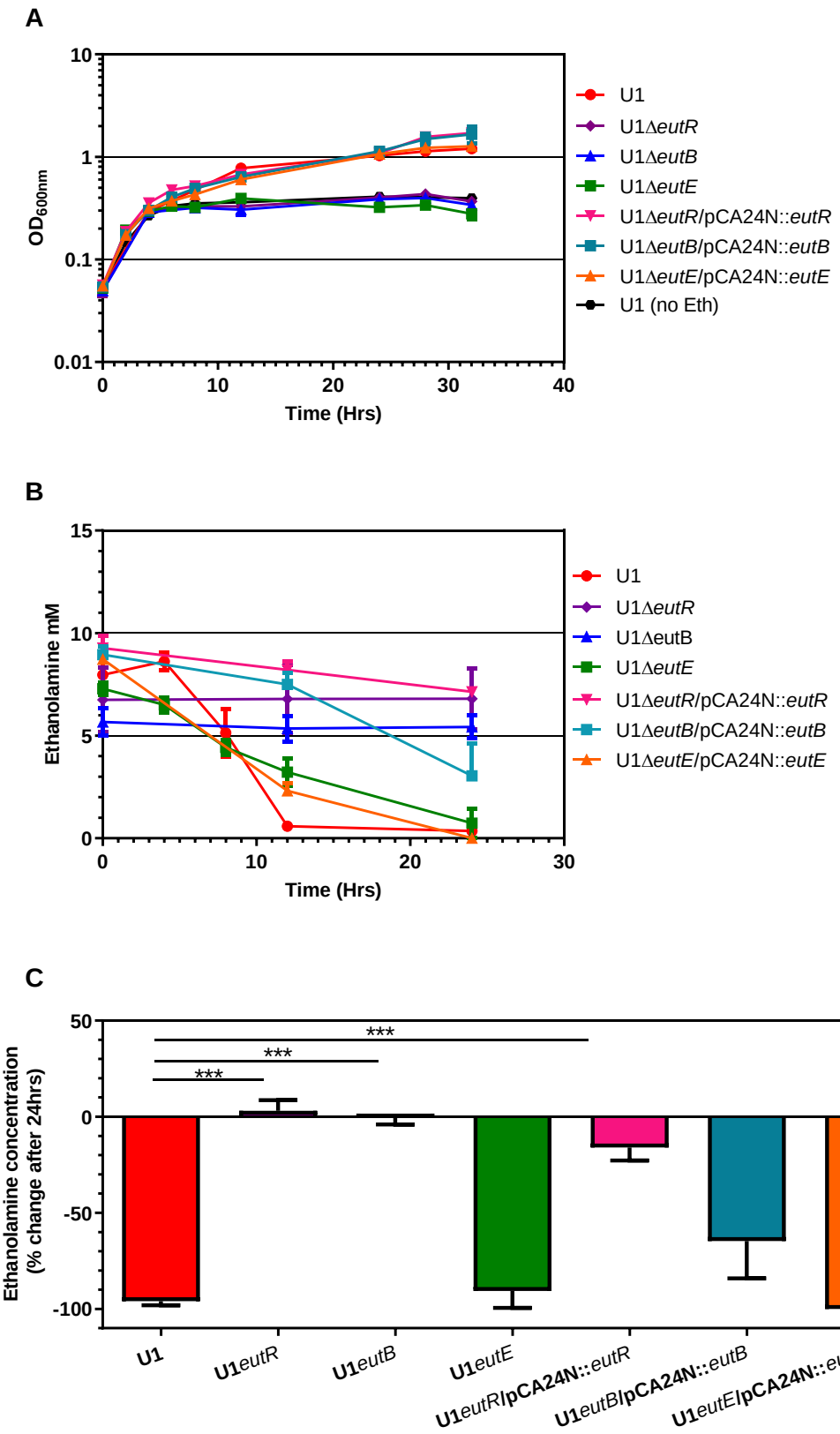

Fig4.6 Ethanolamine does not increase growth in *eut* knock out mutants in AUM

A. Growth of all strains in AUM with 10mM ethanolamine. **B**. HPLC analysis of ethanolamine concentration in AUM with 10mM ethanolamine over 24 hours. **C.** Change in ethanolamine after 24hours. 1-way ANOVA. ***P<0.001. Values are Mean ± SEM. N=3 or more.

4.3.5 Prophage can excise in U1Δ*eutR*/pCA24N::*eutR* when grown in Mod M9 with ethanolamine but not when grown in AUM with ethanolamine

The introduction of the CPZ-55 prophage into the genome of U1 during transduction to form the U1Δ*eutR* prevents complementation of the strain in Mod M9. To investigate whether the prophage could be excised with prolonged nutritional stress, U1Δ*eutR*/pCA24N::*eutR*, was grown for 48hrs in Mod M9 with 10mM ethanolamine. After 30hrs incubation in Mod M9 with 10mM ethanolamine growth of U1Δ*eutR*/pCA24N::*eutR* was detected (Fig 4.8a). After 48hrs the bacterial cultures were grown in Mod M9 with 10mM ethanolamine for a further 24hrs before the strains were screened for the presence of the prophage by colony PCR, using primers that amplify the border between the prophage and *eutB*. Two of the three colonies were negative for the presence of the prophage (lane 9 and 10, Fig 4.8b) while the kanamycin cassette that replaces *eutR* was still present in the bacterial genome (Lanes 1-3, Fig 4.8b). Therefore, this suggest that in situations of nutritional stress the prophage can excise from the *eut* operon. Interestingly, prophage excision when U1Δ*eutR*/pCA24N::*eutR* was grown in AUM plus ethanolamine was not detected (Appendix 4.5).

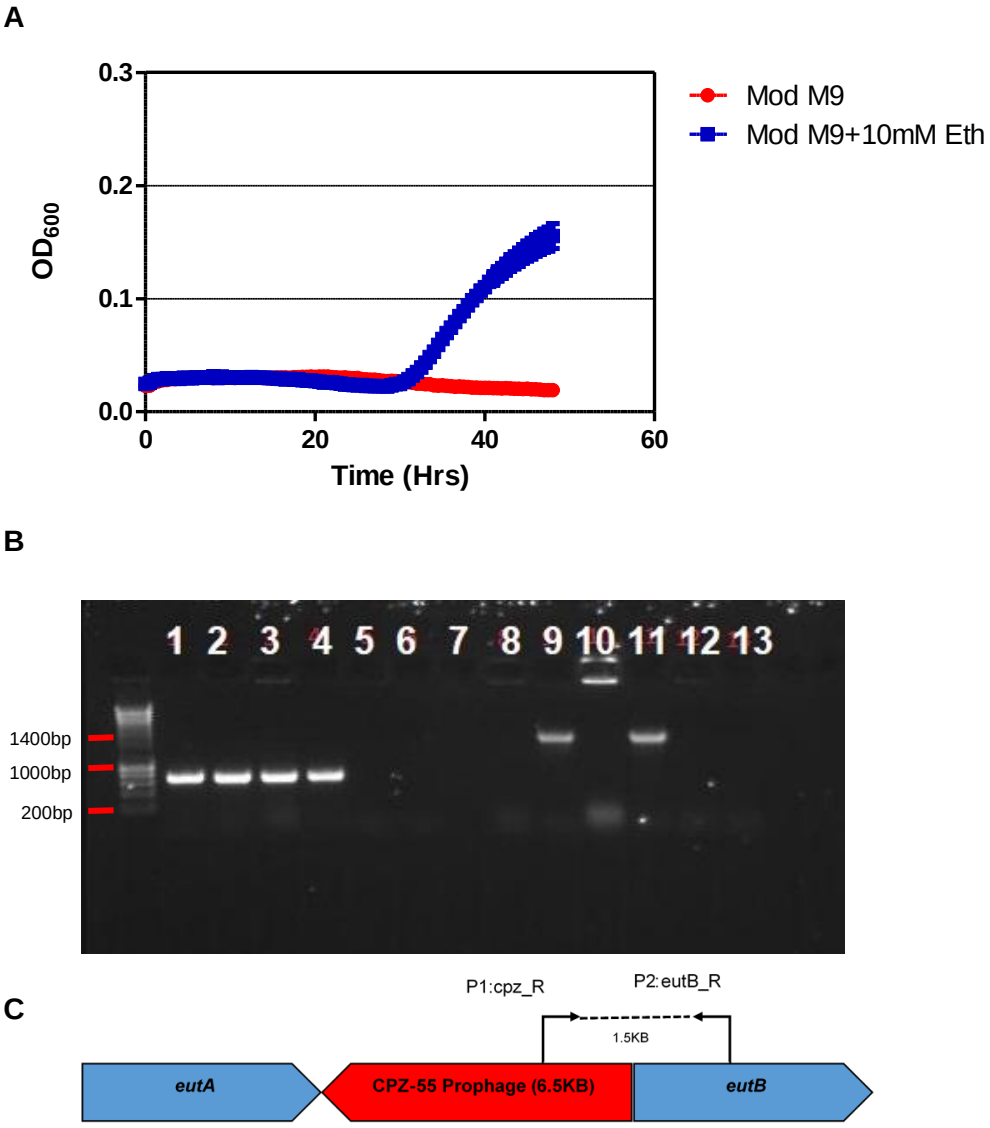

Figure 4.8 Prophage CPZ-55 excises from U1Δ*eutR*/pCA24N::*eutR* during nutrient stress. A. Growth of U1Δ*eutR*/pCA24N::*eutR* in Mod M9 with 10mM ethanolamine for 48 hours. **B.** Colony PCR of strains collected after 48hrs growth. Lanes 1-6 amplify region over Kanamycin cassette. Lanes 8-13 amplify region over CPZ-55 and *eutB* boarder. C. Schematic of PCR amplification over prophage border. Lanes are as follows:
1./8. U1Δ*eutR*/pCA24N::*eutR*.1 **2./9.** U1Δ*eutR*/pCA24N::*eutR*.2
3./10. U1Δ*eutR*/pCA24N::*eutR*.3 **4./11.** U1Δ*eutR*/pCA24N::*eutR* (before growth)
5./12. U1 **6./13.** H_2O. Values are Mean ± SEM N ≥3.

4.3.6 *eut* operon is up regulated in U1 when grown in AUM supplemented with ethanolamine

Expression of the *eut* operon was investigated in AUM to determine the involvement of the *eut* operon in the metabolism of ethanolamine. The *eut* operon expression in U1 was measured by qRT-PCR and compared to the geometric mean of *gyrA* and *rrsA* housekeeping genes via 2-ΔΔCT (190, 217). Gene expression was measured at 4 hrs, 8 hrs and 24 hrs incubation, corresponding to different phases of growth and ethanolamine breakdown as determined by OD_{600nm} measurements and HPLC (Fig 4.3b). Relative expression of *eut* genes, *eutR*, *eutB*, *eutE* and *eutS* in AUM with ethanolamine were compared to relative expression during exponential growth in AUM. All genes are significantly upregulated in U1 when ethanolamine is present at 4hrs and 8 hrs incubation; *eutR*, *eutB* and *eutE* were increased approximately 15-fold (Student t-test or Mann Whitney U when data is not normally distributed) (Fig 4.9a). *eutS* displayed 130-fold increase in expression (Fig 4.9a). At 24 hrs the expression of these genes decreases, which corresponds to ethanolamine depletion (Fig 4.3b; 4.9a).

Expression of the *eut* operon was also measured in the knock-out mutants and compared to expression observed in the wild type. Expression was measured at 4 hrs when all strains were in exponential phase. The data shows that there is negligible induction of the *eut* operon by ethanolamine in the U1Δ*eutR*. These results confirm the positive regulation of the operon by *eutR* as described by Roof and colleagues (141). In U1Δ*eutB, eutR* and *eutE* were upregulated by ethanolamine, 10 and 6-fold respectively, confirming there is no polar effect associated with the insertion of the kanamycin cassette. However, the upregulation of these genes was not significant (Fig 4.9) (Mann-Whiney U). Likewise, *eutB* was upregulated by the addition of ethanolamine in the U1Δ*eutE* strain. This suggest that ethanolamine ammonia lyase enzyme that metabolises ethanolamine to acetaldehyde should still be expressed in U1Δ*eutE* (Fig 4.9) (Mann Whitney U, p=0.0028).

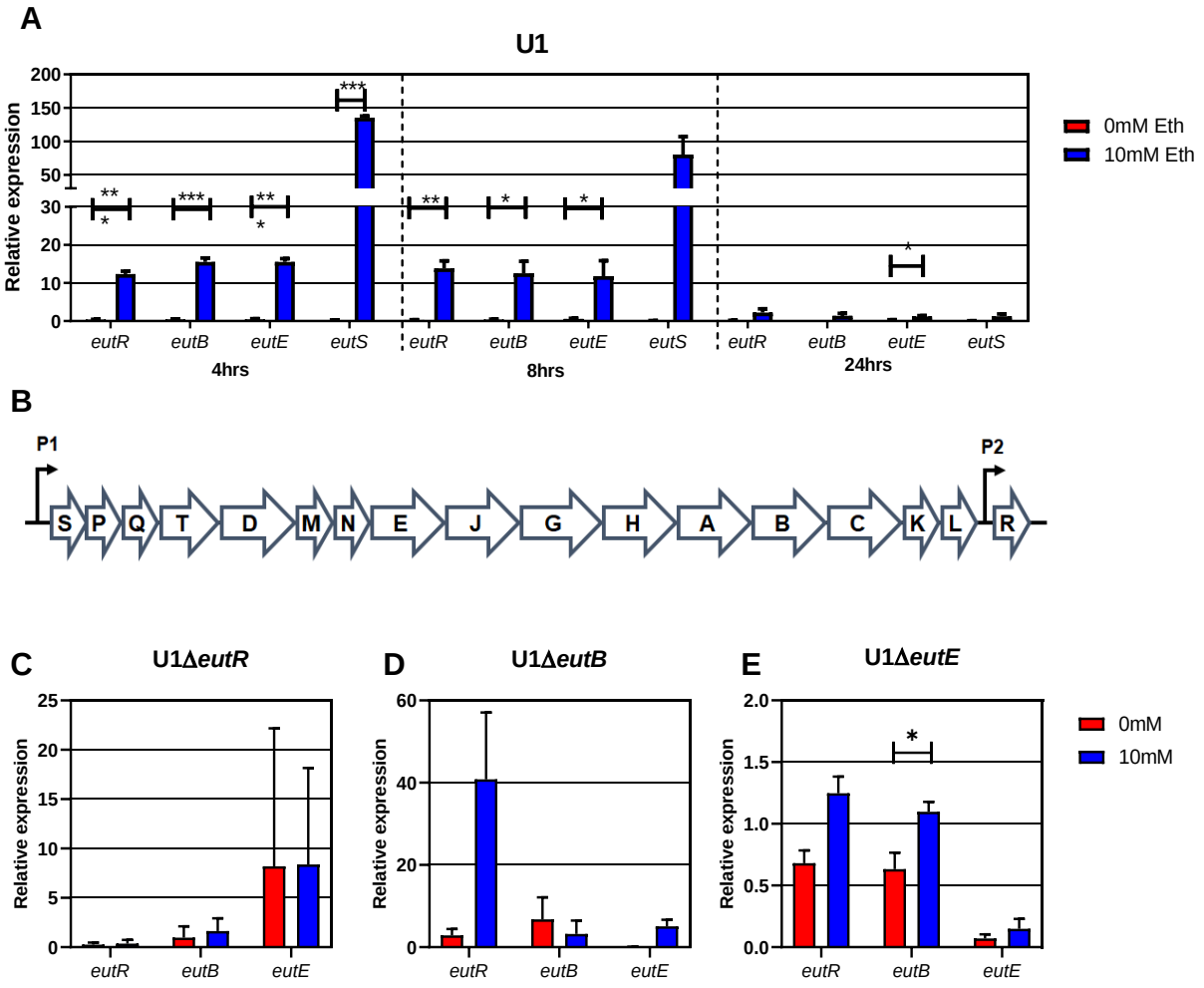

Figure 4.9 The eut operon is upregulated in AUM with the addition of 10mM ethanolamine. **A.** Relative expression of *eutR, eutB, eutE* and *eutS* in U1 grown in AUM with and without 10mM ethanolamine**. B.** Schematic of the *eut* operon. **C** Relative expression of *eutR, eutB* and *eutE* in B U1Δ*eutR* **C.** U1Δ*eutR* and **D.** U1Δ*eutR* after 4 hours growth in AUM with and without 10mM ethanolamine. Expression is measured relative to the geometric mean of *rrsA* and *gyrA*. Values are Mean ± SEM. N=3. Student t-test (or Mann Whitney U where sample is non parametric appropriate) * p<0.05,

4.3.7 Microcompartments are visible during growth in AUM with 10mM Ethanolamine

Gene expression data showed that *eutS* which encodes a shell protein for the Eut bacterial microcompartment was highly upregulated when U1 was grown in AUM with ethanolamine (Fig 4.9a). To investigate whether these microcompartments were visible in U1 in the presence of ethanolamine, bacterial pellets were harvested after 8 hours incubation in AUM with 10mM ethanolamine and fixed for transmission electron microscopy. Imaged sections show numerous straight-edged polyhedral structures 100-150nm in diameter in most cells visualised (Fig 4.10a). This is classical characterisation of the bacterial microcompartment (Fig 4.10a) (165). These structures were not visible in U1 when grown in AUM without ethanolamine or U1Δ*eutR* when grown in AUM with or without ethanolamine (Fig 4.10 b, c and d). This provides further evidence of microcompartment-mediated metabolism of ethanolamine in *E. coli*.

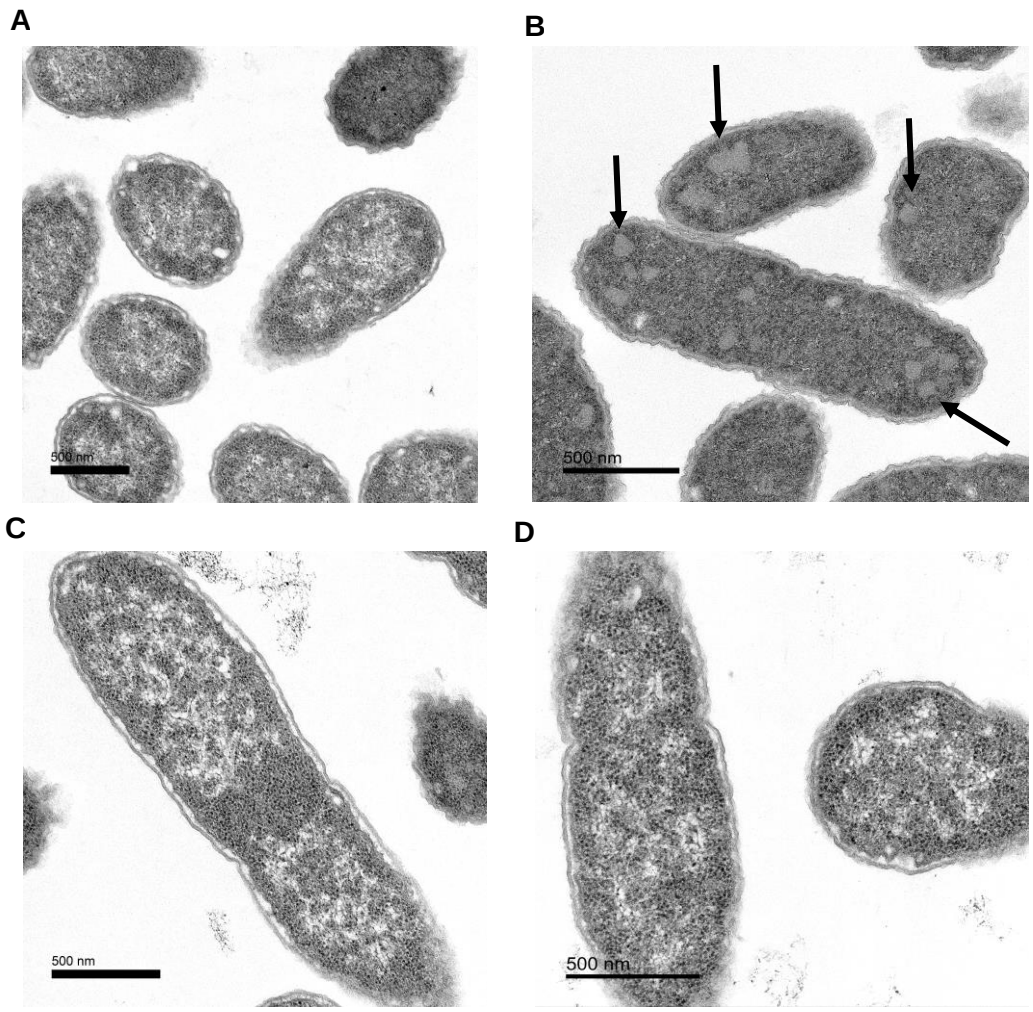

Fig4.10 Transmission electron microscopy of **A** U1 grown in AUM for 8hrs **B** U1 grown in AUM with 10mM ethanolamine for 8hrs. **C** U1Δ*eutR* in AUM for 8hrs. **D** U1Δ*eutR* in AUM with 10mM ethanolamine for 8hrs. Arrow point to microcompartments.

4.3.8 The physiological concentration of ethanolamine in urine increases UPEC growth *in vitro*

In Chapter 3 of this thesis ethanolamine was measured in infected urine by HPLC and detected at a mean concentration of 0.567mM. To test the ability of U1 to metabolise ethanolamine at this physiological level, U1 was grown in Mod M9 with 0.5mM ethanolamine in parallel to the U1 knock-out mutants and their complemented strains for 24hrs (Fig 4.11a). At this concentration U1 has a growth advantage over the *eutR* and *eutB* knock-out mutants, which grow similarly to U1 in the absence of ethanolamine. U1 displays similar growth at 20hrs compared to the *eutE* mutant, and the *eutB*-complemented clone, however the *eutE* mutant and its complemented clone have a higher growth rate than U1 for the first 10 hours (Fig 4.11a).

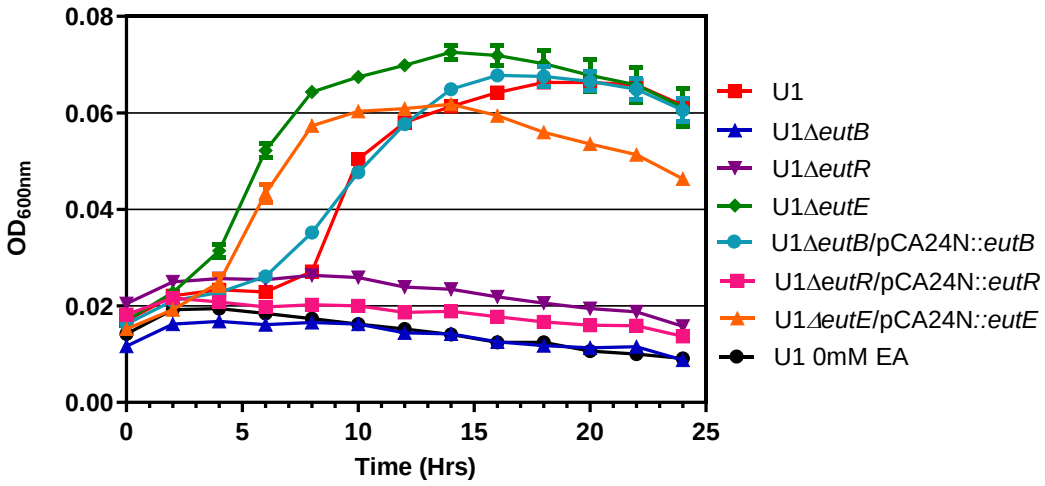

Figure. 4.11 Physiological levels of ethanolamine promote a growth advantage for U1 and complemented mutants. Growth of U1 and related strain grown in Mod M9 with 0.5mM Ethanolamine. Values are Mean ± SEM. N=3.

U1 was also grown in AUM with ethanolamine at this concentration. The difference in growth between 0 and 0.5mM ethanolamine measured by OD_{600nm} is small but there is a positive increment conferred by additional ethanolamine (Fig 4.12a). This difference in U1 growth by OD_{600nm} was calculated to be significant at 8hrs ($p<0.001$) and 24hrs ($p<0.05$) (t-test). When growth of U1 was measured by viable count (CFU $ml^{-1)}$, an increase in bacterial number was seen with additional ethanolamine. There was a significant difference in CFU ml^{-1} at 8hrs with an increase of $1.5x10^{8}$ CFU ml^{-1} ($p<0.05$, Student t-test) (Fig 4.12a). In contrast the *eut* mutants do not display a consistent growth difference with the addition of 0.5mM ethanolamine when measured by OD_{600nm} or viable count (Fig 4.12b, c and d).

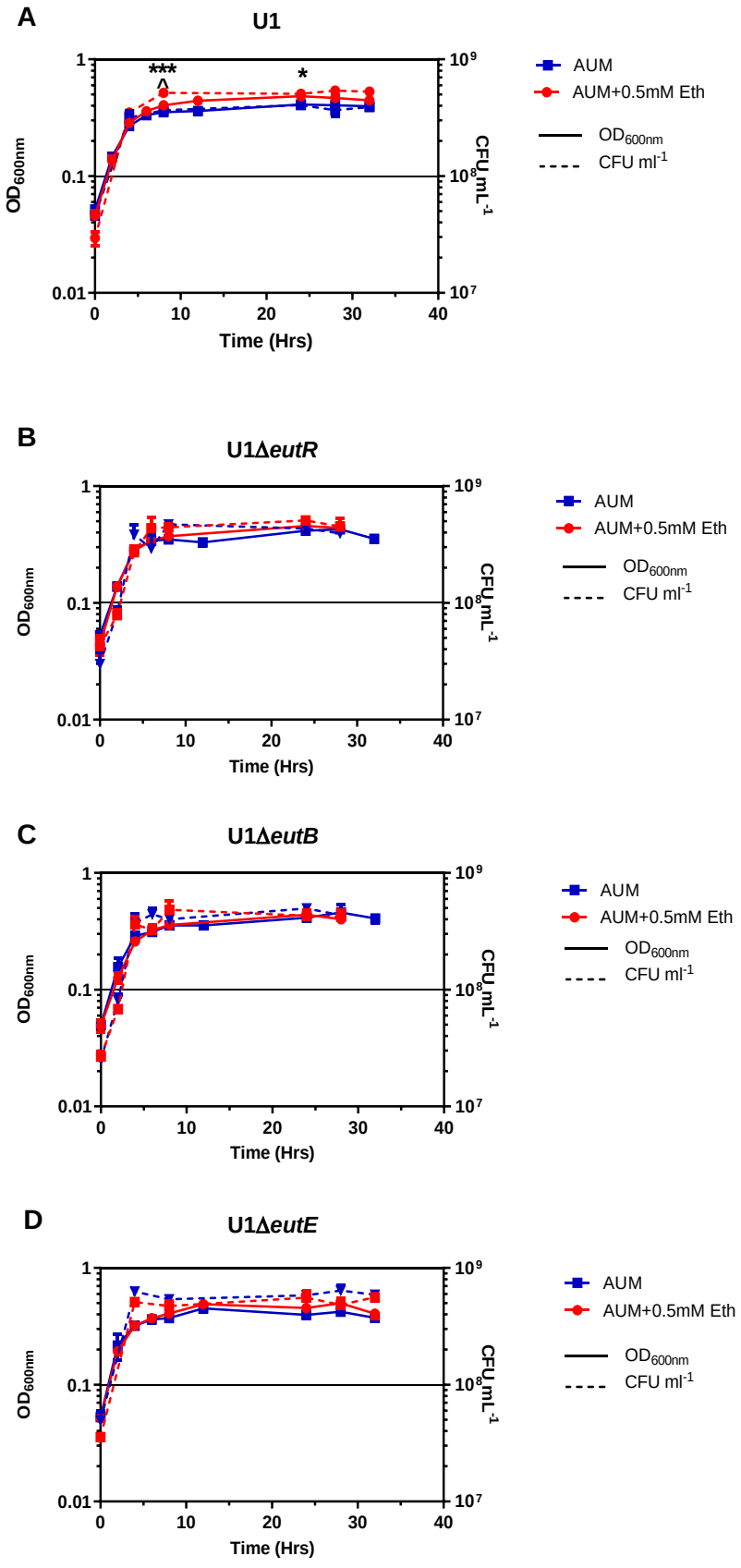

Figure .4.12 Growth of **A** U1; **B** U1Δ*eutR* **C** U1Δ*eutB* **D** U1Δ*eutE* in AUM+0.5mM ethanolamine measured by Optical Density (OD_{600nm} (Solid line) and CFU ml^{-1} (Dashed line). Difference in OD_{600nm} and CFU ml^{-1} was measured by Student t-test: OD_{600nm}. (* $p<0.05$, ***$p<0.001$), CFU ml^{-1} (^ $p<0.05$)

Table 4.1 Summary of growth of U1 strains in media with ethanolamine. + = growth enhancement compared to growth without ethanolamine. - =no growth enhancement compared to growth without ethanolamine. ND=no data. *Growth enhancement only observed after 30 hours

	Mod M9 10mM	***Mod M9 0.5mM***	***AUM 10mM***	***AUM 0.5mM***
U1	+	+	+	+
U1*∆*eutR	-	-	-	-
U1*∆*eutB	-	-	-	-
U1*∆*eutE	+	+	-	-
U1*∆*eutR*/pCA24N *::eutR	+*	-	+	ND
U1*∆*eutB*/pCA24N *::eutB	+	+	+	ND
U1*∆*eutE*/pCA24N *::eutB	+	+	+	ND

4.3.9 Ethanolamine provides a competitive advantage for UPEC in AUM

To determine whether ethanolamine consumption provides a competitive advantage to UPECs, U1 was co-incubated in AUM containing ethanolamine with each of the mutants. The bacteria were incubated for 24hrs before being re-inoculated into fresh AUM and ethanolamine for a second cycle of growth to emphasise any competitive advantage. When incubated with 10mM ethanolamine, the wild type had a clear advantage over all mutants after 36hrs (Fig 4.13). There is a significant difference in CFU ml^{-1} after 32hrs of incubation with U1Δ*eutR* ($p<0.01$, Student's t-test), which is also seen from incubation with U1Δ*eutB* ($p<0.05$, Student's t-test). However, growth of U1 with U1Δ*eutE*, conferred a growth advantage beginning at 12hrs with significant differences measured at most time points (Fig 4.13 f). When the bacteria are grown in physiological levels of ethanolamine the wild type does not appear to have a competitive advantage in this model when raw counts are used. (Fig 4.13)

The competitive index was calculated for the competition of wild type U1 and mutants in AUM with the different concentrations of ethanolamine. The competitive index was calculated, as specified in Chapter 2, and competitive indices of less than 1 represent U1 outcompeting the mutant. With the addition of 10mM ethanolamine the CI indicates that the wild-type outcompetes the mutant strains at all time points tested (Table 4.3). In contrast the CI calculated when grown in AUM with 0.5mM ethanolamine shows that the wild type has an advantage over the mutants at later time points however the advantage is variable over the 48hour period, indicating 0.5mM does not give U1 a clear growth advantage over its isogenic mutants (Table 4.2).

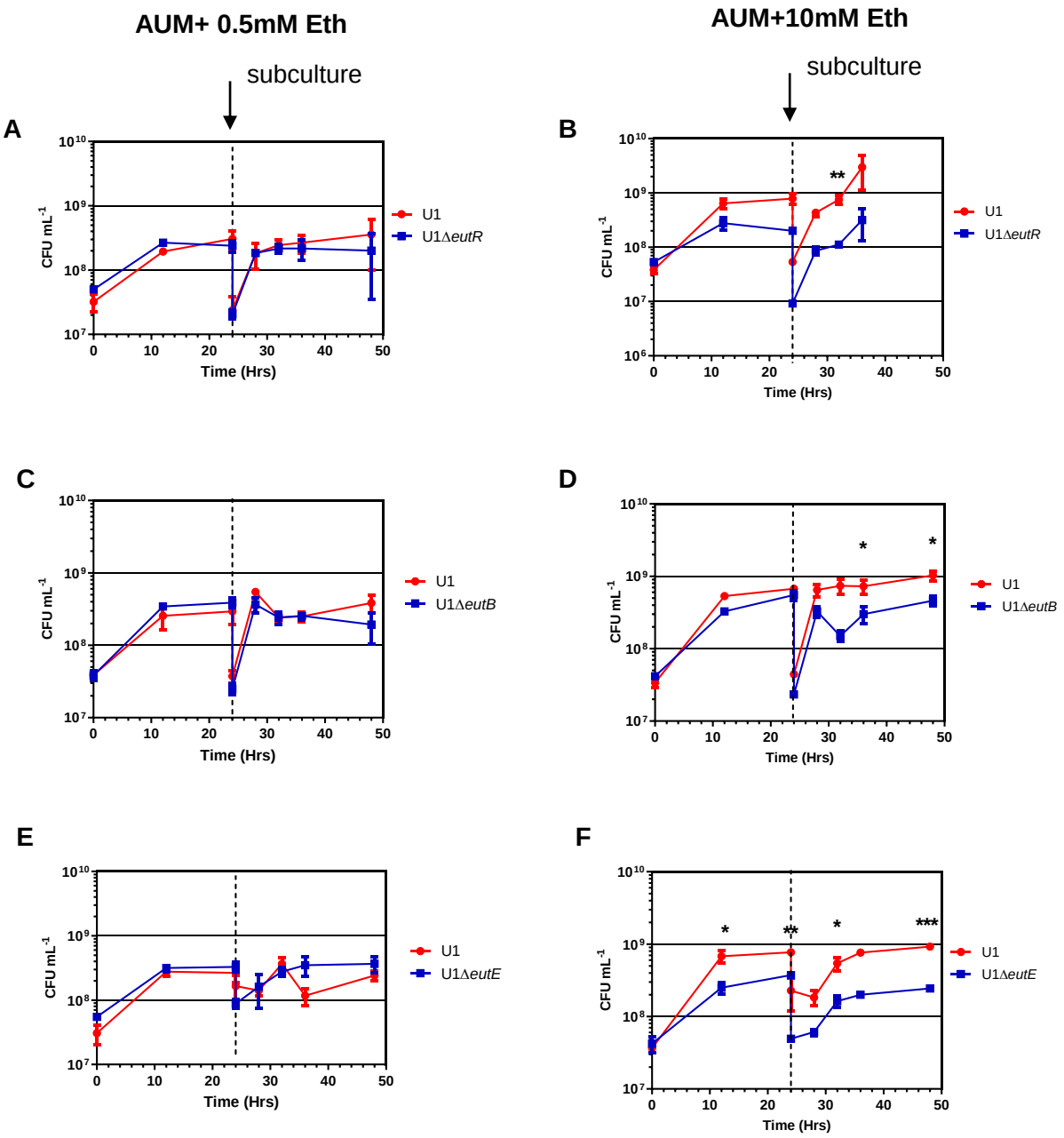

Fig4.13 Ethanolamine provides a competitive advantage for the wild type in AUM. Competition of U1 vs **A.** U1Δ*eutR* with 0.5mM ethanolamine **B** U1Δ*eutR* with 10mM ethanolamine **C** U1Δ*eutB* with 0.5mM ethanolamine **D** U1Δ*eutB* with 10mM ethanolamine **E** U1Δ*eutE* with 0.5mM ethanolamine **F** U1Δ*eutE* with 10mM ethanolamine. Student t-test or Mann Whitney U test (where appropriate) were used to compared CFU. *p<0.05, **p<0.01, ***p<0.001. Values are Mean ± SEM. N=3.

Table 4.2. Competitive index of strains grown in co-culture in AUM with 0.5mM ethanolamine. CI is calculated as described in Chapter 2. CI below 0.8 are in bold. 24 (I) indicates that the bacteria were subcultured. Values are Mean ± SEM. N=3.

	Incubation time (hrs)						
Bacterial Strains	**12**	**24**	**24 (I)**	**28**	**32**	**36**	**48**
U1/U1ΔeutR	0.95	**0.67**	1.89	0.81	0.80	**0.71**	**0.79**
U1/U1ΔeutB	1.68	2.44	**0.74**	**0.69**	1.35	1.27	**0.61**
U1/U1ΔeutE	**0.68**	1.23	**0.71**	**0.40**	**0.60**	1.06	**0.55**

Table 4.3. **Competitive index of strains grown in co-culture in AUM with 10mM** ethanolamine. CI is calculated as described in Chapter 2. CI below 0.8 are in bold. 24 (I) indicates that the bacteria were subcultured. Values are Mean ± SEM. N=3.

	Incubation time (hrs)						
Bacterial Strains	**12**	**24**	**24 (I)**	**28**	**32**	**36**	**48**
U1/U1ΔeutR	**0.37**	**0.22**	**0.13**	**0.15**	**0.11**	**0.09**	**0.10**
U1/U1ΔeutB	**0.51**	**0.72**	**0.42**	**0.52**	**0.19**	**0.42**	**0.40**
U1/U1ΔeutE	**0.36**	**0.48**	**0.36**	**0.40**	**0.28**	**0.24**	**0.26**

4.4 Discussion

During a UTI there is a lack of a dominant virulence factor associated with *E. coli* pathogenesis and colonisation of the bladder. Recent research into UPEC pathogenesis has shifted focus from virulence factors to metabolism (12, 45). In Chapter 3 of this thesis and other studies, it has been established that the *eut* operon is up-regulated in infected urine (149). While ethanolamine metabolism has been found to provide a nutritional advantage for pathogenic bacteria to compete with commensal bacteria in the gut, there are few studies exploring the role of ethanolamine metabolism in the bladder (3, 4). In this study the effect of ethanolamine on the growth of UPECs *in vitro* was investigated.

Previously, whole genome analysis of UPECs collected in this thesis established that 47 out of 48 *E. coli*'s have intact uninterrupted *eut* operons (Chapter 3). Therefore, the strains have the ability to metabolise ethanolamine to ammonia and acetate to use as a source of nitroge n and carbon (Fig 4.3) (142, 148). As *E. coli* lack the urease enzyme which breaks down urea, the main source of nitrogen in the urine, it can be assumed that urine is a relatively nitrogen limited environment for UPEC. Additionally, the high-ammonium affinity glutamine synthase and glutamate oxo-glutarate aminotransferase pathway (GS/GOCAT) for nitrogen assimilation in low nitrogen environments is induced in *E. coli* infected urine (59, 65). Previous work on enteric *E. coli* has found that ethanolamine can be utilised by *E. coli* as a sole source of nitrogen when supplemented at 30mM (3). In this study, 90% of the isolated UPECs were able to utilise ethanolamine as a sole nitrogen source at 10mM concentration *in vitro* (Fig 4.2).

The well characterised UPEC CFT073 has been shown to grow on acetate released during from amino acid metabolism (58). As ethanolamine is metabolised to acetate it is hypothesised that UPECs can use ethanolamine as a sole carbon source. However, UPECs in this study could not utilise 10mM ethanolamine as a carbon source to promote significant growth *in vitro* (Fig 4.2c). While ethanolamine has reported to be utilised as a carbon source in *Salmonella spp*. at a concentration of 20mM (148, 149), higher concentrations of ethanolamine have been reported for successful *E. coli*

utilisation as a sole carbon source (82mM, 1g L^{-1}) (218). O157:H7 EHEC strain EDL933 is unable to utilise ethanolamine as a sole carbon source even at this higher concentration despite evidence of the *eut* operon activity (3). Mutational studies in *Salmonella enterica* show that growth on ethanolamine as a carbon and energy source proceeds via the glyoxylate bypass and the Krebs cycle (148). Acetyl-coA synthetase (Acs) is required to utilise ethanolamine as a carbon source through the operation of an acetate switch (leading to eventual uptake of acetate from the culture medium)(148). Therefore, more research into these pathways in the UPECs would be needed to determine why ethanolamine cannot be utilised as a sole carbon source.

To explore the metabolism of UPECs in urine, an *in vitro* model using an artificial urine medium was used in this study to mimic the nutrient availability in urine(185). Supporting previous work, mutational studies of U1 provide evidence that the ethanolamine ammonia lyase enzyme is crucial for *E. coli* to metabolise ethanolamine to use as a nitrogen source, while breakdown of acetaldehyde by *eutE* is dispensable for growth in minimal medium with ethanolamine as a nitrogen source (Fig 4.1, Fig 4.6)(3). Contrasting with these findings, deletion of *eutE* results in loss of fitness in AUM with ethanolamine (Fig 4.7). While the ethanolamine ammonia lyase is actively breaking down ethanolamine (Fig 4.7) in the *eutE* mutant this does not correlate with enhanced growth which suggests breakdown of acetaldehyde to acetyl Co-A is needed for growth on ethanolamine in the AUM. This data coupled with the high concentration of ammonium chloride in AUM (25mM) suggests that ethanolamine is utilised as an additional source of carbon in AUM and not nitrogen. Another possibility is that the acetaldehyde accumulation by deletion of *eutE* is causing a toxic effect. Despite the formation of the MCP, which is proposed to prevent the toxicity of acetaldehyde in ethanolamine metabolism, there is evidence for low level of intermediates being released (219, 220). Differential toxicity from ethanolamine metabolism in *eutE* deletion mutants has been observed in *Salmonella* depending on added carbon source in minimal medium. For example added ethanolamine prevents growth in the presence of succinate

(149). There is some evidence of growth inhibition with increasing levels of ethanolamine added to a *eutE* deletion mutant in AUM (see Appendix 4.3). Further Investigation into the production of acetaldehyde or acetyl-CoA would be needed to determine how ethanolamine is being utilised in AUM.

An unexpected double mutation provided further evidence that ethanolamine utilisation stimulates growth by different mechanisms in nitrogen-limited M9 Mod and AUM media (Fig 4.7a). When the U1Δ*eutR* mutant was created via P1 transduction, an additional insertion between between *eutA* and *eutB* was introduced to the strain. The CRZ-55 prophage previously seen in the widely used lab strain MG1655 (2, 204) and the KEIO parental strain BW25113 (183, 211), is inserted between *eutA* and *eutB*. The prophage is inserted in reverse orientation to *eut* operon transcription (Appendix 4.2). As *eutR* has only one binding site in the *eut* operon, the presence of the prophage prevents the genes down-stream of *eutA* from being transcribed, including the ethanolamine ammonia lyase enzyme (141). As predicted, complementation of this mutant with the intact *eutR* ASKA clone did not rescue the phenotype in Mod M9 with ethanolamine after 24hrs, as the transcription of the ethanolamine ammonia lyase remains interrupted. However, incubation of *eutR*/pCA24N::*eutR* in Mod M9 with ethanolamine for longer than 30hrs shows restoration of growth. PCR analysis of the resulting strains shows that the prophage excises during prolonged nutritional stress (Fig 4.8). Natural excision of the CPZ-55 prophage has been described before in K12 BW25113 (221). In AUM, the growth phenotype was immediately restored from time zero with 10mM ethanolamine by *eutR* complementation (Fig 4.7a). There was minimal depletion of ethanolamine in the media suggesting this is not due to prophage excision during growth in AUM enabling transcription of *eutBC* and retention of the prophage in AUM after 30hrs was also confirmed by PCR (Appendix 4.5). The insertion of the prophage could result in the overexpression of the proximal portion of the operon, including *eutD*, *eutG* and *eutE* (5). These enzymes could interact with other metabolites in the media to convey this growth advantage. Due to the complexity of the media it is unclear which metabolite it could be utilising (185).

mRNA analysis showed that the *eut* operon was upregulated early (4-8hrs post inoculation) when cultured in growth in AUM (Fig 4.8). As the importance of rapid growth for UPEC survival in the bladder has been established, early induction of the *eut* operon is providing evidence of rapid metabolic adaption (50). Interestingly, with induction of the operon, coincided with upregulation of *eutS*, a shell protein involved with the formation of the ethanolamine BMC. This has also been seen previously in EHECs (3). In this study BMC were visible in U1 when grown in AUM with 10mM ethanolamine. While visualisation of the Eut BMC in *Salmonella* and *E. coli* K-12 has been reported previously, there is no previous depiction of wild-type Eut BMC in pathogenic *E. coli* that the author could find in the literature.

When U1 and its associated strains were grown in Mod M9 with 0.5mM ethanolamine, physiological levels (Chapter3,(47)), the wild type, U1Δ*eutE* and complement Δ*eutE* and Δ*eutB* grew to an OD_{600nm} of 0.08, while the other knockout mutants did not display any growth. Growth of these strains starts at 4hrs post incubation as was seen when U1 is grown Mod M9 with 10mM as the sole nitrogen source and therefore implies ethanolamine is being utilised to facilitate this small increase in OD_{600nm} (Appendix 4.1a). In AUM there is a significant enhancement in growth, by $1.5x10^8$ compared to the wild type strains in AUM and 0.5mM ethanolamine after 8 hours of growth (Fig 4.12). This directly contradicts the assertion that ethanolamine below 1mM does not support growth due to energy requirements needed for the metabolism of the ethanolamine (6).

Previous work has found that deletion of the *eut* operon results in a fitness deficiency in *E. coli* in the UTI mouse model (17). In AUM, 10mM ethanolamine conferred a competitive growth advantage to U1 *in vitro* over an isogenic *eutR* mutant (Fig 4.13). *E. coli* engineered for enhanced amino acid uptake which conferring faster growth than the wild-type parental strain when cultured separately, lose their competitive advantage in co-culture (222). This is because enhanced amino acid uptake and subsequent amino acid metabolism results in ammonia leakage from the engineered cells which can be utilised by the competing wild-type bacteria. The preserved competitive advantage of U1 over Δ*eutR* and Δ*eutB* strains in AUM in the

presence of ethanolamine suggests that either ammonia is not being released from the cell when ethanolamine is utilised as a nitrogen source, or the competitive advantage conferred by ethanolamine metabolism in AUM is based on relief of carbon restriction rather than nitrogen restriction. The contrasting phenotype of Δ*eutE* mutants in nitrogen-restricted M9 Mod with ethanolamine (growth) and AUM with ethanolamine (no growth), and the preserved advantage of wild type U1 over the Δ*eutE* mutant in competitive co-culture in AUM with ethanolamine suggests that ethanolamine provides an additional carbon and energy source in AUM.

When competition was assessed using physiological levels of ethanolamine (0.5mM), there was a small competitive advantage over the *eutR* mutants. Batch culture with physiological levels of ethanolamine in AUM provides a limited window to observe ethanolamine-conferred advantages given that *E. coli* uses it at a rate of 0.75mM/hour after a lag period of 4 hours in this medium (Fig 4.4). Therefore, all ethanolamine would be consumed in the first 5 hours post inoculation compared to over 12 hours for 10mM ethanolamine, and onward metabolism of acetate and ethanol also concluding sooner. The advantage seen of $1.5x10^8$ would be hard to distinguish in a competition assay. Unlike this static model urine is continually being produced and *in vivo* would confer a continual supply of host-derived ethanolamine, passing into the bladder which could provide a competition advantage *in vivo* as seen by Subashchandrabose et al. (9). A continuous culture system would be required to replicate this.

In conclusion, this study has found that UPECs isolated from urine can utilise ethanolamine as a sole nitrogen source. In the *in vitro* artificial urine medium model, ethanolamine also provides a competitive nutritional advantage for UPEC. However, there was evidence ethanolamine was being used as a carbon source in these conditions. Further work is required to confirm this. As a result, the nutritional supplement provides a competitive advantage to bacteria that can metabolise ethanolamine over bacteria that are unable to metabolise ethanolamine. Therefore, ethanolamine in urine appears to be an important nutritional resource that infecting *E. coli* can access by microcompartment- mediated metabolism.

4.5 Appendix

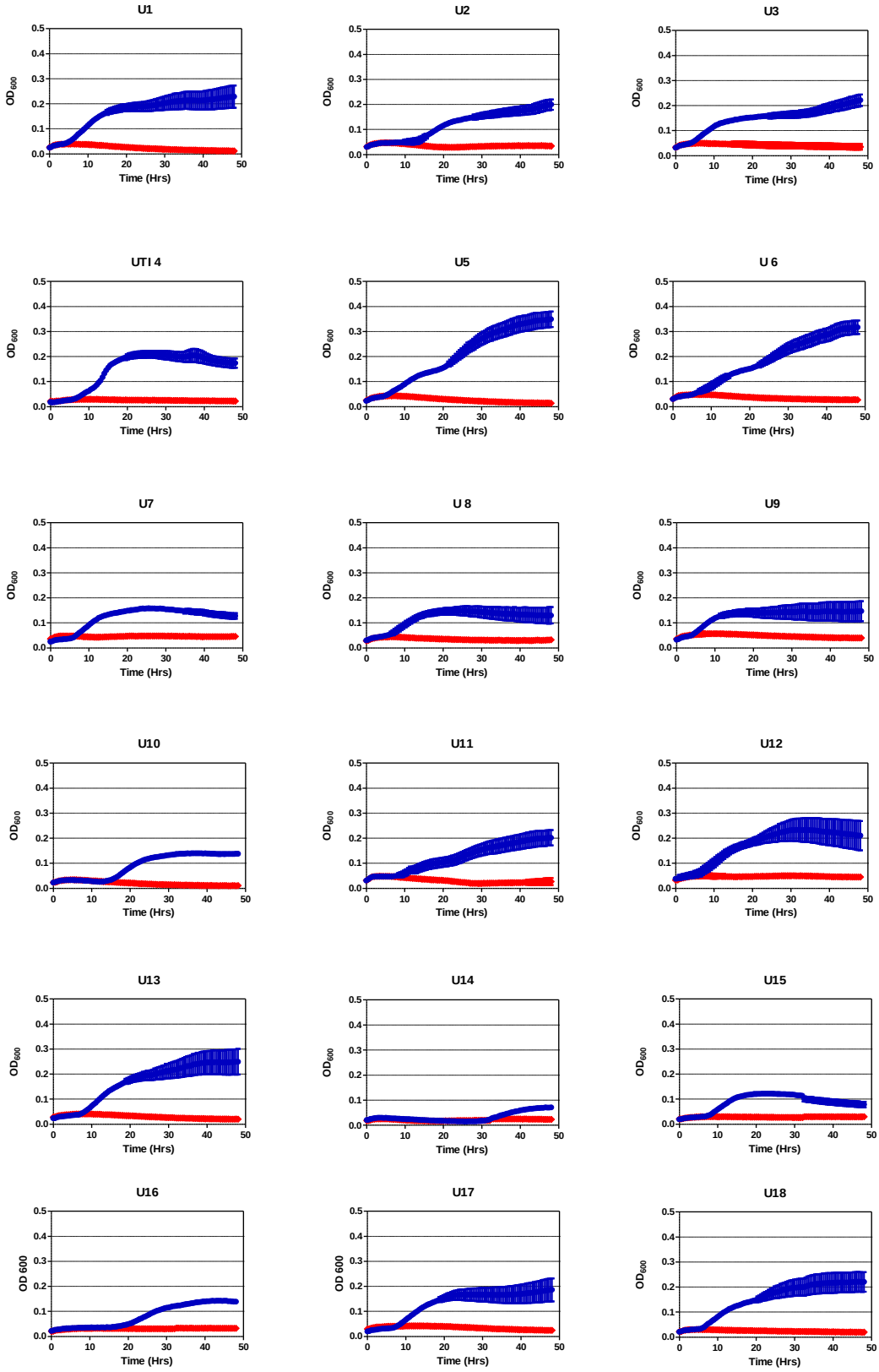

Appendix 4.1a. Automated growth curve of UPEC isolates U1-18 grown in ammonia free modified M9 (red) and ammonia free modified M9 supplemented with 10mM Ethanolamine as nitrogen source. Values are Mean ± SEM. N=3.

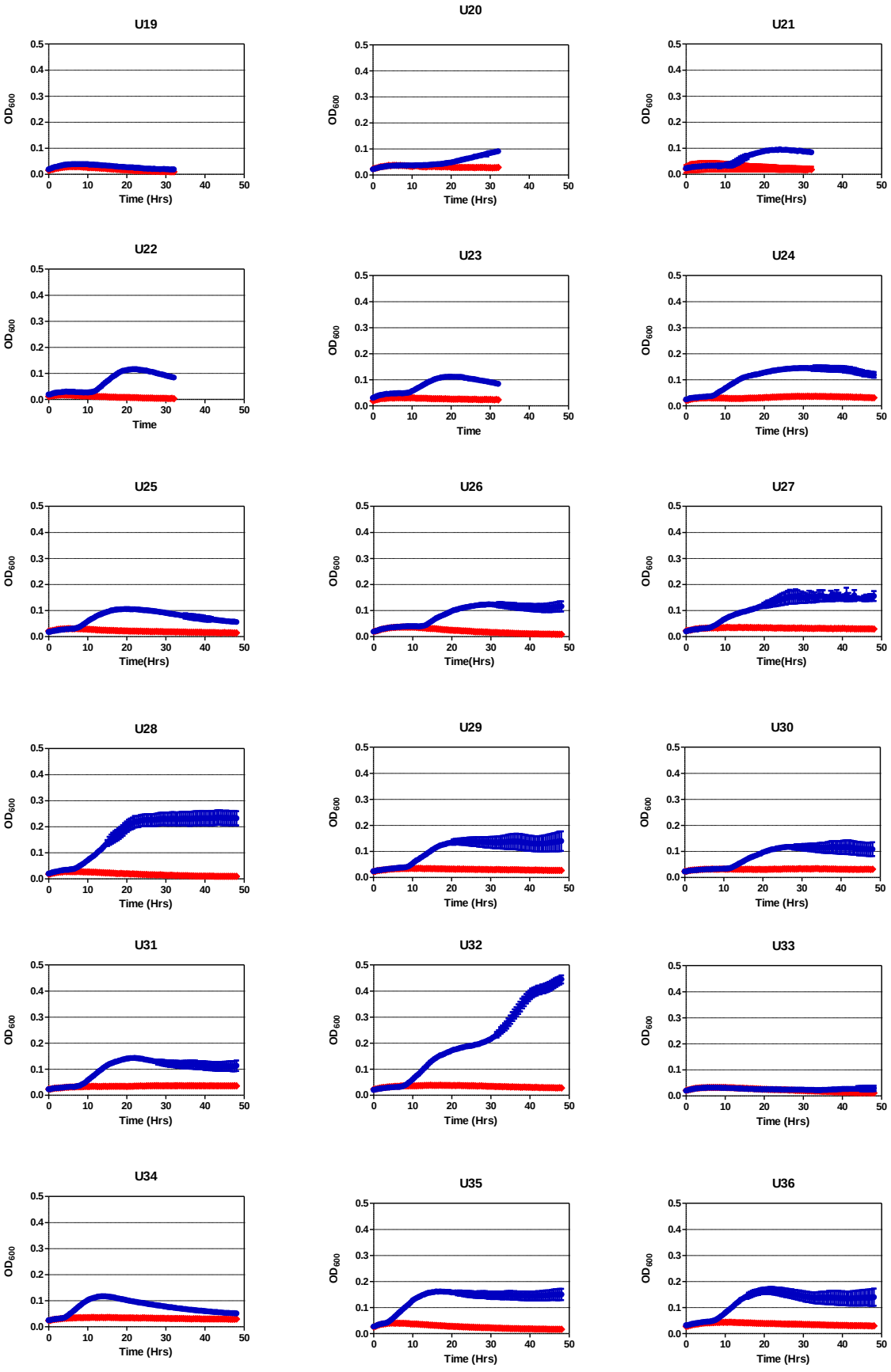

Appendix 1b Automated growth curve of UPECs U19-36 grown in ammonia free modified M9(red) and ammonia free modified M9 supplemented with 10mM Ethanolamine as nitrogen source. Values are Mean ± SEM. N≥3.

.

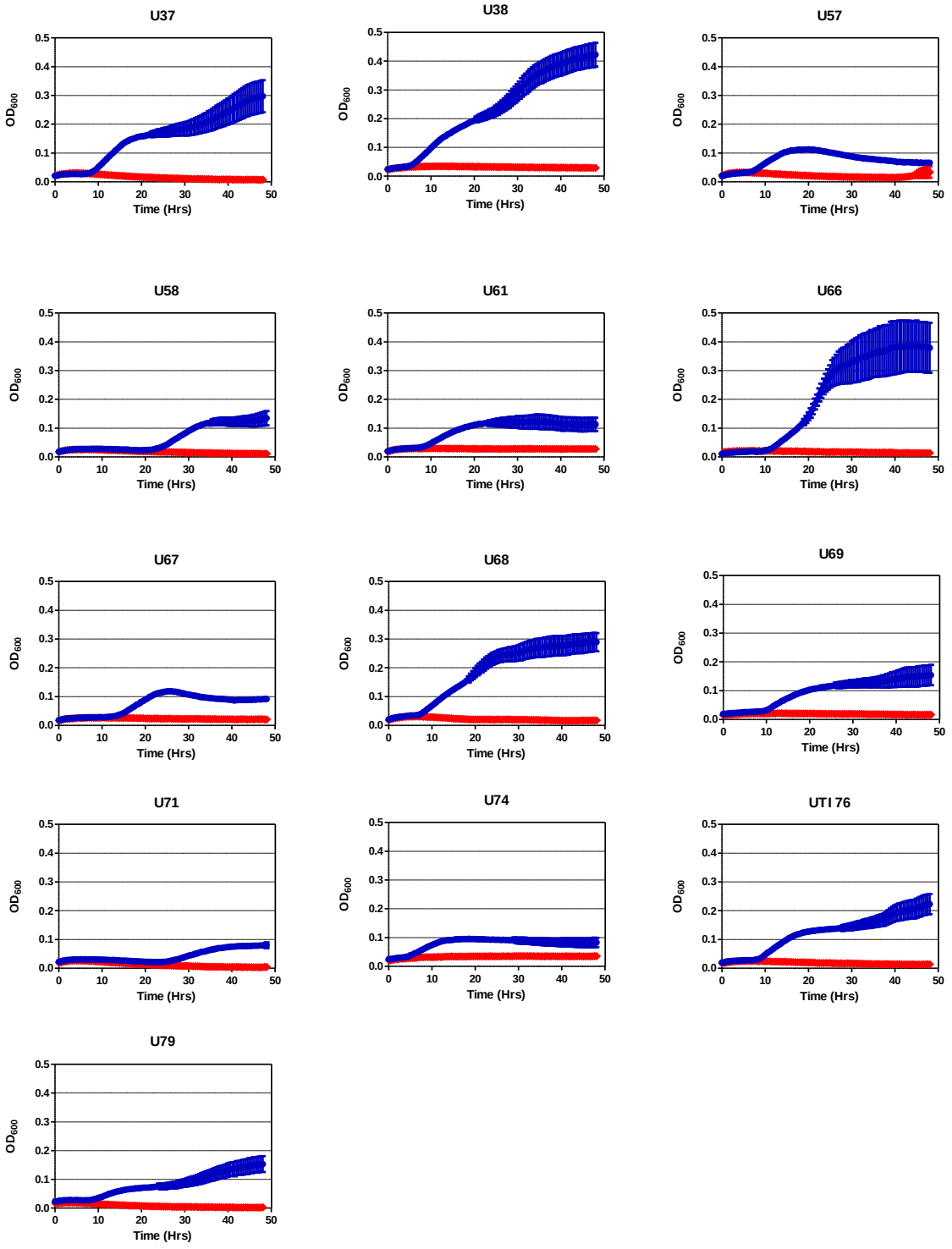

Appendix 4.1c Automated growth curve of UPEC isolated 37-79 grown in ammonia free modified M9(red) and ammonia free modified M9 supplemented with 10mM Ethanolamine as nitrogen source. Values are Mean ± SEM. N≥3.

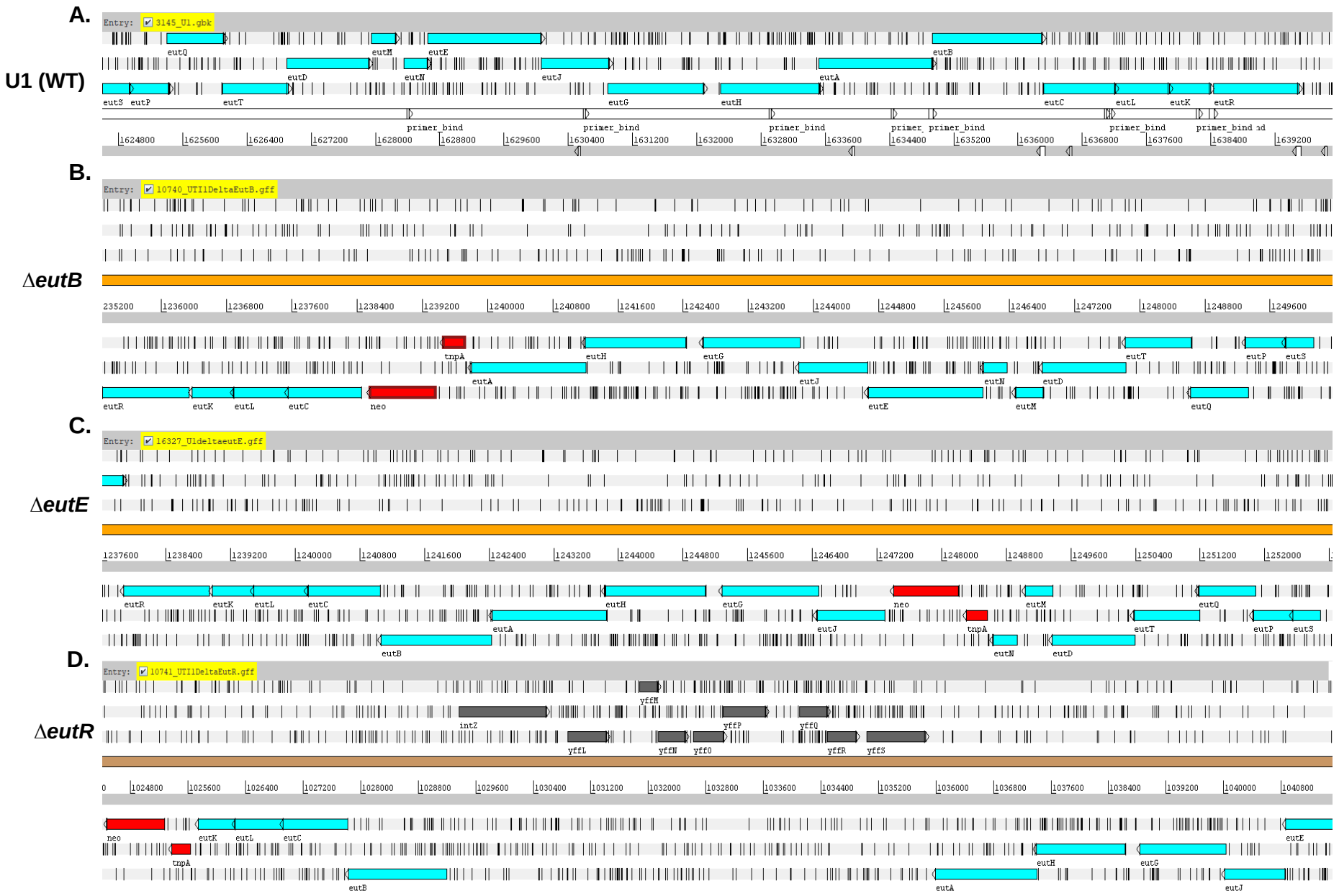

Appendix 4.2.*eut* operon of U1 and respective mutants. **A** U1 (wild type) **B.** U1Δ*eutB* **C**. U1Δ*eutE* **D.** U1Δ*eutR* -prophage between *eutA* and *eutB*. Blue genes are eut operon genes; Red genes are kanamycin cassette insertion; Black genes of CPZ-55 prophage insertion.

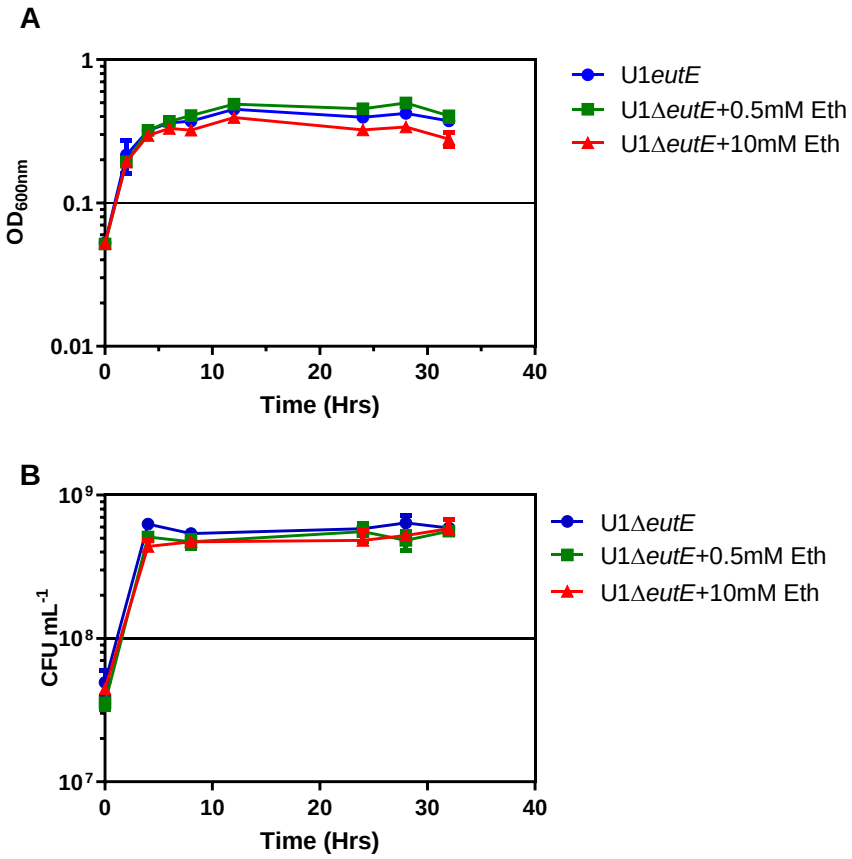

Appendix 4.3. Growth of U1Δ*eutE* in AUM with 0mM (Blue), 0.5mM (Green) and 10mM (Red) ethanolamine. Growth is measured by A. OD_{600} and B CFU ml^{-1}. Values are Mean ± SEM N ≥3.

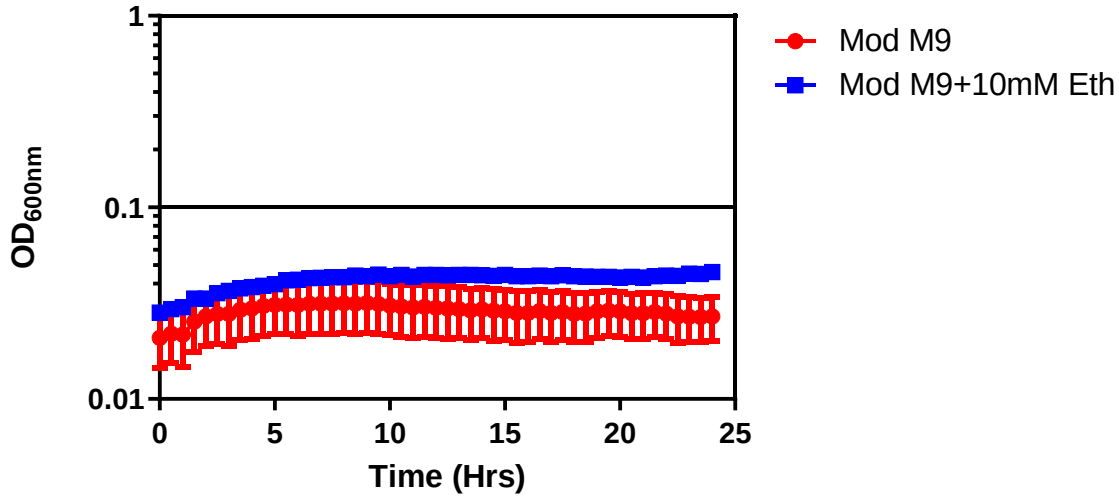

Appendix 4.4 Growth of K-12 MG1655 in Mod M9 with 10mM ethanolamine. Values are Mean ± SEM N ≥3.

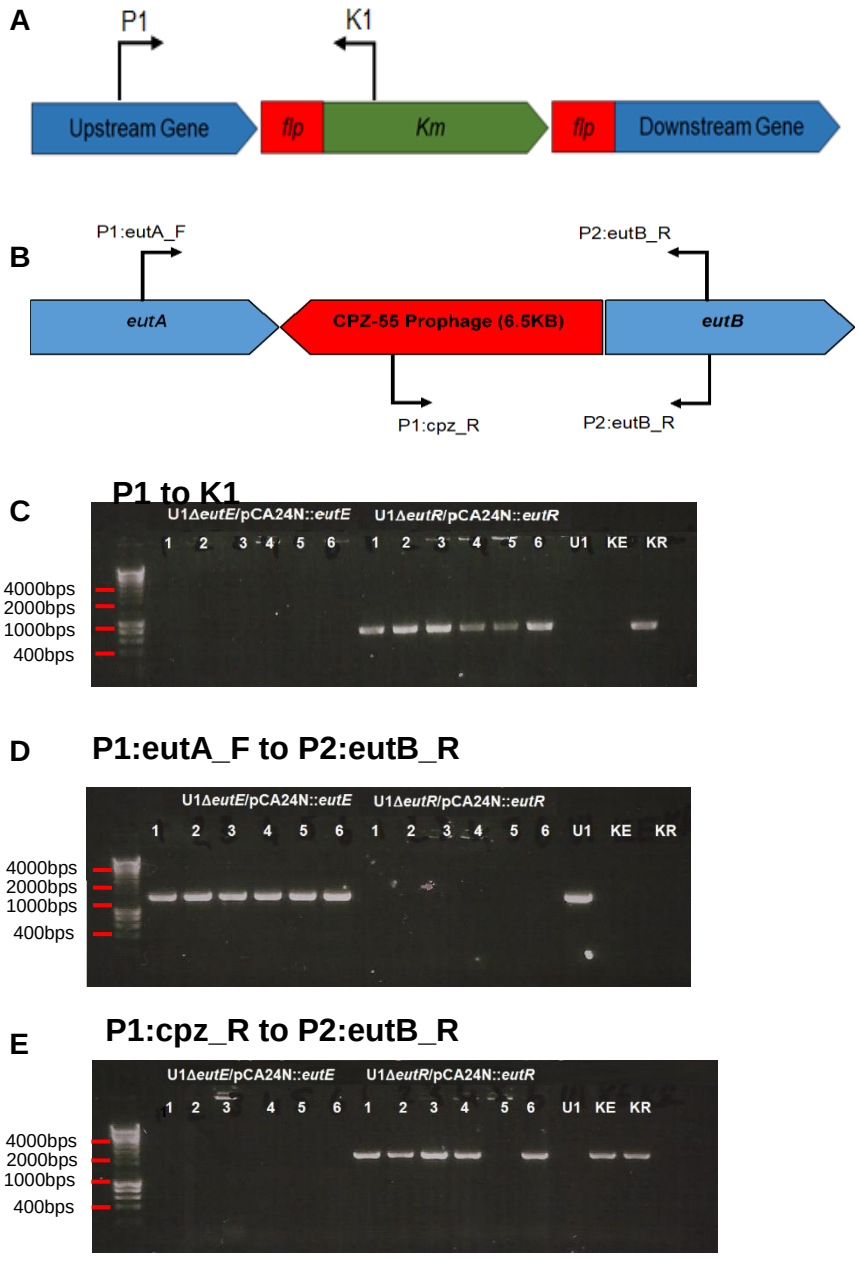

Appendix 4.5. Prophage does not excise when U1Δ*eutR*/pCA24N::*eutR* is grown in AUM with 10mM Ethanolamine. **A.** Schematic of PCR over the kanamycin cassette border. **B.** Schematic of PCR over Prophage border. **C.** Gel image to confirm the presence of the kanamycin cassette in place of *eutR*. **D.** Gel image across the border of *eutA* and *eutB* **E.** Gel image over prophage border with *eutB.* Lanes: **1.** AUM.1 **2.** AUM.2 **3.** AUM.3 **4.** AUM+10mM Eth.1 **5.** AUM+10mM Eth.2 **6.** AUM+10mM Eth.3. KE is the Keio strain JW2439-1. KR is Keio strains JW2430-1.

Chapter 5 Investigation into Ethanolamine Regulation of Virulence Factors in Uropathogenic *E. coli*.

5.1 Abstract

Colonisation of a host is dependent on the pathogen's ability to acquire nutrients and express virulence factors. Ethanolamine can be used by bacteria as a nutrient as shown in Chapter 4 and has more recently been seen to regulate the expression of virulence genes in enteric pathogens (3, 4, 6-8, 16, 168). The regulator *eutR* has been found to directly regulate the expression of the locus of enterocyte effacement (LEE) in EHEC and the *Salmonella* Pathogenicity island 2 (SPI-2) (7, 16). Additionally, ethanolamine has been seen to promote the expression of fimbriae in EHEC (8). Fimbriae are key colonisation factors for uropathogenic *E. coli* (UPEC) during urinary tract infection (UTI) and for long term colonisation of the gastrointestinal (GI) tract (9, 223). Recent expression analysis has shown that the *eut* operon is upregulated *in vivo* during UTI, therefore it can be hypothesised that ethanolamine may be a regulator of fimbriae and other virulence factors in UPECs in different environments (10, 17).

In this study the ability of ethanolamine to promote virulence factors in UPECs was investigated *in vitro*. The ability of two UPEC strains to produce fimbriae in the presence of ethanolamine was measured by agglutination and cell attachment assays. Ethanolamine did not affect these phenotypic assays of fimbriae; however ethanolamine appears to influence the ability of a *eutR* mutant of UPEC strain U1 to invade bacterial epithelial cells *in vitro*. Gene expression analysis in artificial urine media (AUM) detected differential expression of *fimE* and *fimH* type 1 fimbrial operon genes in UPEC strain U1 in the presence of ethanolamine after 8 hours. Therefore, these studies suggest that ethanolamine may enhance fimbriae expression in AUM in some UPEC strains, however further studies would be needed to confirm these findings phenotypically.

5.2 Introduction

The ability of a pathogen to colonise a host environment and cause infection is controlled by the acquisition of nutrients and the expression of virulence factors. Ethanolamine which is derived from the host can be utilised by bacteria as a nutrient through its catabolism by a series of enzymatic reactions encoded in the ethanolamine utilisation (*eut*) operon (3, 13). A form of the 17-gene *eut* operon was first identified in *Salmonella sp*. is conserved across many species of bacteria (5, 224). Comparative genome analyses of pathogenic bacteria have associated the presence of the *eut* operon with the ability to cause infection (138, 167, 225). However, it is unclear whether this is due to ethanolamine metabolism itself or via another mechanism.

Ethanolamine metabolism can promote a growth advantage for bacteria by being utilised as a nutrient as has been seen in *E. coli* (Chapter 4) (3). Induction of *eut* operon genes has also been detected in intracellular *Listeria monocytogenes* (170). *L. monocytogenes* are intracellular pathogens that invade epithelial cells as part of their infective cycle. Mutations within the ethanolamine ammonia lyase enzyme major subunit gene (*eutB*) reduces invasion of the epithelial cell line, Caco-2, by *L. monocytogenes* compared to the wild type, suggesting ethanolamine metabolism is important for cell invasion (170). Similarly, to *L. monocytogenes*, metabolism of ethanolamine provides a colonisation advantage for *Salmonella enterica* serotype Typhimurium (*S.* Typhimurium) in the GI tract. However the ability of *S.* Typhimurium to gain a growth advantage by ethanolamine metabolism in the anaerobic environment of the GI tract is dependent on the presence of inflammation derived tetrathionate as a final electron receptor (4, 172). Further work in *S.* Typhimurium reveals that while mutants in *eutB* and *eutC*, and therefore ethanolamine metabolism, were attenuated in colonising the mouse intestine, mutation in *eutR,* the operon regulator caused a greater colonisation defect when disseminating to other niches within the host such as within macrophages (16). This therefore suggests that the *eut* operon has a role in pathogenesis independent of ethanolamine metabolism.

In *S.* Typhimurium and Enterohaemorrhagic *E. coli* (EHEC), the *eut* operon has been found to directly regulate virulence factors. *S.* Typhimurium is a

facultative intracellular pathogen, invading epithelial cells and macrophages in the GI tract to cause acute gastroenteritis. Survival within the macrophage is mediated by the expression of type three secretion systems (T3SS) that are encoded on Salmonella pathogenicity island 2 (SPI-2)(175). EutR was found to regulate expression of T3SSs by directly binding the promoter of *ssrB,* the regulator of SPI-2, and aid survival in macrophages and progression to systemic infection (16). Ethanolamine also mediates the expression of virulence factors in EHEC (6-8). EHECs bind to the epithelium of the intestine and form attaching and effacing (AE) lesions which destroy the structure of the villi and cause diarrhoeal disease (226). The majority of the genes needed for the formation of AE lesions are found on the locus of enterocyte effacement (LEE) Pathogenicity Island. EHEC preferentially bind to phosphatidylethanolamine phospholipids in enterocytes during infection, the source of ethanolamine in the host (214). Studies have found that ethanolamine upregulates genes involved in EHEC virulence which include *ler*, the transcriptional regulator of the LEE operon, histidine sensor kinases *qseC* and *qseE,* and Shiga toxin *stx* (6). Expression of these virulence genes are independent of ethanolamine metabolism and later experiments confirmed that *eutR* directly binds to *ler* to regulate the transcription of the LEE operon (7). These studies however did reveal that micromolar concentrations of ethanolamine which induced the LEE operon did not induce expression of *eutR,* and therefore there may be an unidentified regulator that is responsible for ethanolamine-dependent virulence gene expression at these concentrations (6). More recently ethanolamine has been shown to promote expression of putative and characterised fimbriae which facilitate EHEC attachment to HeLa cells, however only a minority of the fimbriae induced by ethanolamine were regulated by *eutR*, again indicating the presence of another regulatory gene responding to ethanolamine (8).

In addition to a role in intestinal infection the *eut* operon has found to be upregulated during UTI (17). Within the urinary tract *E. coli* utilise many virulence factors to colonise and cause infection. Adherence is crucial to *E. coli* survival in the urinary tract and as such uropathogenic *E. coli* (UPEC)

can encode at least 12 fimbriae in its genome (227). Type 1 fimbriae mediate the attachment and subsequent invasion required for formation of bacteria type communities in bladder epithelium cells (BECs) (41, 90, 91). Close association between infecting *E. coli* and host cells in urine has been seen in Chapter 3 of this thesis (Fig 3.8). Deletion of type 1 fimbriae results in colonisation defects in mouse urinary tract infection models (91).

As the *eut* operon has been found to regulate expression of virulence factors in EHEC, and ethanolamine has been found to enhance growth of UPECs *in vitro* (Chapter 4), and regulate *eut* operon genes in infected urine (Chapter 3), it can be hypothesized that ethanolamine may promote expression of virulence factors in UPECs to assist colonisation of the urinary tract, as has been seen in EHEC in the intestine. This study extends the findings from Chapter 3 and 4 and investigates whether ethanolamine could provide a regulatory role for virulence genes involved with UPEC pathogenesis. The ability of UPECs to produce fimbriae in the presence of ethanolamine were investigated using an agglutination assay and by measuring adherence to and invasion of the cell line HT1376. In addition, gene expression of U1 in AUM was examined for the expression of fimbriae.

5.3 Results

5.3.1 Strain U1 binds erythrocytes via mannose resistant fimbriae

During UTI bacteria attach to epithelial cells to colonise the urinary tract. They do this by forming fimbriae which bind to receptors on the Bladder Epithelial Cells (BEC) surface. To detect fimbriae formation by UPECs, bacteria were incubated with guinea pig erythrocytes (Chapter 2) to measure haemagglutination. The UPEC strains U1, U13, U17 and U38 were grown in fimbriae-inducing conditions (statically) in LB media in the presence or absence of 10mM ethanolamine. U1, U1Δ*eutB*, U1Δ*eutR* and U38 have high haemagglutination titres (2^{3-4}) when grown in LB compared to U13 and U17 where haemagglutination does not occur (Fig 5.1b). Growth in the presence of ethanolamine did not cause a significant difference in the ability of the UPECs to cause haemagglutination, however there does appear to be a decrease in the agglutination ability of U1 in the presence of ethanolamine (Mann Whitney-U test) (Fig 5.1b).

To assess whether the fimbriae produced by U1, U1Δ*eutB*, U1Δ*eutR* and U38 were mannose sensitive, which is characteristic of type 1 fimbriae, the bacterial dilutions were incubated with 4% mannose before the erythrocytes were added. After overnight incubation with erythrocytes, U38 was unable to bind to erythrocytes and unable to cause haemagglutination (Fig 5.1c). U1, U1Δ*eutB* and U1Δ*eutR* were however still able to bind to erythrocytes after incubation with 4% mannose indicating the fimbriae expressed by U1 are mannose resistant (Fig 5.1c).

In parallel to the haemagglutination assay, the expression of type I fimbriae was tested with a yeast agglutination assay. The UPECs were grown overnight in fimbriae-inducing conditions with and without 10mM ethanolamine. Bacteria were incubated with 1% *Saccharomyces cerevisiae* and agglutination was determined after 10mins as being positive (+) or negative (-). Agglutination was only detected in U38 and this was prevented with the addition of mannose (Table 5.1). This suggest that U38 is the only strain to produce mannose sensitive fimbriae in these conditions confirming the observation shown by the haemagglutination assay.

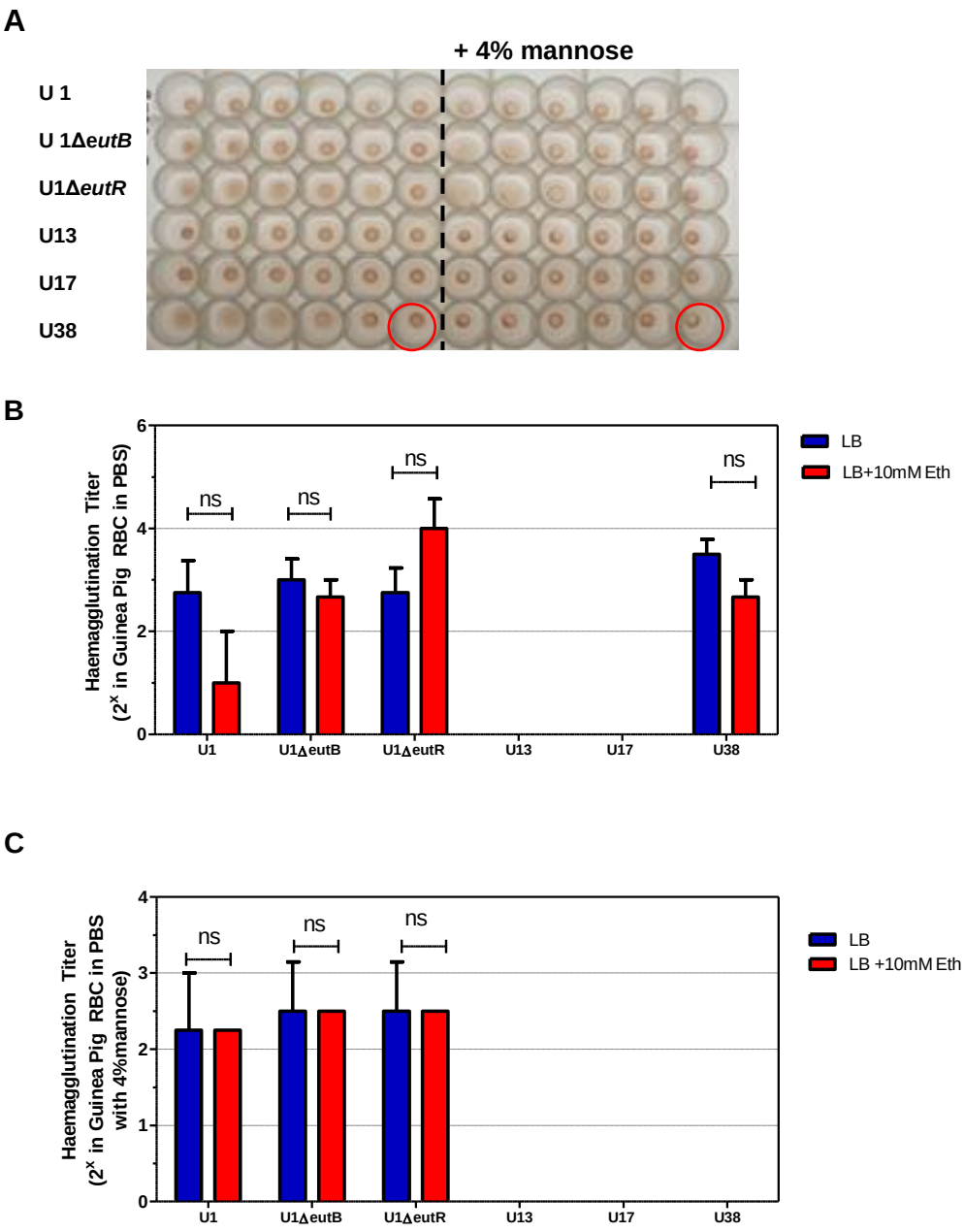

Figure 5.1 UPECs bind to Guinea Pig red blood cells. **A**. Photo representation of haemagglutination. Negative PBS/PBS+4% mannose controls are circled in red. Haemagglutination titre of bacteria grown statically overnight in LB or LB+10mM ethanolamine and incubated with: **B** defibrinated guinea pig erythrocytes; **C** defibrinated guinea pig erythrocytes and 4% mannose. Values are Mean ± SEM N=4

5.3.2

Table 5.1 Yeast Agglutination Assay. + indicates positive agglutination and – indicates negative agglutination after 10minutes incubation with 1% Saccharomyces cerevisiae. Values are Mean ± SEM N=3

			4% Mannose	
Bacterial Strain	LB	LB+10mM EA	LB	LB+10mM EA
U1	-	-	-	-
U1Δ*eutB*	-	-	-	-
U1Δ*eutR*	-	-	-	-
U13	-	-	-	-
U17	-	-	-	-
U38	+	+	-	-

5.3.3 Ethanolamine does not affect *E. coli* adhesion to human bladder epithelial cell line HT1376

To assess whether utilising ethanolamine alters the ability of U1 and U13 to attach to epithelium, a cell culture model was set up using the bladder epithelial carcinoma cell line, HT1376. The bacteria were cultured with the epithelial cells for 3 hours before the epithelial cells were removed, lysed and the lysate containing attached bacteria plated on agar. Comparing the CFU ml^{-1} of U1 and the *eut* knock out mutants, U1Δ*eutB* and U1Δ*eutR*, there was no significant difference in the ability of the mutants to colonise the epithelial cells compared to the wild type (ANOVA) (Fig 5.2a). However, there was a significant difference in adherence of U1 and the *eut* mutants compared to U13 and HM605, a well-studied adherent-invasive *E. coli* strain, which was used as a positive control in this study ($p<0.001$, 1-way ANOVA) (Fig 5.2). This increase in adherence is not attributed to an increase in growth rate, as all bacteria grow to the same OD_{600nm} after 3-hour incubation in DMEM (Appendix 5.1). Comparing the difference in adherence within strains, the metabolism of ethanolamine does not appear to enhance adherence to epithelial cells. There was no significant difference in the ability of individual strains to bind with the addition of ethanolamine to the cell culture (Mann Whitney-U test) (Fig 5.2). This suggests that the ability of the *E. coli* to produce fimbriae in the presence of epithelial cells is unaffected by the ability to detect or metabolise ethanolamine.

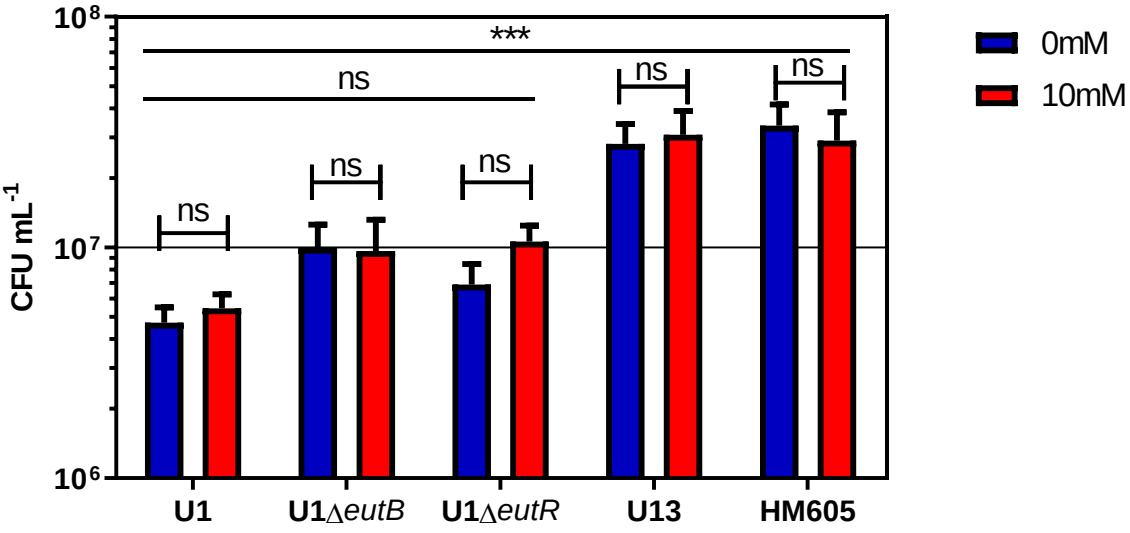

c**Figure 5.2 Association of *E. coli* to HT1376**. CFU ml^{-1} of bacteria associated with HT1376 after 3 hours incubation in low glucose DMEM with and without 10mM ethanolamine. Comparison by Mann Whitney U. Values are Mean ± SEM N=3

5.3.4 UPEC do not easily invade bladder epithelial cells HT1376

During infection UPEC evade the host immune system by invading epithelial cells and replicating to form intracellular bacterial communities, and this is facilitated by the formation of fimbriae (90). Therefore the ability of UPEC strains to invade BECs was measured using a BEC cell lysis model similar to section 5.3.2 with an additional step in which adherent bacteria were killed with gentamicin prior to lysis (Chapter 2). Comparing the CFU ml^{-1} of bacteria that invade the epithelial cells, there is no significant difference in the ability of different bacterial strains to invade the BECs (ANOVA), however U13 and the adherent invasive *E. coli* HM605 appear to invade in higher numbers compared to U1 strains. When ethanolamine was added to the incubation media, no significant difference was calculated between DMEM and DMEM with 10mM ethanolamine in most strains, however U1Δ*eutR* there was a decrease in CFU ml^{-1} recovered when incubated in the presence of ethanolamine ($p<0.05$, Mann Whitney-U test) (Fig 5.3).

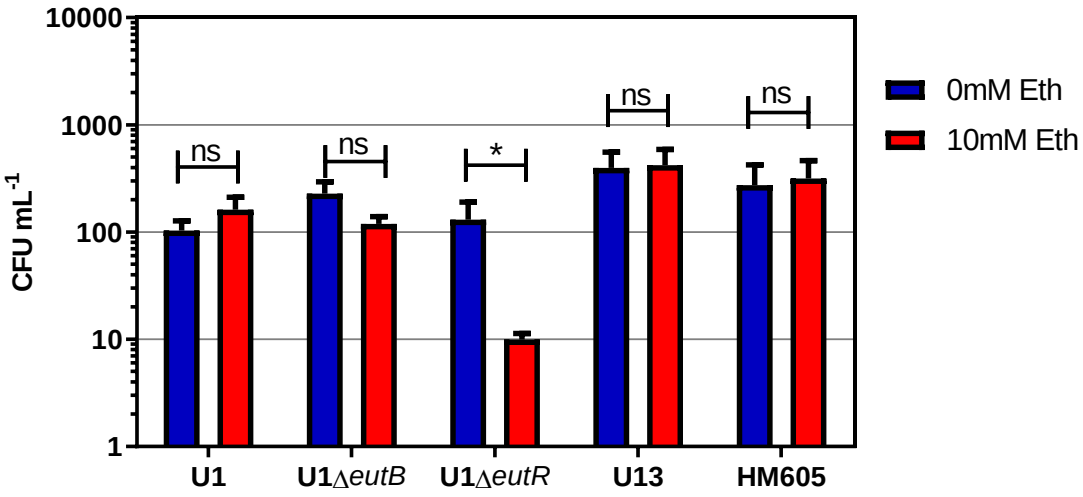

Figure 5.3 Invasion of *E. coli* in HT1376. **A**. CFU ml^{-1} of bacteria invasion of HT1376 after 4 hours incubation in low glucose DMEM with and without 10mM ethanolamine. Comparison by Mann Whitney U. Values are Mean ± SEM N=3

5.3.5 Expression of Fimbriae in Artificial Urine Medium (AUM)

In Chapter 4 *E. coli* metabolism of ethanolamine was assessed for its ability to cause a growth advantage in AUM. RNA analysis showed that the *eut* operon was upregulated during growth in AUM with ethanolamine, with highest expression after 4 hours and 8 hours of growth (Chapter 4, Fig 4.7). However it was not assessed whether expression of the *eut* operon regulated the expression of genes known to be involved with virulence. As there is evidence of ethanolamine regulating epithelial invasion (Fig 5.3) which is mediated by type 1 fimbriae (90), expression of the *fim* operon that encode type 1 fimbriae was measured in RNA from U1 and U1Δ*eutR* grown in AUM (Chapter 4).

The expression of *fimE*, the phase variation recombinase which regulates expression of the *fim* operon, and *fimH,* the adhesion protein that tips the fimbriae and facilitates binding to mannose residues on epithelial cells, was detected in U1(40, 228). In AUM the expression of *fimE* and *fimH* was highest after 8 hours incubation, with 10mM ethanolamine (Fig 5.4 a). The expression of *fimE* after 8 hours with 10mM ethanolamine was not significantly different compared to 4hrs and 24hrs incubation (Kruskal-Wallis test). However there was a significant difference in *fimE* expression when the effect of different concentrations of ethanolamine was measured at 8 hours (Kruskal-Wallis test, $p<0.05$) (Fig 5.4a).

There was a significant 50-fold increase in *fimH* expression between 4 hours and 8 hours when U1 was grown in 10mM ethanolamine (Kruskal-Wallis test, $p<0.05$) (Fig 5.4a), and similarly to *fimE* there was a significant different in *fimH* expression when the effect of different concentrations of ethanolamine was measured at 8 hours (Fig 5.4 a). The expression of *fimH* was measured in the *eutR* knockout mutant at 8 hours, when expression of *fimH* appears to be highest in U1. A 30-fold decrease in expression in the U1Δ*eutR* was measured compared to U1 when grown in AUM with 10mM ethanolamine, this difference however was not significant (Mann-Whitney U) (Fig 5.4 b). These results suggest that ethanolamine does affect type 1 fimbriae expression in AUM and this may be at least partly mediated by *eutR*.

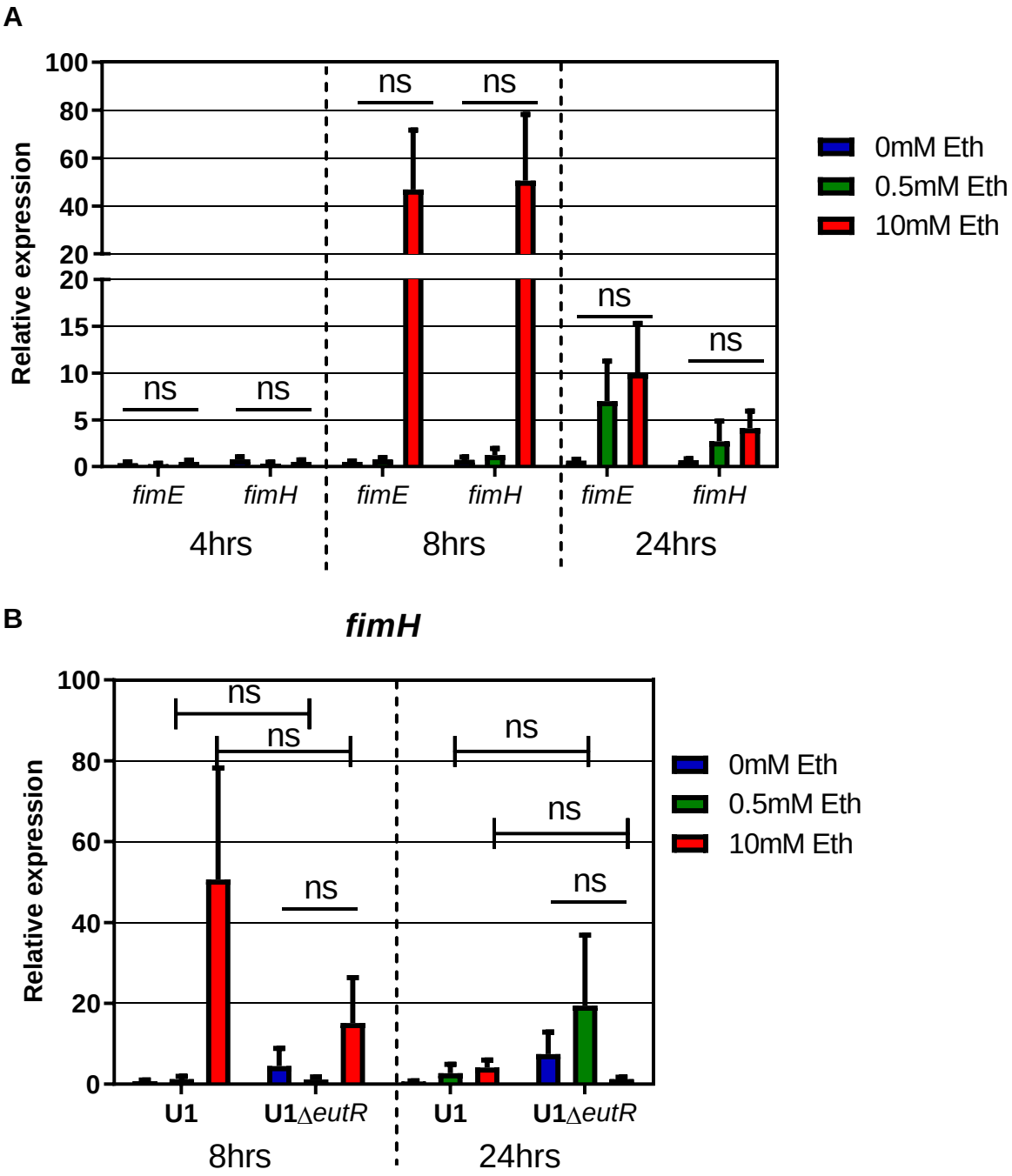

Figure 5.4 Expression of type 1 fimbrae A. Relative expression of *fimE* and *fimH* in U1 after 4, 8 and 24hours growth in AUM with different concentration of ethanolamine. **B**. Relative expression of *fimH* in U1 and U1Δ*eutR* 8 hours growth in AUM with different concentration of ethanolamine. Relative expression to the geometric mean of housekeeper genes *rrsA* and *gyrB*. Comparison by 1-way ANOVA (straight line) or Mann Whitney U (edged line). Values are Mean ± SEM N=3.

5.4 Discussion

Pathogens express virulence factors to colonise and acquire nutrients within the host environment to cause infection. Ethanolamine is known to be metabolised by enteric pathogens to provide additional nutritional support in the GI tract (3, 4). Previously in this thesis it has been shown that ethanolamine can be metabolised by UPEC to provide them with a nutritional advantage *in vitro* (Chapter 4). However, there is growing research demonstrating the ability of ethanolamine to act as a signalling molecule to regulate virulence (6, 16). EutR, the regulator of the *eut* operon has been found to directly regulate virulence factors in EHEC (6-8). One virulence mechanism that has been shown to be regulated by ethanolamine in EHEC is the expression of fimbria proteins, although EutR is not always the regulator involved (8). As there is a recently recognised role for ethanolamine in regulating pathogenicity of UPEC (10, 17), and fimbriae are crucial to the successful colonisation of the urinary tract (93, 94), it was hypothesised in this thesis that ethanolamine regulates expression of fimbriae in UPECs. Furthermore, ethanolamine regulates the locus of enterocyte effacement (LEE) operon in EHEC, which mediates attachment to host cells and the characteristic attaching and effacing (A/E) lesions affecting host cells, respectively (7, 8). It was therefore hypothesised that equivalent properties of cell attachment and invasion in UPECs could be similarly regulated.

Type1 fimbriae are the most studied fimbriae expressed by UPECs. They enable the adhesion of bacteria to mannose moieties on the surface of BECs and have been found to facilitate the invasion of BECs (87, 90). Bacterial adherence to host cells was visible in infected urines collected in this study and expression of *fimH* was detected in half the UPEC RNA analysed in Chapter 3 (Fig 3.8). Additionally, the ability to express type 1 fimbriae *in vitro* has been shown to increase colonisation of the murine urinary tract (38). Through agglutination assays it was determined that UPEC strains U1 and U38 express fimbriae *in vitro* and that while those expressed by U38 were mannose sensitive, those in U1 were not (Fig 5.1 and Fig 5.3). There was no apparent effect of ethanolamine addition to LB growth medium in this

phenotypic assay. If time had permitted this experiment would have been repeated with AUM-grown cells.

RT-PCR provided evidence of ethanolamine the significant induction of Type 1 fimbria genes *fimE* and *fimH* after eight hours in AUM with 10mM ethanolamine compared to when ethanolamine was not added (Fig 5.4a). *fimH* induction by 10mM ethanolamine was greatly reduced by *eutR* knockout, but not abolished, suggesting a role for *eutR* as well as another regulatory circuit in this process, however this finding was not significant (Fig 5.4b). Further experimentation looking at gene expression when grown in static conditions examining the expression of the *fim* operon in the other U1 mutants would further this area of study.

The ability of UPECs to attach and invade bladder epithelial cell line HT1376 was measured in the presence of ethanolamine. Incubation in ethanolamine for 4 hours did not affect the ability of UPECs to bind to the epithelial cells in the assay used (Fig 5.3). Additionally, mutations in *eutB* and *eutR* did not affect the ability of UPEC strain U1 to bind to HT1376 in the presence or absence of ethanolamine, suggesting that ethanolamine does not affect bacterial attachment to epithelial cells. Surprisingly, however, U1Δ*eutR* demonstrated a significant decrease in the ability to invade epithelial cells when ethanolamine was supplemented (Fig 5.4). If this defect was due to *eut* operon inactivation alone, this would imply that the ability to sense and/or metabolise ethanolamine is important for the invasion of epithelial cells, but only when ethanolamine is present, which is difficult to explain. However, this phenotype is only present in U1Δ*eutR* and not U1Δ*eutB* which suggest invasion is independent of ethanolamine metabolism. A more likely explanation is that *eutR* is a direct or indirect repressor of another ethanolamine sensor or regulator outside the *eut* operon that in turn represses a bacterial factor required for invasion, or *eutR* and the unidentified ethanolamine sensor co-regulate an invasion factor. This is compatible with data collected from EHEC indicating the existence of an unidentified regulator responsible for ethanolamine-dependent virulence gene expression and expression of putative and characterised fimbriae (6,

8). Experimentation with the complemented *eutR* mutant to examine this further was not possible in the time available.

In summary, RT-PCR evidence was found supporting the hypothesis that induction of genes encoding Type 1 fimbriae in a UPEC strain are influenced by ethanolamine. Phenotypic evidence for the induction of Type 1 fimbriae by ethanolamine in UPEC strains was not found, and mutation of the *eut* operon had no effect on haemagglutination titres. However, haemagglutination experiments were not carried out in AUM media where high expression of the *eut* operon is detected when ethanolamine is added (Chapter 4, Fig 4.9). Ethanolamine and *eut* operon mutants did not affect the attachment of UPECs U1 and U13 to attach to the uroepithelial cell line HT1376. However, U1Δ*eutR* mutation abolished cell invasion in the presence of ethanolamine, suggesting an indirect role for the *eut* operon in uroepithelial cell invasion.

Future experiments would be required to extend this area of investigation. This includes experimentation with the complemented mutant strains to confirm the phenotypes seen in this chapter. Additionally, measuring fimbriae expression by qRT-PCR and phenotypic assay when grown in a static culture of AUM with ethanolamine to determine whether ethanolamine influences expression of fimbriae in conditions similar to those seen in the bladder. In this study the ability of UPEC adhere and invade bladder epithelial cells was measured after 4 hours co-incubations. However, from qRT-PCR data this this chapter *fim* genes are upregulated after 8 hours growth in AUM with ethanolamine. Therefore, the ability of U1 to attach to HT1376 should be measured after 8 hours pre-growth in AUM with ethanolamine. Finally, further investigation in UPEC strains that have increased attachment potential such as U38 that produce mannose sensitive fimbriae, or U13 that has greater binding ability in the *in vitro* cell assay could enhance investigation into ethanolamine regulation of fimbriae.

5.5 Appendix

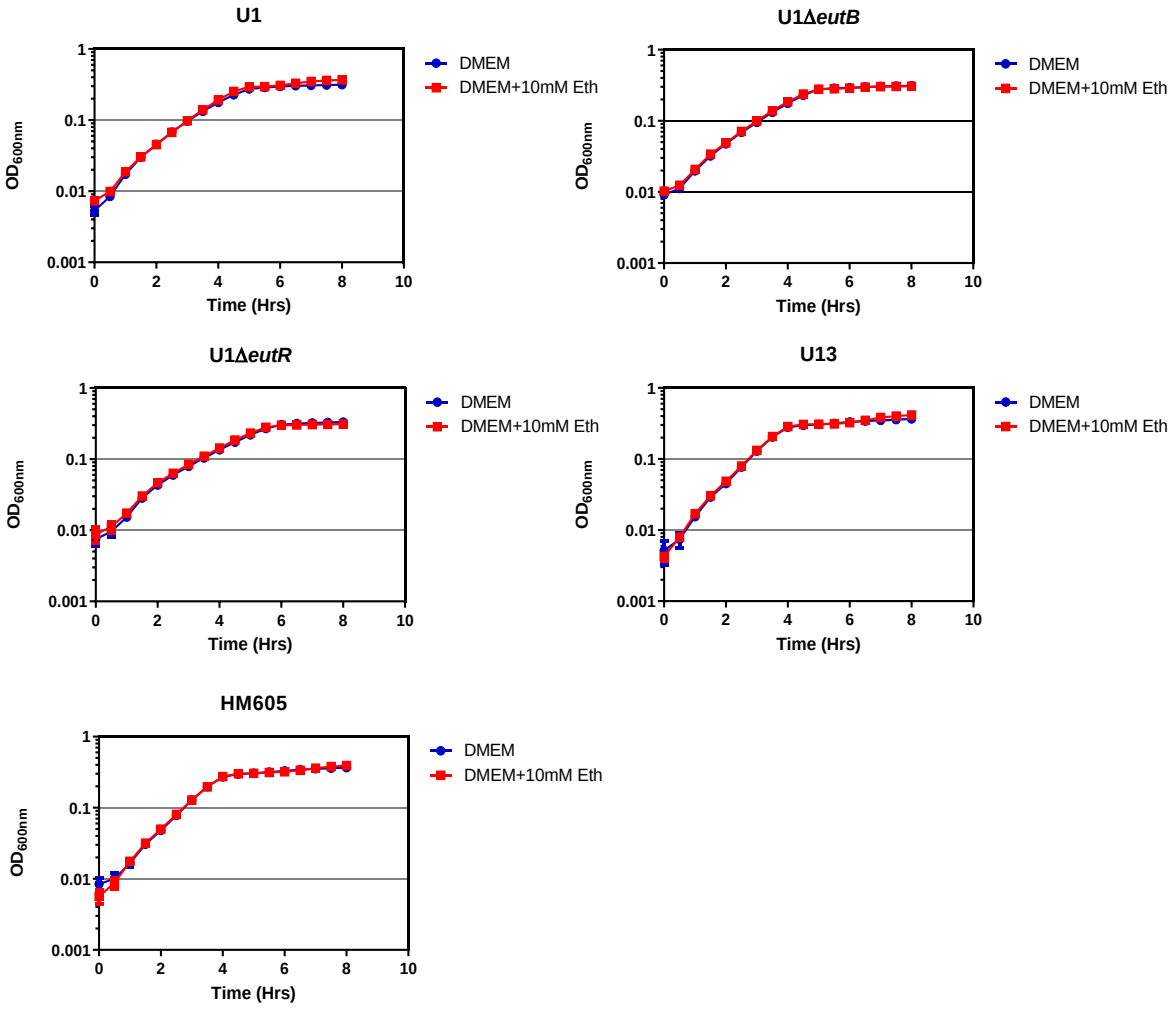

Appendix 5.1. Growth of *E. coli* strains in Low glucose DMEM with and without 10mM ethanolamine. Values are Mean ± SEM N=3

Chapter 6 Thesis Discussion and Conclusion

Urinary tract infections (UTIs) are a significant burden on healthcare systems worldwide and are primarily caused by Uropathogenic *E. coli* (UPEC) which account for 75% of all UTIs (1, 11). There is a lack of conserved virulence factors in UPEC, unlike other pathogenic *E. coli* strains (38). However, pathogenesis studies into UPEC are shifting focus from putative uropathogenic virulence factors and are beginning to investigate the role of adaptive metabolism (12, 45). Ethanolamine can be metabolised by *E. coli* as a source of carbon and nitrogen and has been linked to enteric bacterial pathogenesis by providing pathogenic bacteria with a competitive advantage (3, 4, 170). Additional studies have found that ethanolamine can be utilised as a regulatory molecule, controlling expression of virulence factors in EHEC (6-8). Recently the role of the ethanolamine utilisation (*eut*) operon in the urinary tract has been investigated (10, 17). Studies have found that the *eut* operon is upregulated in human UTI and promotes colonisation in a murine UTI model. However, it is unknown whether the *eut* operon is facilitating the metabolism of ethanolamine in the urinary tract or is sensing ethanolamine as a signal used to regulate colonisation factors, both functions have been seen in enteric pathogenesis. In this thesis the role of ethanolamine utilisation by UPEC in the urinary tract was investigated. The overall aim of this thesis was to determine whether ethanolamine is metabolised in the urine, whether metabolising ethanolamine confers a competitive advantage for UPECs, and whether other virulence factors are regulated by ethanolamine.

The initial aim of this study was to characterise clinically collected UPECs to determine whether they were metabolically active in urine (Chapter 3). Within urine, peptides and amino acids are the main source of carbon (49). UPECs have adapted to metabolise amino acids for acetogenic growth (58). The most abundant amino acid in urine, D-serine (0.38mM) is preferentially utilised by *E. coli in vitro* (1, 205). Similarly, ethanolamine can be metabolised by bacteria as a source of carbon by producing acetyl-CoA and acetate (148, 206). Analysis of 52 infected urine samples collected from Cork University Hospital, detected ethanolamine in urine at an approximate concentration of 0.57mM. This is more abundant than D-serine in urine

(137). In the intestine ethanolamine is believed to derive from epithelial cell turnover and other microbes, however in the bladder uroepithelial cell turnover is 50-fold slower and therefore would not appear to provide a viable source of ethanolamine in the urine. A characteristic of UTI, however, is the large influx of neutrophils, driven by expression of IL-8. It was hypothesised in this study that immune cells could provide the ethanolamine detected in urine. However, no correlation was detected between cytokine expression and urinary ethanolamine concentration, and similar ethanolamine levels were detected in healthy control urine samples with no white cells. This suggests ethanolamine in the urine is more likely to derive from excretion from the kidneys. Cytospin and TEM showed that *E. coli* adheres tightly to host cells in infected urine suggesting another possible source for ethanolamine. Previous studies with EHEC have found that they preferentially bind phosphatidylethanolamine (PE) rather than other phospholipids (214). *E. coli* binding PE on urinary neutrophils or epithelium could be facilitating local ethanolamine metabolism without increasing urinary ethanolamine. However further studies would be needed to examine this.

Genomic analysis of UPEC strains (Chapter 3) isolated at Cork University Hospital showed that the *eut* operon was conserved in all 47 strains, however the D-serine tolerance locus (*dsdCXA*) needed to metabolise D-serine was only present in 53% of the UPEC (216). mRNA analysis conducted in this thesis provides evidence that the *eut* operon is upregulated in UPEC-infected urine, which supports previous published findings (17). However, a novel finding in this thesis was that the degree of upregulation of the *eutB* gene encoding the first step in ethanolamine metabolism correlates with the concentration of ethanolamine detected in urine. This suggests ethanolamine is being actively metabolised during UTI rather than just acting as a regulatory molecule. In urine, UPECs show some signs of nitrogen stress, as they are unable to utilise urea, the primary source of nitrogen in urine and are known to be utilising amino acids for gluconeogenesis (12, 45). Therefore, it is unclear whether metabolism of ethanolamine in urine could provide *E. coli* with a nitrogen source, a carbon source, or both.

To explore how metabolised ethanolamine is utilised in urine, growth of UPECs with ethanolamine was assessed *in vitro* (Chapter 4). Most studies to date have used K12-laboratory strains and enteric pathogenic *E. coli* to investigate ethanolamine metabolism in *E. coli* (3, 144, 206). However, this thesis provides evidence that UPECs actively metabolise ethanolamine *in vitro* to provide a growth advantage. It has been documented that *E. coli* can utilise ethanolamine as a sole nitrogen source, however it is unclear in which circumstances ethanolamine can be used as a sole carbon source by *E. coli* (3, 218). An early study showed that ethanolamine can be used as a carbon source by some *E. coli* strains (but not others) at relatively high concentrations (82mM)(218). A more recent study was unable to show ethanolamine use as a carbon source in EHEC (3). It has been shown that other enzymes of central metabolism, such as the Acetyl-CoA synthetase (Acs), are required for the use of ethanolamine use as a carbon source in *Salmonella*, and a full TCA cycle is known to be required by *E. coli* in UTI (12, 147, 148). Therefore, mutations or global regulatory differences outside the *eut* operon could explain why ethanolamine cannot be used as a carbon source by all *E. coli*

In this study (Chapter 4) evidence is provided that 10mM ethanolamine can be used by UPEC strains as a sole nitrogen source in minimal (Mod M9) media, and *eutR* (operon regulator) and *eutB* (major component of ethanolamine ammonia lyase) are essential for this. Additionally, it was found that ethanolamine could be used at the physiological concentration found in urine (0.5mM) by a UPEC strain as a nitrogen source to provide a growth advantage, contradicting the published assertion that ethanolamine cannot support growth at concentrations lower than 1mM (6). Again, *eutR* and *eutB* were essential for this. UPEC culture in an artificial urine medium (185) (AUM) showed upregulation of *eut* operon enzyme and shell protein genes and growth enhancement when 10 mM ethanolamine was added, with the appearance of microcompartment structures in the cytoplasm. However, in AUM, unlike ModM9 medium, *eutE* (acetaldehyde dehydrogenase) was essential for growth enhancement with ethanolamine. Ethanolamine ammonia lyase activity alone, releasing ammonia and acetaldehyde, did not

appear to provide UPEC with a growth enhancement in AUM, unlike in ModM9 minimal medium. A need for acetaldehyde to be further metabolised to acetyl-CoA and acetate to provide a growth advantage suggests that ethanolamine could be acting as a carbon source in this medium. Previous studies have found that the accumulation of acetaldehyde can cause a toxic effect and prevent cell growth, therefore the production of acetaldehyde and the viability of bacterial cells in culture would be required to exclude acetaldehyde toxicity as a cause for this phenotype.

In the K12 strains MG1655 and BW25113, the prophage CPZ-55 is inserted between *eutA* and *eutB* of the *eut* operon (204, 211). The CPZ-55 prophage inserted in this region is transcribed in the reverse orientation compared to the *eut* operon. As there is only one promotor of the *eut* operon it is assumed that the genes downstream of the insert are not transcribed (see Fig 4.1), therefore ethanolamine cannot be metabolised (2, 141, 143). In this thesis a novel prophage was identified *eutA* and *eutB* in UPEC strain U71 (Chapter 3). Additionally, the CPZ-55 prophage was introduced into the U1 genomes during transduction forming U1Δ*eutR* (Chapter 4). Investigations into *E. coli* prophage have found that some prophage including CPZ-55 excise naturally at very low rates of less than 1 per 100,000 cells (221). Within this thesis it was found that the prophage can excise from the *eut* operon when faced with prolonged nutritional stress in Mod M9 (Chapter 4). Interestingly, the prophage does not appear to excise from complemented U1 in AUM despite the growth phenotype being restored. This phenomenon remains to be explained; it is proposed that the enzymes transcribed from the proximal region of the operon interact with other metabolites in the cytoplasm as a complete BMC cannot be formed. An additional hypothesis is that *eutR* might be regulating other metabolic pathways to provide a growth advantage. Further studies in this area would be needed to explain this finding.

The Eut microcompartment is a proteinaceous structure that encases the metabolism of ethanolamine (5). The presence of the Eut bacterial microcompartment (BMC) is hypothesised to protect the bacteria from the toxic effect of acetaldehyde (15). Additionally, the Eut BMC has been proposed to concentrate enzymes and intermediates to speed up the

transition of acetaldehyde to the non-toxic acetyl-coA (14). The genes that encode the Eut BMC shell proteins have been identified as core genes in *Salmonella* and *E. coli*, however there are limited images of Eut BMC and these are in *E. coli* K-12(5, 164). In this thesis, *eutS,* one of the shell proteins was highly upregulated in AUM with 10mM ethanolamine and TEM confirmed the presence of BMC-like structures in the bacterial cytoplasm. To the author's knowledge, the images presented in this thesis are the first images of native *eut* BMC in UPEC *E. coli* and suggest AUM facilitates ethanolamine induction of microcompartments (Fig 4.10b).

Work in Chapter 4 has provided evidence that ethanolamine metabolism promotes a growth advantage and also a competitive advantage in co-culture for UPEC in AUM, *in vitro*. Studies to date have shown that activation of the *eut* operon occurs in human urinary tract infection and knockout impairs fitness in a murine model of urinary tract infection. However, no study has shown this is because of ethanolamine metabolism in the urinary tract (10, 17). Studies using UPEC mutants interrupting key parts of the ethanolamine metabolic pathway, such as those constructed in this thesis, could be used to determine which parts of ethanolamine metabolism are important for UTI *in vivo*, and could determine whether utilisation of ethanolamine as a nitrogen source or a carbon source is key to colonisation.

A secondary aim in this thesis was to determine whether the *eut* operon can regulate the expression of putative urovirulence gene in UPECs (Chapter 5). Metabolism of ethanolamine can produce acetyl phosphate which can be converted to acetate (148). There is evidence to show that acetyl phosphate influences cell division, expression of flagella, type 1 fimbriae, capsular proteins, biofilm and stress response in *E. coli* (205). While there is a lack of conserved virulence factors in UPEC, putative urovirulence factors such as fimbriae, are crucial for the colonisation of the murine urinary tract, and flagella are important for the ascent of bacteria into the kidney to cause disease (44, 90, 91). In addition to metabolism, the *eut* operon directly regulates the expression of virulence factor in enteric pathogens (7). This include regulating the Locus of Enterocyte Effacement (LEE) operon, which encode genes involved with characteristic virulence genes for EHEC

pathogenesis (6, 7). Work by the same group found that ethanolamine helped regulate putative fimbriae in EHEC (8). Cytospins in Chapter 3 of this thesis presents evidence that bacteria adhere to the surface of host cells and fimbriae genes are expressed in infected urine (Fig 3.8). In this study there is evidence of *fim* operon expression in U1 grown in AUM at time points where ethanolamine is being actively metabolised, however as the expression of *fimH* was still upregulated in U1*ΔeutR* in the presence of ethanolamine, *fim* expression cannot be assumed to be regulated by the *eut* operon alone or by metabolism of ethanolamine. *In vitro* investigation using the bladder epithelial cell line HT1376 found that ethanolamine incubation did not enhance the adhesion of two selected UPEC strains. However, ethanolamine negatively affected the ability of U1Δ*eutR* mutants, in principle unable to sense or metabolise ethanolamine, to invade the epithelial cells (See Fig 5.3). Therefore, a secondary ethanolamine sensor/regulator outside of the *eut* operon could be responsible for an effect of ethanolamine on epithelial cell invasion and expression of the *fim* operon. The presence of a secondary ethanolamine sensor has previously been proposed in EHEC, and more work would be needed to confirm this hypothesis in UPEC (6).

In conclusion, this thesis has provided evidence that ethanolamine is utilised as a nutrient source by UPECs in different *in vitro* environments. It has shown that ethanolamine is present in the urine (0.57mM) and that this level of ethanolamine is sufficient to confer an *in vitro* growth advantage and the *eut* operon is upregulated in relation to metabolising ethanolamine at this level. Investigation using artificial urine medium suggests that ethanolamine may provide an additional source of carbon in urine, through microcompartment mediated metabolism of ethanolamine. Additionally, this study has found that the border between *eutA* and *eutB* in *E. coli* is prone to prophage insertion, therefore care is needed in future experimentation into ethanolamine metabolism to ensure this site is not compromised. This study has provided evidence that ethanolamine does not promote expression of fimbriae in the UPEC strain U1 to enhance attachment to epithelial cells in the conditions tested. However, ethanolamine has a negative impact on U1's ability to invade BEC when the *eut* operon is inactivated, suggesting a

regulatory circuit depending on ethanolamine outside the *eut* operon. The findings presented in this thesis supports the hypothesis that ethanolamine can be utilised by UPEC as a nutrient to provide a competitive growth advantage in UTIs. Further studies are needed to confirm a role for ethanolamine as a signalling molecule in UPEC pathogenesis.

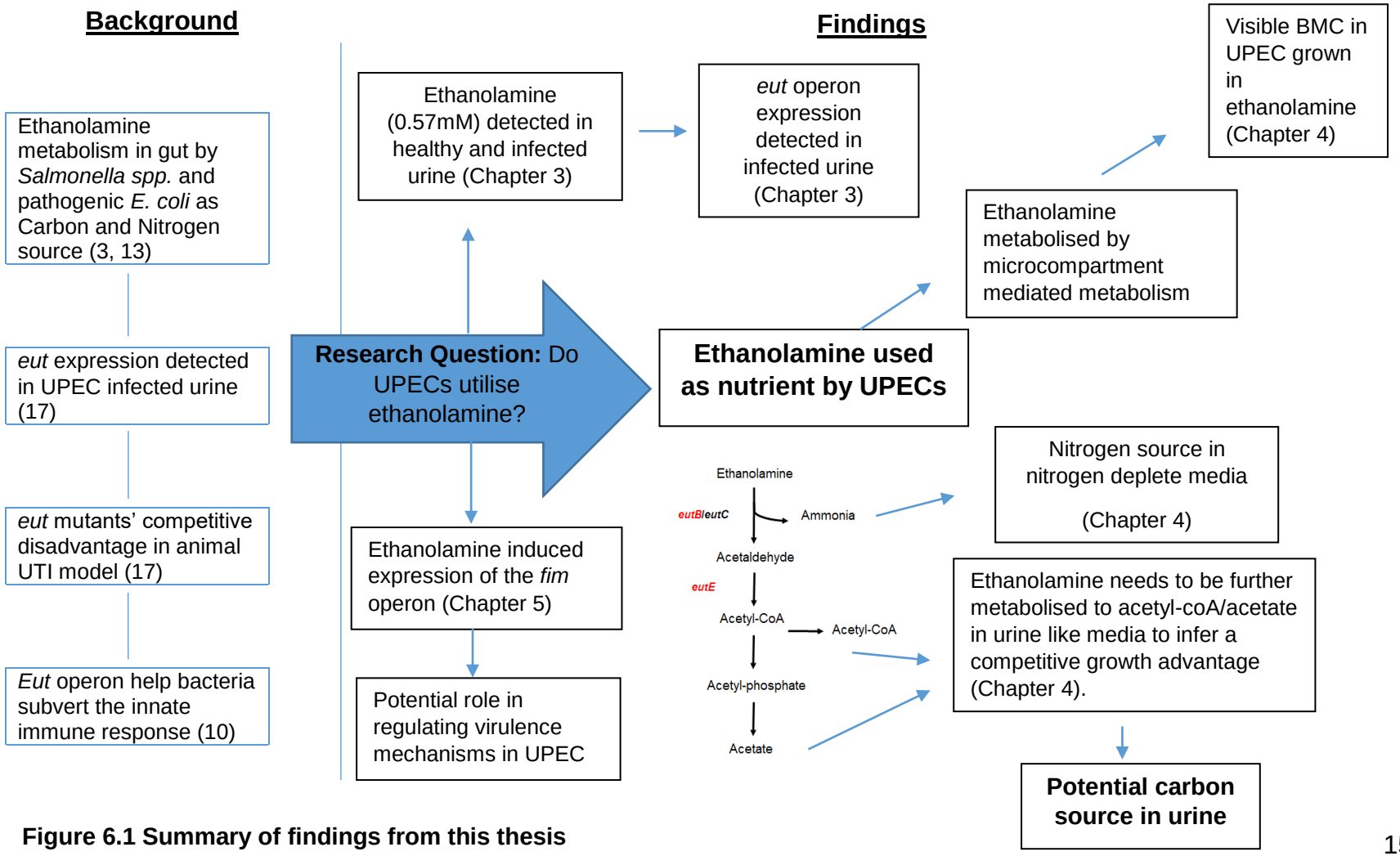

Figure 6.1 Summary of findings from this thesis

Bibliography

1. Mann R, Mediati DG, Duggin IG, Harry EJ, Bottomley AL. Metabolic Adaptations of Uropathogenic *E. coli* in the Urinary Tract. Frontiers in Cellular and Infection Microbiolgy. 2017;7:241.
2. Stojiljkovic I, Bäumler AJ, Heffron F. Ethanolamine Utilization in *Salmonella typhimurium*: Nucleotide Sequence, Protein Expression, and Mutaional Analysis of the *cchA cchB eutE eutG eut H* gene cluster. Journal of Bacteriology. 1995;177(5):1357-66.
3. Bertin Y, Girardeau JP, Chaucheyras-Durand F, Lyan B, Pujos-Guillot E, Harel J, et al. Enterohaemorrhagic *Escherichia coli* gains a competitive advantage by using ethanolamine as a nitrogen source in the bovine intestinal content. Environmental Microbiology. 2011;13(2):365-77.
4. Thiennimitr P, Winter SE, Winter MG, Xavier MN, Tolstikov V, Huseby DL, et al. Intestinal inflammation allows Salmonella to use ethanolamine to compete with the microbiota. Proceedings of the National Academy of Sciences. 2011;108(42):17480-5.
5. Koifoid E, Rappleye C, Stojiljkovic I, Roth J. The 17-Gene Ethanolamine Operon of *Salmonella typhimurium* Encodes Five Homologues of Carboxysome Shell Proteins. Journal of Bacteriology. 1999;181(17):5317-29.
6. Kendall MM, Gruber CC, Parker CT, Sperandio V. Ethanolamine controls expression of genes encoding components involved in interkingdom signaling and virulence in enterohemorrhagic *Escherichia coli* O157:H7. mBio. 2012;3(3).
7. Luzader DH, Clark DE, Gonyar LA, Kendall MM. EutR Is a Direct Regulator of Genes That Contribute to Metabolism and Virulence in Enterohemorrhagic *Escherichia coli* O157:H7. Journal of Bacteriology. 2013;195(21):4947-53.
8. Gonyar LA, Kendall MM. Ethanolamine and choline promote expression of putative and characterized fimbriae in enterohemorrhagic *Escherichia coli* O157:H7. Infection and Immunity. 2014;82(1):193-201.
9. Subashchandrabose S, Mobley HL. Virulence and Fitness Determinants of Uropathogenic *Escherichia coli*. Microbiology Spectrum. 2015;3(4).

10. Sintsova A, Smith S, Subashchandrabose S, Mobley HL. Role of ethanolamine utilization genes in host colonization during urinary tract infection. Infection and Immunity. 2017.
11. Flores-Mireles AL, Walker JN, Caparon M, Hultgren SJ. Urinary tract infections: epidemiology, mechanisms of infection and treatment options. Nature Reviews Microbiology. 2015;13(5):269-84.
12. Alteri CJ, Smith SN, Mobley HL. Fitness of *Escherichia coli* during urinary tract infection requires gluconeogenesis and the TCA cycle. PLoS Pathogens. 2009;5(5):e1000448.
13. Roof DM, Roth JR. Ethanolamine Utilization in *Salmonella typhimurium*. Journal of Bacteriology. 1988;170(9):3588-863.
14. Brinsmade SR, Paldon T, Escalante-Semerena JC. Minimal functions and physiological conditions required for growth of *salmonella enterica* on ethanolamine in the absence of the metabolosome. Journal of Bacteriology. 2005;187(23):8039-46.
15. Penrod JT, Roth JR. Conserving a volatile metabolite: a role for carboxysome-like organelles in *Salmonella enterica*. Journal of Bacteriology. 2006;188(8):2865-74.
16. Anderson CJ, Clark DE, Adli M, Kendall MM. Ethanolamine Signaling Promotes Salmonella Niche Recognition and Adaptation during Infection. PLoS Pathogens. 2015;11(11):e1005278.
17. Subashchandrabose S, Hazen TH, Brumbaugh AR, Himpsl SD, Smith SN, Ernst RD, et al. Host-specific induction of *Escherichia coli* fitness genes during human urinary tract infection. Proceedings of the National Academy of Sciences of the United States of America. 2014;111(51):18327-32.
18. Stamm WE, Norrby SR. Urinary Tract Infections: Disease Panorama and Challenges. The Journal of Infectious Diseases. 2001;183(Supplement_1):S1-S4.
19. Foxman B, Brown P. Epidemiology of urinary tract infections: transmission and risk factors, incidence, and costs. Infectious Disease Clinics of North America. 2003;17(2):227-41.
20. Foxman B. Epidemiology of urinary tract infections: incidence, morbidity, and economic costs. Disease-a-month : DM. 2003;49(2):53-70.

21. Foxman B. Recurring urinary tract infection: incidence and risk factors. American Journal of Public Health. 1990;80(3):331-3.
22. Foxman B. Epidemiology of urinary tract infections: incidence, morbidity, and economic costs. The American Journal of Medicine. 2002;113(1, Supplement 1):5-13.
23. Mehnert-Kay SA. Diagnosis and management of uncomplicated urinary tract infections. American Family Physician. 2005;72.
24. Lichtenberger P, Hooton TM. Complicated urinary tract infections. Current Infectious Disease Reports. 2008;10(6):499-504.
25. Weber DJ, Sickbert-Bennett EE, Gould CV, Brown VM, Huslage K, Rutala WA. Incidence of Catheter-Associated and Non-Catheter-Associated Urinary Tract Infections in a Healthcare System. Infection Control and Hospital Epidemiology. 2011;32(8):822-3.
26. Wiles TJ, Kulesus RR, Mulvey MA. Origins and Virulence Mechanisms of Uropathogenic *Escherichia coli*. Experimental and Molecular Pathology. 2008;85(1):11-9.
27. Berg RD. The indigenous gastrointestinal microflora. Trends in Microbiology. 1996;4(11):430-5.
28. Tenaillon O, Skurnik D, Picard B, Denamur E. The population genetics of commensal *Escherichia coli*. Nature Reviews Microbiology. 2010;8(3):207-17.
29. Croxen MA, Finlay BB. Molecular mechanisms of *Escherichia coli* pathogenicity. Nature Reviews Microbiology. 2010;8(1):26-38.
30. Dobrindt U, Chowdary MG, Krumbholz G, Hacker J. Genome dynamics and its impact on evolution of *Escherichia coli*. Medical Microbiology and Immunology. 2010;199(3):145-54.
31. Touchon M, Hoede C, Tenaillon O, Barbe V, Baeriswyl S, Bidet P, et al. Organised Genome Dynamics in the *Escherichia coli* Species Results in Highly Diverse Adaptive Paths. PLOS Genetics. 2009;5(1):e1000344.
32. Kaas RS, Friis C, Ussery DW, Aarestrup FM. Estimating variation within the genes and inferring the phylogeny of 186 sequenced diverse *Escherichia coli* genomes. BMC Genomics. 2012;13(1):577.

33. Land M, Hauser L, Jun S-R, Nookaew I, Leuze MR, Ahn T-H, et al. Insights from 20 years of bacterial genome sequencing. Functional & Integrative Genomics. 2015;15(2):141-61.
34. Rasko DA, Rosovitz MJ, Myers GSA, Mongodin EF, Fricke WF, Gajer P, et al. The pangenome structure of *Escherichia coli*: comparative genomic analysis of *E. coli* commensal and pathogenic isolates. Journal of Bacteriology. 2008;190(20):6881-93.
35. Clermont O, Christenson J, Denamur E, M Gordon D. The Clermont *Escherichia coli* phylo-typing method revisited: Improvement of specificity and detection of new phylo-groups 2013. 58-65 p.
36. Chaudhuri RR, Henderson IR. The evolution of the *Escherichia coli* phylogeny. Infection, Genetics and Evolution. 2012;12(2):214-26.
37. White AP, Sibley KA, Sibley CD, Wasmuth JD, Schaefer R, Surette MG, et al. Intergenic Sequence Comparison of *Escherichia coli* Isolates Reveals Lifestyle Adaptations but Not Host Specificity. Applied and Environmental Microbiology. 2011;77(21):7620-32.
38. Schreiber HL, Conover MS, Chou W-C, Hibbing ME, Manson AL, Dodson KW, et al. Bacterial virulence phenotypes of *Escherichia coli* and host susceptibility determine risk for urinary tract infections. Science Translational Medicine. 2017;9.
39. Yamamoto S, Tsukamoto T, Terai A, Kurazono H, Takeda Y, Yoshida O. Genetic Evidence Supporting the Fecal-Perineal-Urethral Hypothesis in Cystitis Caused by *Escherichia Coli*. The Journal of Urology. 1997;157(3):1127-9.
40. Eto DS, Jones TA, Sundsbak JL, Mulvey MA. Integrin-mediated host cell invasion by type 1-piliated uropathogenic *Escherichia coli*. PLoS Pathogens. 2007;3(7):e100.
41. Wright KJ, Seed PC, Hultgren SJ. Development of intracellular bacterial communities of uropathogenic *Escherichia coli* depends on type 1 pili. Cellular Microbiology. 2007;9(9):2230-41.
42. Mulvey MA, Lopez-Boado YS, Wilson CL, Roth R, Parks WC, Heuser J, et al. Induction and evasion of host defenses by type 1-piliated uropathogenic *Escherichia coli*. Science (New York, NY). 1998;282(5393):1494-7.

43. Blango MG, Ott EM, Erman A, Veranic P, Mulvey MA. Forced resurgence and targeting of intracellular uropathogenic *Escherichia coli* reservoirs. PloS One. 2014;9(3):e93327-e.
44. Lane MC, Alteri CJ, Smith SN, Mobley HLT. Expression of flagella is coincident with uropathogenic Escherichia coli ascension to the upper urinary tract. Proceedings of the National Academy of Sciences of the United States of America. 2007;104(42):16669-74.
45. Alteri CJ, Himpsl SD, Mobley HL. Preferential use of central metabolism *in vivo* reveals a nutritional basis for polymicrobial infection. PLoS Pathogens. 2015;11(1):e1004601.
46. Bielecki P, Muthukumarasamy U, Eckweiler D, Bielecka A, Pohl S, Schanz A, et al. In Vivo mRNA Profiling of Uropathogenic *Escherichia coli* from Diverse Phylogroups Reveals Common and Group-Specific Gene Expression Profiles. mBio. 2014;5(4).
47. Bouatra S, Aziat F, Mandal R, Guo AC, Wilson MR, Knox C, et al. The human urine metabolome. PLOS ONE. 2013;8(9):e73076.
48. Vejborg RM, de Evgrafov MR, Phan MD, Totsika M, Schembri MA, Hancock V. Identification of genes important for growth of asymptomatic bacteriuria *Escherichia coli* in urine. Infection and Immunity. 2012;80(9):3179-88.
49. Alteri CJ, Mobley HL. Metabolism and Fitness of Urinary Tract Pathogens. Microbiology Spectrum. 2015;3(3).
50. Forsyth VS, Armbruster CE, Smith SN, Pirani A, Springman AC, Walters MS, et al. Rapid Growth of Uropathogenic *Escherichia coli* during Human Urinary Tract Infection. mBio. 2018;9.
51. Møller AK, Leatham MP, Conway T, Nuijten PJM, de Haan LAM, Krogfelt KA, et al. An *Escherichia coli* MG1655 Lipopolysaccharide Deep-Rough Core Mutant Grows and Survives in Mouse Cecal Mucus but Fails To Colonize the Mouse Large Intestine. Infection and Immunity. 2003;71(4):2142-52.
52. Fabich AJ, Jones SA, Chowdhury FZ, Cernosek A, Anderson A, Smalley D, et al. Comparison of carbon nutrition for pathogenic and commensal *Escherichia coli* strains in the mouse intestine. Infection and Immunity. 2008;76(3):1143-52.
53. Chang DE, Smalley DJ, Tucker DL, Leatham MP, Norris WE, Stevenson SJ, et al. Carbon nutrition of *Escherichia coli* in the mouse intestine. Proceedings

of the National Academy of Sciences of the United States of America. 2004;101(19):7427-32.

54. Sweeney NJ, Laux DC, Cohen PS. *Escherichia coli* F-18 and *E. coli* K-12 *eda* mutants do not colonize the streptomycin-treated mouse large intestine. Infection and Immunity. 1996;64(9):3504-11.

55. Conway T, Cohen PS. Commensal and Pathogenic *Escherichia coli* Metabolism in the Gut. Microbiology Spectrum. 2015;3(3).

56. Miranda RL, Conway T, Leatham MP, Chang DE, Norris WE, Allen JH, et al. Glycolytic and gluconeogenic growth of *Escherichia coli* O157:H7 (EDL933) and *E. coli* K-12 (MG1655) in the mouse intestine. Infection and Immunity. 2004;72(3):1666-76.

57. Conover MS, Hadjifrangiskou M, Palermo JJ, Hibbing ME, Dodson KW, Hultgren SJ. Metabolic Requirements of *Escherichia coli* in Intracellular Bacterial Communities during Urinary Tract Infection Pathogenesis. mBio. 2016;7(2):e00104-e116.

58. Anfora AT, Halladin DK, Haugen BJ, Welch RA. Uropathogenic *Escherichia coli* CFT073 is adapted to acetatogenic growth but does not require acetate during murine urinary tract infection. Infection and Immunity. 2008;76(12):5760-7.

59. Snyder JA, Haugen BJ, Buckles EL, Lockatell CV, Johnson DE, Donnenberg MS, et al. Transcriptome of uropathogenic *Escherichia coli* during urinary tract infection. Infection and Immunity. 2004;72(11):6373-81.

60. Pätzold R, Schieber A, Brückner H. Gas chromatographic quantification of free D-amino acids in higher vertebrates. Biomedical Chromatography. 2005;19(6):466-73.

61. Brückner H, Haasmann S, Friedrich A. Quantification of D-amino acids in human urine using GC-MS and HPLC. Amino Acids. 1994;6(2):205-11.

62. Connolly JPR, Roe AJ. When and where? Pathogenic *Escherichia coli* differentially sense host D-serine using a universal transporter system to monitor their environment. Microbial Cell. 2016;3(4):181-4.

63. Hryckowian AJ, Baisa GA, Schwartz KJ, Welch RA. *dsdA* Does Not Affect Colonization of the Murine Urinary Tract by *Escherichia coli* CFT073. PLoS One. 2015;10(9):e0138121.

64. van Heeswijk WC, Westerhoff HV, Boogerd FC. Nitrogen assimilation in *Escherichia coli*: putting molecular data into a systems perspective. Microbiology and Molecular Biology Reviews 2013;77(4):628-95.
65. Hagan EC, Lloyd AL, Rasko DA, Faerber GJ, Mobley HL. *Escherichia coli* global gene expression in urine from women with urinary tract infection. PLoS Pathogens. 2010;6(11):e1001187.
66. Reigstad CS, Hultgren SJ, Gordon JI. Functional Genomic Studies of Uropathogenic *Escherichia coli* and Host Urothelial Cells when Intracellular Bacterial Communities Are Assembled. Journal of Biological Chemistry. 2007;282(29):21259-67.
67. Henderson JP, Crowley JR, Pinkner JS, Walker JN, Tsukayama P, Stamm WE, et al. Quantitative metabolomics reveals an epigenetic blueprint for iron acquisition in uropathogenic *Escherichia coli*. PLoS Pathogens. 2009;5(2):e1000305-e.
68. Garcia EC, Brumbaugh AR, Mobley HLT. Redundancy and Specificity of *Escherichia coli* Iron Acquisition Systems during Urinary Tract Infection. Infection and Immunity. 2011;79(3):1225.
69. McHugh JP, Rodriguez-Quinones F, Abdul-Tehrani H, Svistunenko DA, Poole RK, Cooper CE, et al. Global iron-dependent gene regulation in *Escherichia coli*. A new mechanism for iron homeostasis. The Journal of Biological Chemistry. 2003;278(32):29478-86.
70. Subashchandrabose S, Mobley HL. Back to the metal age: battle for metals at the host-pathogen interface during urinary tract infection. Metallomics. 2015;7(6):935-42.
71. Hagan EC, Mobley HLT. Uropathogenic *Escherichia coli* outer membrane antigens expressed during urinary tract infection. Infection and Immunity. 2007;75(8):3941-9.
72. Hagan EC, Mobley HLT. Haem acquisition is facilitated by a novel receptor Hma and required by uropathogenic *Escherichia coli* for kidney infection. Molecular Microbiology. 2009;71(1):79-91.
73. Larsen RA, Thomas MG, Postle K. Protonmotive force, ExbB and ligand-bound FepA drive conformational changes in TonB. Molecular Microbiology. 1999;31(6):1809-24.

74. Torres AG, Redford P, Welch RA, Payne SM. TonB-dependent systems of uropathogenic *Escherichia coli*: aerobactin and heme transport and TonB are required for virulence in the mouse. Infection and Immunity. 2001;69(10):6179-85.
75. Steigedal M, Marstad A, Haug M, Damås JK, Strong RK, Roberts PL, et al. Lipocalin 2 imparts selective pressure on bacterial growth in the bladder and is elevated in women with urinary tract infection. Journal of Immunology 2014;193(12):6081-9.
76. Hantke K, Nicholson G, Rabsch W, Winkelmann G. Salmochelins, siderophores of *Salmonella enterica* and uropathogenic *Escherichia coli* strains, are recognized by the outer membrane receptor IroN. Proceedings of the National Academy of Sciences. 2003;100(7):3677-82.
77. Smith KD. Iron metabolism at the host pathogen interface: Lipocalin 2 and the pathogen-associated iroA gene cluster. The International Journal of Biochemistry & Cell Biology. 2007;39(10):1776-80.
78. Sabri M, Houle S, Dozois CM. Roles of the Extraintestinal Pathogenic *Escherichia coli* ZnuACB and ZupT Zinc Transporters during Urinary Tract Infection. Infection and Immunity. 2009;77(3):1155.
79. Dessing MC, Butter LM, Teske GJ, Claessen N, van der Loos CM, Vogl T, et al. S100A8/A9 is not involved in host defense against murine urinary tract infection. PLOS ONE. 2010;5(10):e13394-e.
80. Djoko KY, Ong C-lY, Walker MJ, McEwan AG. The Role of Copper and Zinc Toxicity in Innate Immune Defense against Bacterial Pathogens. The Journal of biological chemistry. 2015;290(31):18954-61.
81. Nies DH, Herzberg M. A fresh view of the cell biology of copper in enterobacteria. Molecular Microbiology. 2013;87(3):447-54.
82. Outten FW, Huffman DL, Hale JA, O'Halloran TV. The Independent *cue* and *cus* Systems Confer Copper Tolerance during Aerobic and Anaerobic Growth in *Escherichia coli*. Journal of Biological Chemistry. 2001;276(33):30670-7.
83. Rensing C, Fan B, Sharma R, Mitra B, Rosen BP. CopA: An *Escherichia coli* Cu(I)-translocating P-type ATPase. Proceedings of the National Academy of Sciences of the United States of America. 2000;97(2):652-6.

84. Grass G, Rensing C. Genes involved in copper homeostasis in *Escherichia coli*. Journal of Bacteriology. 2001;183(6):2145-7.
85. Tree JJ, Ulett GC, Ong C-LY, Trott DJ, McEwan AG, Schembri MA. Trade-Off between Iron Uptake and Protection against Oxidative Stress: Deletion of *cueO* Promotes Uropathogenic *Escherichia coli* Virulence in a Mouse Model of Urinary Tract Infection. Journal of Bacteriology. 2008;190(20):6909.
86. Welch RA, Burland V, Plunkett G, 3rd, Redford P, Roesch P, Rasko D, et al. Extensive mosaic structure revealed by the complete genome sequence of uropathogenic *Escherichia coli*. Proceedings of the National Academy of Sciences of the United States of America. 2002;99(26):17020-4.
87. Zhou G, Mo W-J, Sebbel P, Min G, Neubert TA, Glockshuber R, et al. Uroplakin Ia is the urothelial receptor for uropathogenic *Escherichia coli* evidence from *in vitro* FimH binding. Journal of Cell Science. 2001;114(22):4095.
88. Miller E, Garcia T, Hultgren S, Oberhauser AF. The mechanical properties of *E. coli* type 1 pili measured by atomic force microscopy techniques. Biophysical Journal. 2006;91(10):3848-56.
89. Martinez JJ, Hultgren SJ. Requirement of Rho-family GTPases in the invasion of Type 1-piliated uropathogenic *Escherichia coli*. Cellular Microbiology. 2002;4(1):19-28.
90. Martinez JJ, Mulvey MA, Schilling JD, Pinkner JS, Hultgren SJ. Type 1 pilus-mediated bacterial invasion of bladder epithelial cells. The EMBO Journal. 2000;19(12):2803-12.
91. Connell I, Agace W, Klemm P, Schembri M, Mărild S, Svanborg C. Type 1 fimbrial expression enhances *Escherichia coli* virulence for the urinary tract. Proceedings of the National Academy of Sciences of the United States of America. 1996;93(18):9827-32.
92. Nowicki B, Rhen M, Väisänen-Rhen V, Pere A, Korhonen TK. Immunofluorescence study of fimbrial phase variation in *Escherichia coli* KS71. Journal of Bacteriology. 1984;160(2):691-5.
93. Holden NJ, Totsika M, Mahler E, Roe AJ, Catherwood K, Lindner K, et al. Demonstration of regulatory cross-talk between P fimbriae and type 1 fimbriae in uropathogenic *Escherichia coli*. Microbiology. 2006;152(Pt 4):1143-53.

94. Snyder JA, Haugen BJ, Lockatell CV, Maroncle N, Hagan EC, Johnson DE, et al. Coordinate expression of fimbriae in uropathogenic *Escherichia coli*. Infection and Immunity. 2005;73(11):7588-96.
95. Lane MC, Lockatell V, Monterosso G, Lamphier D, Weinert J, Hebel JR, et al. Role of motility in the colonization of uropathogenic *Escherichia coli* in the urinary tract. Infection and Immunity. 2005;73(11):7644-56.
96. Pichon C, Hechard C, du Merle L, Chaudray C, Bonne I, Guadagnini S, et al. Uropathogenic *Escherichia coli* AL511 requires flagellum to enter renal collecting duct cells. Cellular Microbiology. 2009;11(4):616-28.
97. Lane MC, Simms AN, Mobley HLT. complex interplay between type 1 fimbrial expression and flagellum-mediated motility of uropathogenic *Escherichia coli*. Journal of Bacteriology. 2007;189(15):5523-33.
98. Luterbach CL, Mobley HLT. Cross Talk between MarR-Like Transcription Factors Coordinates the Regulation of Motility in Uropathogenic *Escherichia coli*. Infection and Immunity. 2018;86(12).
99. Wiles TJ, Dhakal BK, Eto DS, Mulvey MA. Inactivation of host Akt/protein kinase B signaling by bacterial pore-forming toxins. Molecular Biology of the Cell. 2008;19(4):1427-38.
100. Dhakal BK, Mulvey MA. The UPEC pore-forming toxin alpha-hemolysin triggers proteolysis of host proteins to disrupt cell adhesion, inflammatory, and survival pathways. Cell Host Microbe. 2012;11(1):58-69.
101. Lemonnier M, Landraud L, Lemichez E. Rho GTPase-activating bacterial toxins: from bacterial virulence regulation to eukaryotic cell biology. FEMS Microbiology Reviews. 2007;31(5):515-34.
102. Rippere-Lampe KE, O'Brien AD, Conran R, Lockman HA. Mutation of the Gene Encoding Cytotoxic Necrotizing Factor Type 1 (*cnf 1*) Attenuates the Virulence of Uropathogenic *Escherichia coli*. Infection and Immunity. 2001;69(6):3954-64.
103. Grist M, Chakraborty J. Identification of a mucin layer in the urinary bladder. Urology. 1994;44(1):26-33.
104. Cornish J, Lecamwasam JP, Harrison G, Vanderwee MA, Miller TE. Host defence mechanisms in the bladder. II. Disruption of the layer of mucus. British Journal of Experimental Pathology. 1988;69(6):759-70.

105. Wu X-R, Kong X-P, Pellicer A, Kreibich G, Sun T-T. Uroplakins in Urothelial Biology, Function and Disease. Kidney International. 2009;75(11):1153-65.
106. Song J, Duncan MJ, Li G, Chan C, Grady R, Stapleton A, et al. A Novel TLR4-Mediated Signaling Pathway Leading to IL-6 Responses in Human Bladder Epithelial Cells. PLoS Pathogens. 2007;3(4):e60.
107. Nagamatsu K, Hannan TJ, Guest RL, Kostakioti M, Hadjifrangiskou M, Binkley J, et al. Dysregulation of *Escherichia coli* alpha-hemolysin expression alters the course of acute and persistent urinary tract infection. Proceedings of the National Academy of Sciences of the United States of America. 2015;112(8):E871-80.
108. Chromek M, Slamová Z, Bergman P, Kovács L, Podracká Lu, Ehrén I, et al. The antimicrobial peptide cathelicidin protects the urinary tract against invasive bacterial infection. Nature Medicine. 2006;12:636.
109. Valore EV, Park CH, Quayle AJ, Wiles KR, McCray PB, Ganz T. Human beta-defensin-1: an antimicrobial peptide of urogenital tissues. Journal of Clinical Investigation. 1998;101(8):1633-42.
110. Danka ES, Hunstad DA. Cathelicidin augments epithelial receptivity and pathogenesis in experimental *Escherichia coli* cystitis. The Journal of Infectious Diseases. 2015;211(7):1164-73.
111. Carattino MD, Prakasam HS, Ruiz WG, Clayton DR, McGuire M, Gallo LI, et al. Bladder filling and voiding affect umbrella cell tight junction organization and function. American Journal of Physiology-Renal Physiology. 2013;305(8):F1158-F68.
112. Chen Y, Guo X, Deng FM, Liang FX, Sun W, Ren M, et al. Rab27b is associated with fusiform vesicles and may be involved in targeting uroplakins to urothelial apical membranes. Proceedings of the National Academy of Sciences of the United States of America. 2003;100(24):14012-7.
113. Bishop BL, Duncan MJ, Song J, Li G, Zaas D, Abraham SN. Cyclic AMP-regulated exocytosis of *Escherichia coli* from infected bladder epithelial cells. Nature Medicine. 2007;13(5):625-30.
114. Song J, Bishop BL, Li G, Grady R, Stapleton A, Abraham SN. TLR4-mediated expulsion of bacteria from infected bladder epithelial cells. Proceedings of the National Academy of Sciences of the United States of America. 2009;106(35):14966-71.

115. Hayes BW, Abraham SN. Innate Immune Responses to Bladder Infection. Microbiology Spectrum. 2016;4(6).
116. Godaly G, Bergsten G, Hang L, Fischer H, Frendeus B, Lundstedt AC, et al. Neutrophil recruitment, chemokine receptors, and resistance to mucosal infection. Journal of Leukocyte Biology. 2001;69(6):899-906.
117. Chan CY, St John AL, Abraham SN. Mast cell interleukin-10 drives localized tolerance in chronic bladder infection. Immunity. 2013;38(2):349-59.
118. Schiwon M, Weisheit C, Franken L, Gutweiler S, Dixit A, Meyer-Schwesinger C, et al. Crosstalk between sentinel and helper macrophages permits neutrophil migration into infected uroepithelium. Cell. 2014;156(3):456-68.
119. Shahin RD, Engberg I, Hagberg L, Svanborg Eden C. Neutrophil recruitment and bacterial clearance correlated with LPS responsiveness in local gram-negative infection. The Journal of Immunology. 1987;138(10):3475-80.
120. Haraoka M, Hang L, Frendeus B, Godaly G, Burdick M, Strieter R, et al. Neutrophil recruitment and resistance to urinary tract infection. The Journal of Infectious Diseases. 1999;180(4):1220-9.
121. Hannan TJ, Roberts PL, Riehl TE, van der Post S, Binkley JM, Schwartz DJ, et al. Inhibition of Cyclooxygenase-2 Prevents Chronic and Recurrent Cystitis. EBioMedicine. 2014;1(1):46-57.
122. Jaillon S, Moalli F, Ragnarsdottir B, Bonavita E, Puthia M, Riva F, et al. The humoral pattern recognition molecule PTX3 is a key component of innate immunity against urinary tract infection. Immunity. 2014;40(4):621-32.
123. Abraham SN, Shin J-S, Malaviya R.
124. Zec K, Volke J, Vijitha N, Thiebes S, Gunzer M, Kurts C, et al. Neutrophil Migration into the Infected Uroepithelium Is Regulated by the Crosstalk between Resident and Helper Macrophages. Pathogens. 2016;5(1):15.
125. Anderson M, Bollinger D, Hagler A, Hartwell H, Rivers B, Ward K, et al. Viable but nonculturable bacteria are present in mouse and human urine specimens. Journal of Clinical Microbiology. 2004;42(2):753-8.
126. Siddiqui H, Nederbragt AJ, Lagesen K, Jeansson SL, Jakobsen KS. Assessing diversity of the female urine microbiota by high throughput sequencing of 16S rDNA amplicons. BMC microbiology. 2011;11:244.

127. Aragón IM, Herrera-Imbroda B, Queipo-Ortuño MI, Castillo E, Del Moral JS-G, Gómez-Millán J, et al. The Urinary Tract Microbiome in Health and Disease. European Urology Focus. 2018.
128. Lewis DA, Brown R, Williams J, White P, Jacobson SK, Marchesi JR, et al. The human urinary microbiome; bacterial DNA in voided urine of asymptomatic adults. Frontiers in Cellular and Infection Microbiology. 2013;3:41.
129. Fouts DE, Pieper R, Szpakowski S, Pohl H, Knoblach S, Suh MJ, et al. Integrated next-generation sequencing of 16S rDNA and metaproteomics differentiate the healthy urine microbiome from asymptomatic bacteriuria in neuropathic bladder associated with spinal cord injury. Journal of Translational Medicine. 2012;10:174.
130. Walker AW, Lawley TD. Therapeutic modulation of intestinal dysbiosis. Pharmacological Research. 2013;69(1):75-86.
131. Liévin-Le Moal V, Servin AL. Anti-Infective Activities of *Lactobacillus* Strains in the Human Intestinal Microbiota: from Probiotics to Gastrointestinal Anti-Infectious Biotherapeutic Agents. Clinical Microbiology Reviews. 2014;27(2):167-99.
132. Randle CL, Albro PW, Dittmer JC. The phosphoglyceride composition of gram-negative bacteria and the changes in composition during growth. Biochimica et Biophysica Acta (BBA) - Lipids and Lipid Metabolism. 1969;187(2):214-20.
133. Garsin DA. Ethanolamine utilization in bacterial pathogens: roles and regulation. Nature Reviews Microbiology. 2010;8(4):290-5.
134. Larson TJ, Ehrmann M, Boos W. Periplasmic glycerophosphodiester phosphodiesterase of *Escherichia coli,* a new enzyme of the *glp* regulon. Journal of Biological Chemistry. 1983;258(9):5428-32.
135. Proulx P, Fung CK. Metabolism of phosphoglycerides in *E. coli* IV. The positional specificity and properties of phospbolipase A. Canadian Journal of Biochemistry. 1969;47(12):1125-8.
136. Snoeck V, Goddeeris B, Cox E. The role of enterocytes in the intestinal barrier function and antigen uptake. Microbes and Infection. 2005;7(7-8):997-1004.

137. Wishart DS, Tzur D, Knox C, Eisner R, Guo AC, Young N, et al. HMDB: the Human Metabolome Database. Nucleic Acids Research. 2007;35(Database issue):D521-D6.
138. Tsoy O, Ravcheev D, Mushegian A. Comparative genomics of ethanolamine utilization. Journal of Bacteriology. 2009;191(23):7157-64.
139. Roof DM, Roth JR. Functions required for vitamin B12-dependent ethanolamine utilization in *Salmonella typhimurium*. Journal of Bacteriology. 1989;171(6):3316-23.
140. Sheppard DE, Roth JR. A rationale for autoinduction of a transcriptional activator: ethanolamine ammonia-lyase (EutBC) and the operon activator (EutR) compete for adenosyl-cobalamin in *Salmonella typhimurium*. Journal of Bacteriology. 1994;176(5):1287-96.
141. Roof DM, Roth JR. Autogenous regulation of ethanolamine utilization by a transcriptional activator of the eut operon in *Salmonella typhimurium*. Journal of Bacteriology. 1992;174(20):6634-43.
142. Blackwell CM, Turner JM. Purification and Properties of Coenzyme B12-dependent Ethanolamine Ammonia Lysase. Journal of Biochemistry. 1978;175(1):555-63.
143. Scarlett AF, Turner JM. Microbial metabolism of Amino Alcohols. Ethanolamine Catabolism Mediated by Coenzyme B12-dependent Ethanolamine Ammonia-Lyase in *Escherichia col*i and *Klebsiella aerogenes*. Journal of General Microbiology. 1976;95:173-6.
144. Blackwell CM, Scarlett AF, Turner JM. Microbial Metabolism of Amino Alcohols. Control of Formation and Stability of Partially Purified Ethanolamine Ammonia-lyase in *Escherichia coli*. Journal of General Microbiology. 1977;98:133-9.
145. Buan NR, Suh S-J, Escalante-Semerena JC. The eutT gene of *Salmonella enterica* Encodes an oxygen-labile, metal-containing ATP:corrinoid adenosyltransferase enzyme. Journal of Bacteriology. 2004;186(17):5708-14.
146. Mori K, Bando R, Hieda N, Toraya T. Identification of a Reactivating Factor for Adenosylcobalamin-Dependent Ethanolamine Ammonia Lyase. Journal of Bacteriology. 2004;186(20):6845.

147. Brinsmade SR, Escalante-Semerena JC. The eutD Gene of *Salmonella enterica* Encodes a Protein with Phosphotransacetylase Enzyme Activity. Journal of Bacteriology. 2004;186(6):1890-2.
148. Starai VJ, Garrity J, Escalante-Semerena JC. Acetate excretion during growth of *Salmonella enterica* on ethanolamine requires phosphotransacetylase (EutD) activity, and acetate recapture requires acetyl-CoA synthetase (Acs) and phosphotransacetylase (Pta) activities. Microbiology. 2005;151(Pt 11):3793-801.
149. Penrod JT, Mace CC, Roth JR. A pH-sensitive function and phenotype: evidence that EutH facilitates diffusion of uncharged ethanolamine in *Salmonella enterica*. Journal of Bacteriology. 2004;186(20):6885-90.
150. Moore TC, Escalante-Semerena JC. The EutQ and EutP proteins are novel acetate kinases involved in ethanolamine catabolism: physiological implications for the function of the ethanolamine metabolosome in *Salmonella enterica*. Molecular Microbiology. 2016;99(3):497-511.
151. Kaval KG, Garsin DA. Ethanolamine Utilization in Bacteria. mBio. 2018;9.
152. Chowdhury C, Sinha S, Chun S, Yeates TO, Bobik TA. Diverse bacterial microcompartment organelles. Microbiology and Molecular Biology Reviews. 2014;78(3):438-68.
153. Niklowitz W, Drews G. [Cytology of Cyanophycea. I. Research on the substructure of *Phormidium uncinatum* Gom]. Archiv für Mikrobiologie. 1956;24(2):134-46.
154. Shively JM, Ball F, Brown DH, Saunders RE. Functional organelles in prokaryotes: polyhedral inclusions (carboxysomes) of *Thiobacillus neapolitanus*. Science (New York, NY). 1973;182(4112):584-6.
155. Axen SD, Erbilgin O, Kerfeld CA. A taxonomy of bacterial microcompartment loci constructed by a novel scoring method. PLoS Computational Biology. 2014;10(10):e1003898.
156. Chen P, Andersson DI, Roth JR. The control region of the *pdu/cob* regulon in *Salmonella typhimurium*. Journal of Bacteriology. 1994;176(17):5474-82.
157. Bobik TA, Lehman BP, Yeates TO. Bacterial microcompartments: widespread prokaryotic organelles for isolation and optimization of metabolic pathways. Molecular Microbiology. 2015;98(2):193-207.

158. English RS, Lorbach SC, Qin X, Shively JM. Isolation and characterization of a carboxysome shell gene from *Thiobacillus neapolitanus*. Molecular Microbiology. 1994;12(4):647-54.
159. Kerfeld CA, Erbilgin O. Bacterial microcompartments and the modular construction of microbial metabolism. Trends in Microbiology. 2015;23(1):22-34.
160. Kerfeld CA, Sawaya MR, Tanaka S, Nguyen CV, Phillips M, Beeby M, et al. Protein structures forming the shell of primitive bacterial organelles. Science (New York, NY). 2005;309(5736):936-8.
161. Cai F, Menon BB, Cannon GC, Curry KJ, Shively JM, Heinhorst S. The pentameric vertex proteins are necessary for the icosahedral carboxysome shell to function as a CO2 leakage barrier. PLOS ONE. 2009;4(10):e7521-e.
162. Sutter M, Greber B, Aussignargues C, Kerfeld CA. Assembly principles and structure of a 6.5-MDa bacterial microcompartment shell. Science (New York, NY). 2017;356(6344):1293-7.
163. Pang A, Frank S, Brown I, Warren MJ, Pickersgill RW. Structural insights into higher order assembly and function of the bacterial microcompartment protein PduA. The Journal of Biological Chemistry. 2014;289(32):22377-84.
164. Shively JM BC, Aldrich CH, Bobik TA, Meglman JL, Jin S, Baker SH. Sequence homologs of the carboxysomal polypeptide CsoS1 of the thiobacilli are present in cyanobacteria and enteric bacteria that form carboxysomes-polyhedral bodies. Canadian Journal of Botany. 1998;76(6):906-16.
165. Held M, Kolb A, Perdue S, Hsu SY, Bloch SE, Quin MB, et al. Engineering formation of multiple recombinant Eut protein nanocompartments in *E. coli*. Scientific Reports. 2016;6:24359.
166. Havemann GD, Sampson EM, Bobik TA. PduA Is a Shell Protein of Polyhedral Organelles Involved in Coenzyme B12-Dependent Degradation of 1,2-Propanediol in *Salmonella enterica* Serovar Typhimurium LT2. Journal of Bacteriology. 2002;184(5):1253-61.
167. Korbel JO, Doerks T, Jensen LJ, Perez-Iratxeta C, Kaczanowski S, Hooper SD, et al. Systematic association of genes to phenotypes by genome and literature mining. PLoS biology. 2005;3(5):e134.

168. Toledo-Arana A, Dussurget O, Nikitas G, Sesto N, Guet-Revillet H, Balestrino D, et al. The *Listeria* transcriptional landscape from saprophytism to virulence. Nature. 2009;459(7249):950-6.
169. Janoir C, Denève C, Bouttier S, Barbut F, Hoys S, Caleechum L, et al. Adaptive Strategies and Pathogenesis of *Clostridium difficile* from *In Vivo*Transcriptomics. Infection and Immunity. 2013;81(10):3757.
170. Joseph B, Przybilla K, Stühler C, Schauer K, Slaghuis J, Fuchs TM, et al. Identification of *Listeria monocytogenes* Genes Contributing to Intracellular Replication by Expression Profiling and Mutant Screening. Journal of Bacteriology. 2006;188(2):556.
171. Winter SE, Thiennimitr P, Winter MG, Butler BP, Huseby DL, Crawford RW, et al. Gut inflammation provides a respiratory electron acceptor for Salmonella. Nature. 2010;467(7314):426-9.
172. Price-Carter M, Tingey J, Bobik TA, Roth JR. The alternative electron acceptor tetrathionate supports B12-dependent anaerobic growth of *Salmonella enterica serovar typhimurium* on ethanolamine or 1,2-propanediol. Journal of Bacteriology. 2001;183(8):2463-75.
173. Nawrocki KL, Wetzel D, Jones JB, Woods EC, McBride SM. Ethanolamine is a valuable nutrient source that impacts *Clostridium difficile* pathogenesis. Environmental Microbiology. 2018;20(4):1419-35.
174. Rowley CA, Anderson CJ, Kendall MM. Ethanolamine Influences Human Commensal *Escherichia coli* Growth, Gene Expression, and Competition with Enterohemorrhagic *E. coli* O157:H7. mBio. 2018;9(5).
175. Hensel M, Shea JE, Waterman SR, Mundy R, Nikolaus T, Banks G, et al. Genes encoding putative effector proteins of the type III secretion system of Salmonella pathogenicity island 2 are required for bacterial virulence and proliferation in macrophages. Molecular Microbiology. 1998;30(1):163-74.
176. Bolger AM, Lohse M, Usadel B. Trimmomatic: a flexible trimmer for Illumina sequence data. Bioinformatics (Oxford, England). 2014;30(15):2114-20.
177. Bankevich A, Nurk S, Antipov D, Gurevich AA, Dvorkin M, Kulikov AS, et al. SPAdes: A New Genome Assembly Algorithm and Its Applications to Single-Cell Sequencing. Journal of Computational Biology. 2012;19(5):455-77.
178. Seemann T. Prokka: rapid prokaryotic genome annotation. Bioinformatics (Oxford, England). 2014;30(14):2068-9.

179. Treangen TJ, Ondov BD, Koren S, Phillippy AM. The Harvest suite for rapid core-genome alignment and visualization of thousands of intraspecific microbial genomes. Genome Biology. 2014;15(11):524.
180. Letunic I, Bork P. Interactive tree of life (iTOL) v3: an online tool for the display and annotation of phylogenetic and other trees. Nucleic Acids Research. 2016;44(W1):W242-5.
181. Price MN, Dehal PS, Arkin AP. FastTree 2 – Approximately Maximum-Likelihood Trees for Large Alignments. PLOS ONE. 2010;5(3):e9490.
182. Dixit PD, Pang TY, Studier FW, Maslov S. Recombinant transfer in the basic genome of *Escherichia coli*. Proceedings of the National Academy of Sciences of the United States of America. 2015;112(29):9070-5.
183. Baba T, Ara T, Hasegawa M, Takai Y, Okumura Y, Baba M, et al. Construction of *Escherichia coli* K-12 in-frame, single-gene knockout mutants: the Keio collection. Molecular Systems Biology. 2006;2:2006 0008.
184. Martin HM, Campbell BJ, Hart CA, Mpofu C, Nayar M, Singh R, et al. Enhanced *Escherichia coli* adherence and invasion in Crohn's disease and colon cancer. Gastroenterology. 2004;127(1):80-93.
185. Brooks T, Keevil CW. A simple artificial urine for the growth of urinary pathogens. Letters in Applied Microbiology. 1997;24(3):203-6.
186. Hall BG, Acar H, Nandipati A, Barlow M. Growth Rates Made Easy. Molecular Biology and Evolution. 2014;31(1):232-8.
187. Thomason LC, Costantino N, Court DL. *E. coli* genome manipulation by P1 transduction. Current Protocols in Molecular Biology. 2007;Chapter 1:Unit 1 17.
188. Kitagawa M, Ara T, Arifuzzaman M, Ioka-Nakamichi T, Inamoto E, Toyonaga H, et al. Complete set of ORF clones of *Escherichia coli* ASKA library (a complete set of *E. coli* K-12 ORF archive): unique resources for biological research. DNA Research. 2005;12(5):291-9.
189. Sturms R, Streauslin NA, Cheng S, Bobik TA. In *Salmonella enterica*, Ethanolamine Utilization Is Repressed by 1,2-Propanediol To Prevent Detrimental Mixing of Components of Two Different Bacterial Microcompartments. Journal of Bacteriology. 2015;197(14):2412-21.

190. Livak KJ, Schmittgen TD. Analysis of relative gene expression data using real-time quantitative PCR and the 2(-Delta Delta C(T)) Method. Methods. 2001;25(4):402-8.
191. Hagberg L, Jodal U, Korhonen TK, Lidin-Janson G, Lindberg U, Svanborg Edén C. Adhesion, hemagglutination, and virulence of *Escherichia coli* causing urinary tract infections. Infection and Immunity. 1981;31(2):564-70.
192. Hultgren SJ, Schwan WR, Schaeffer AJ, Duncan JL. Regulation of production of type 1 pili among urinary tract isolates of *Escherichia coli*. Infection and Immunity. 1986;54(3):613-20.
193. Dale AP, Woodford N. Extra-intestinal pathogenic *Escherichia coli* (ExPEC): Disease, carriage and clones. Journal of Infection. 2015;71(6):615-26.
194. Czaja CA, Stamm WE, Stapleton AE, Roberts PL, Hawn TR, Scholes D, et al. Prospective cohort study of microbial and inflammatory events immediately preceding *Escherichia coli* recurrent urinary tract infection in women. The Journal of Infectious Diseases. 2009;200(4):528-36.
195. Bergthorsson U, Ochman H. Distribution of chromosome length variation in natural isolates of *Escherichia coli*. Molecular Biology and Evolution. 1998;15(1):6-16.
196. Wirth T, Falush D, Lan R, Colles F, Mensa P, Wieler LH, et al. Sex and virulence in *Escherichia coli*: an evolutionary perspective. Molecular Microbiology. 2006;60(5):1136-51.
197. Moreno E, Andreu A, Pigrau C, Kuskowski MA, Johnson JR, Prats G. Relationship between *Escherichia coli* strains causing acute cystitis in women and the fecal *E. coli* population of the host. Journal of Clinical Microbiology. 2008;46(8):2529-34.
198. Zhang L, Foxman B, Marrs C. Both urinary and rectal *Escherichia coli* isolates are dominated by strains of phylogenetic group B2. Journal of Clinical Microbiology. 2002;40(11):3951-5.
199. Cao X, Cavaco LM, Lv Y, Li Y, Zheng B, Wang P, et al. Molecular characterization and antimicrobial susceptibility testing of *Escherichia coli* isolates from patients with urinary tract infections in 20 Chinese hospitals. Journal of Clinical Microbiology. 2011;49(7):2496-501.

200. Huang Y, Nishikawa T, Satoh K, Iwata T, Fukushima T, Santa T, et al. Urinary excretion of D-serine in human: comparison of different ages and species. Biological & Pharmaceutical Bulletin. 1998;21(2):156-62.
201. Jost SP. Cell cycle of normal bladder urothelium in developing and adult mice. Virchows Archiv B, Cell Pathology Including Molecular Pathology. 1989;57(1):27-36.
202. Chaudhari PP, Monuteaux MC, Bachur RG. Urine Concentration and Pyuria for Identifying UTI in Infants. Pediatrics. 2016;138(5).
203. Roesch PL, Redford P, Batchelet S, Moritz RL, Pellett S, Haugen BJ, et al. Uropathogenic *Escherichia coli* use d-serine deaminase to modulate infection of the murine urinary tract. Molecular Microbiology. 2003;49(1):55-67.
204. Blattner FR, Plunkett G, Bloch CA, Perna NT, Burland V, Riley M, et al. The Complete Genome Sequence of *Escherichia coli* K-12. Science. 1997;277(5331):1453.
205. Wolfe AJ. The acetate switch. Microbiology and Molecular Biology Reviews. 2005;69(1):12-50.
206. Bologna FP, Campos-Bermudez VA, Saavedra DD, Andreo CS, Drincovich MF. Characterization of *Escherichia coli* EutD: a phosphotransacetylase of the ethanolamine operon. The Journal of Microbiology. 2010;48(5):629-36.
207. Gupta A, Dwivedi M, Mahdi AA, Khetrapal CL, Bhandari M. Broad Identification of Bacterial Type in Urinary Tract Infection Using 1H NMR Spectroscopy. Journal of Proteome Research. 2012;11(3):1844-54.
208. Johnson JR, Porter S, Johnston B, Kuskowski MA, Spurbeck RR, Mobley HL, et al. Host Characteristics and Bacterial Traits Predict Experimental Virulence for *Escherichia coli* Bloodstream Isolates From Patients With Urosepsis. Open Forum Infectious Diseases. 2015;2(3):ofv083.
209. Rijavec M, Starcic Erjavec M, Ambrozic Avgustin J, Reissbrodt R, Fruth A, Krizan-Hergouth V, et al. High prevalence of multidrug resistance and random distribution of mobile genetic elements among uropathogenic *Escherichia coli* (UPEC) of the four major phylogenetic groups. Current Microbiology. 2006;53(2):158-62.
210. Nowrouzian FL, Adlerberth I, Wold AE. Enhanced persistence in the colonic microbiota of *Escherichia coli* strains belonging to phylogenetic group B2:

role of virulence factors and adherence to colonic cells. Microbes and Infection. 2006;8(3):834-40.

211. Grenier F, Matteau D, Baby V, Rodrigue S. Complete Genome Sequence of *Escherichia coli* BW25113. Genome Announcements. 2014;2(5).
212. Ding W, Baumdicker F, Neher RA. panX: pan-genome analysis and exploration. Nucleic Acids Research. 2018;46(1):e5-e.
213. Guo K, Li L. Differential 12C-/13C-isotope dansylation labeling and fast liquid chromatography/mass spectrometry for absolute and relative quantification of the metabolome. Analytical chemistry. 2009;81(10):3919-32.
214. Barnett Foster D, Philpott D, Abul-Milh M, Huesca M, Sherman PM, Lingwood CA. Phosphatidylethanolamine recognition promotes enteropathogenic *E. coli* and enterohemorrhagic *E. coli* host cell attachment. Microbial Pathogenesis. 1999;27(5):289-301.
215. Barnett Foster D, Abul-Milh M, Huesca M, Lingwood CA. Enterohemorrhagic *Escherichia coli* Induces Apoptosis Which Augments Bacterial Binding and Phosphatidylethanolamine Exposure on the Plasma Membrane Outer Leaflet. Infection and Immunity. 2000;68:3108-15.
216. Bloom FR, McFall E. Isolation and characterization of D-serine deaminase constitutive mutants by utilization of D-serine as sole carbon or nitrogen source. Journal of Bacteriology. 1975;121(3):1078-84.
217. Vandesompele J, De Preter K, Pattyn F, Poppe B, Van Roy N, De Paepe A, et al. Accurate normalization of real-time quantitative RT-PCR data by geometric averaging of multiple internal control genes. Genome Biology. 2002;3(7):RESEARCH0034-RESEARCH.
218. Jones PW, Turner JM. A Model for the Common Control of Enzymes of Ethanolamine Catabolism in *Escherichia coli*. Microbiology. 1984;130(4):849-60.
219. Sampson EM, Bobik TA. Microcompartments for B12-dependent 1,2-propanediol degradation provide protection from DNA and cellular damage by a reactive metabolic intermediate. Journal of Bacteriology. 2008;190(8):2966-71.
220. Sriramulu DD, Liang M, Hernandez-Romero D, Raux-Deery E, Lünsdorf H, Parsons JB, et al. *Lactobacillus reuteri* DSM 20016 produces cobalamin-dependent diol dehydratase in metabolosomes and metabolizes 1,2-

propanediol by disproportionation. Journal of Bacteriology. 2008;190(13):4559-67.

221. Wang X, Kim Y, Ma Q, Hong SH, Pokusaeva K, Sturino JM, et al. Cryptic prophages help bacteria cope with adverse environments. Nature Communications. 2010;1:147.

222. Wang J, Yan D, Dixon R, Wang Y-P. Deciphering the Principles of Bacterial Nitrogen Dietary Preferences: a Strategy for Nutrient Containment. mBio. 2016;7(4):e00792-16.

223. Spaulding CN, Klein RD, Ruer S, Kau AL, Schreiber HL, Cusumano ZT, et al. Selective depletion of uropathogenic *E. coli* from the gut by a FimH antagonist. Nature. 2017;546:528.

224. Chang GW, Chang JT. Evidence for the B12-dependent enzyme ethanolamine deaminase in *Salmonella*. Nature. 1975;254(5496):150-1.

225. Li H, Kristensen DM, Coleman MK, Mushegian A. Detection of biochemical pathways by probabilistic matching of phyletic vectors. PLOS ONE. 2009;4(4):e5326.

226. Kaper JB, Nataro JP, Mobley HL. Pathogenic *Escherichia coli*. Nature Reviews Microbiology. 2004;2(2):123-40.

227. Luo C, Hu G-Q, Zhu H. Genome reannotation of *Escherichia coli* CFT073 with new insights into virulence. BMC Genomics. 2009;10:552-.

228. Lim JK, Gunther NWt, Zhao H, Johnson DE, Keay SK, Mobley HL. *In vivo* phase variation of *Escherichia coli* type 1 fimbrial genes in women with urinary tract infection. Infection and Immunity. 1998;66(7):3303-10.